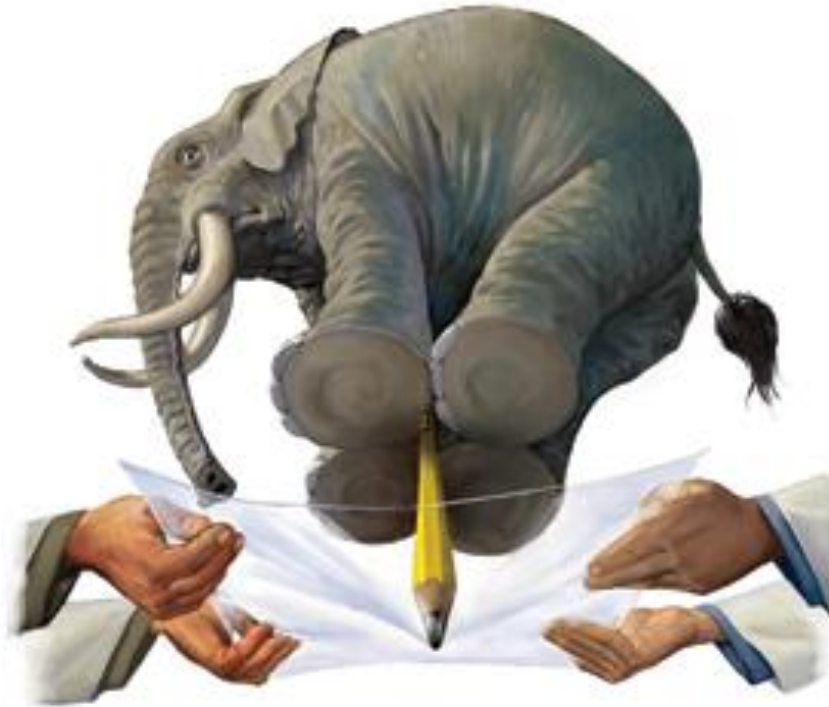


Physics and Mechanics of Graphene



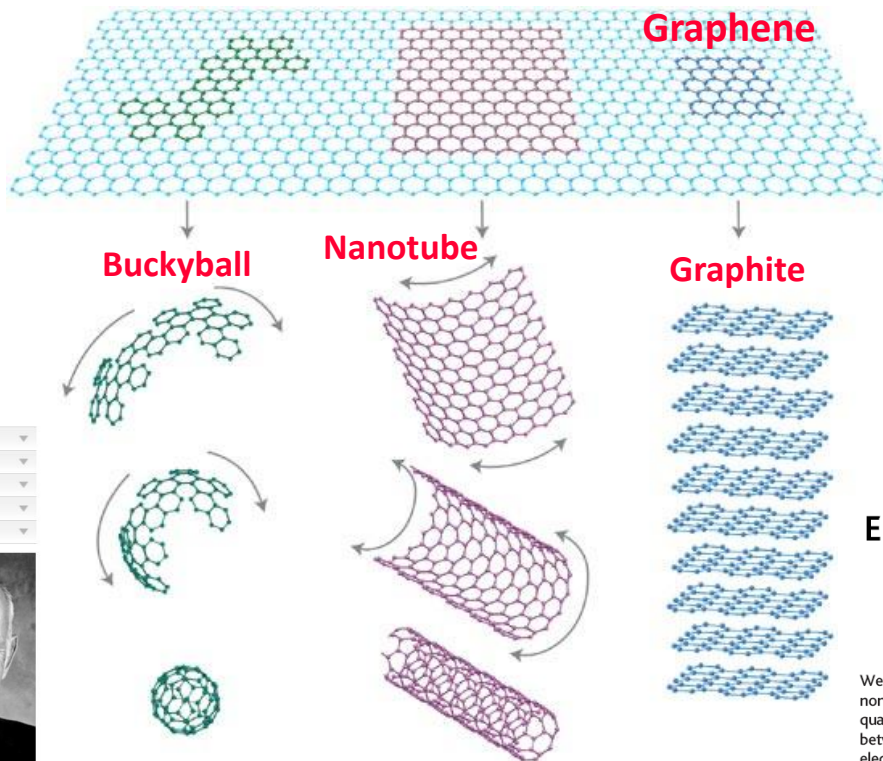
Asst. Prof. K. Papagelis

Department of Materials Science, University of Patras (Greece)
ICE-HT, FORTH, Patras (Greece)



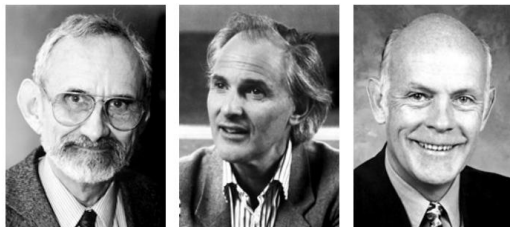
Graphene: Mother of all graphitic forms

Graphene is a flat monolayer of C atoms tightly packed into a 2D honeycomb lattice. It can be wrapped up into 0D fullerenes, rolled into 1D nanotubes or stacked into 3D graphite.



The Nobel Prize in Chemistry 1996
Robert F. Curl Jr., Sir Harold Kroto, Richard E. Smalley

The Nobel Prize in Chemistry 1996
Nobel Prize Award Ceremony
Robert F. Curl Jr.
Sir Harold Kroto
Richard E. Smalley



Robert F. Curl Jr. Sir Harold W. Kroto Richard E. Smalley

The Nobel Prize in Physics 2010
Andre Geim, Konstantin Novoselov

The Nobel Prize in Physics 2010
Andre Geim
Konstantin Novoselov



Photo: Sergeon, Wikimedia Commons Photo: University of Manchester, UK

Andre Geim Konstantin Novoselov

22 OCTOBER 2004 VOL 306 SCIENCE

Electric Field Effect in Atomically Thin Carbon Films

K. S. Novoselov,¹ A. K. Geim,^{1*} S. V. Morozov,² D. Jiang,¹ Y. Zhang,¹ S. V. Dubonos,² I. V. Grigorieva,¹ A. A. Firsov²

We describe monocrystalline graphitic films, which are a few atoms thick but are nonetheless stable under ambient conditions, metallic, and of remarkably high quality. The films are found to be a two-dimensional semimetal with a tiny overlap between valence and conduction bands, and they exhibit a strong ambipolar electric field effect such that electrons and holes in concentrations up to 10¹³ per

162 LETTERS TO NATURE

NATURE VOL. 318 14 NOVEMBER 1985

C₆₀: Buckminsterfullerene

H. W. Kroto*, J. R. Heath, S. C. O'Brien, R. F. Curl & R. E. Smalley

Rice Quantum Institute and Departments of Chemistry and Electrical Engineering, Rice University, Houston, Texas 77251, USA

Fig. 1 A football (in the United States, a soccerball) on Texas grass. The C₆₀ molecule featured in this letter is suggested to have the truncated icosahedral structure formed by replacing each vertex on the seams of such a ball by a carbon atom.



graphite fused six-membered ring structure. We believe that the

LETTERS TO NATURE (1991)

Helical microtubules of graphitic carbon

Sumio Iijima

NEC Corporation, Fundamental Research Laboratories, 34 Miyukigaoka, Tsukuba, Ibaraki 305, Japan

THE synthesis of molecular carbon structures in the form of and other fullerenes¹ has stimulated intense interest in the structures accessible to graphitic carbon sheets. Here I report preparation of a new type of finite carbon structure consisting of needle-like tubes. Produced using an arc-discharge evaporation method similar to that used for fullerene synthesis, the ne

LETTERS TO NATURE (1993)

Single-shell carbon nanotubes of 1-nm diameter

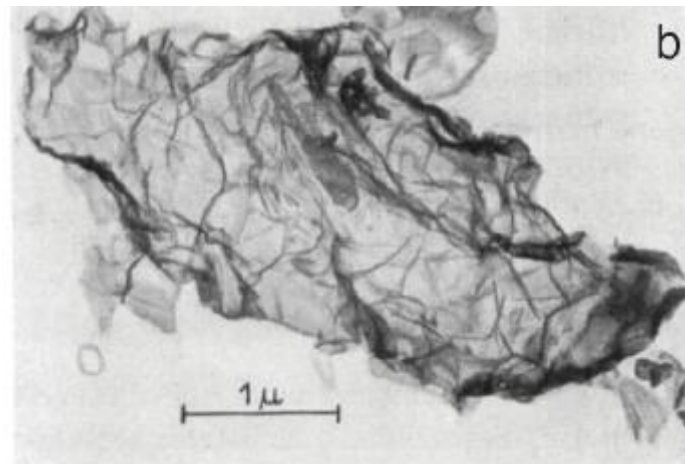
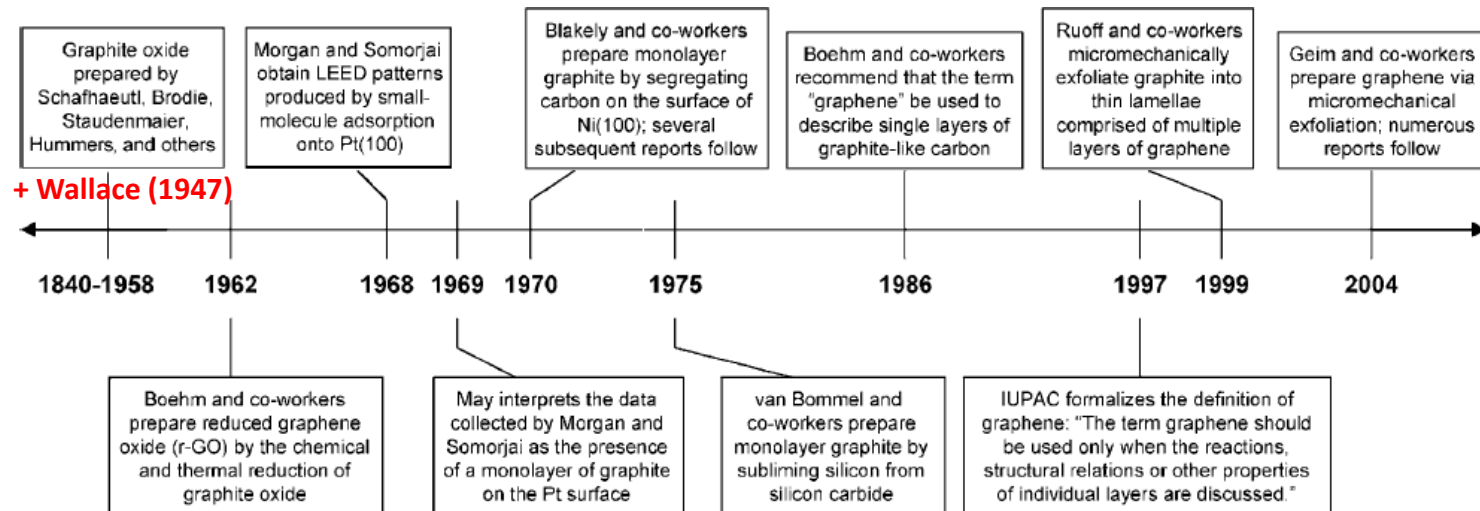
Sumio Iijima & Toshinari Ichihashi

Fundamental Research Laboratories, NEC Corporation, 34 Miyukigaoka, Tsukuba, Ibaraki 305, Japan

CARBON nanotubes¹ are expected to have a wide variety of interesting properties. Capillarity in open tubes has already been

Η μακρά ιστορία του γραφενίου

For a nice Review of the history of graphene see D. R. Dreyer et al, *Angew. Chem. Int. Ed.* 49, 9336 (2010)



...in my opinion, stand as the first observation of graphene because monolayers should have been present among the residue, and the idea was correct...

A. Geim, Nobel Lecture: Random walk to graphene, *Rev. Mod. Phys.* (2011)

[H. P. Boehm et al, *Z. Anorg. Allg. Chem.* 316, 119 (1962)]

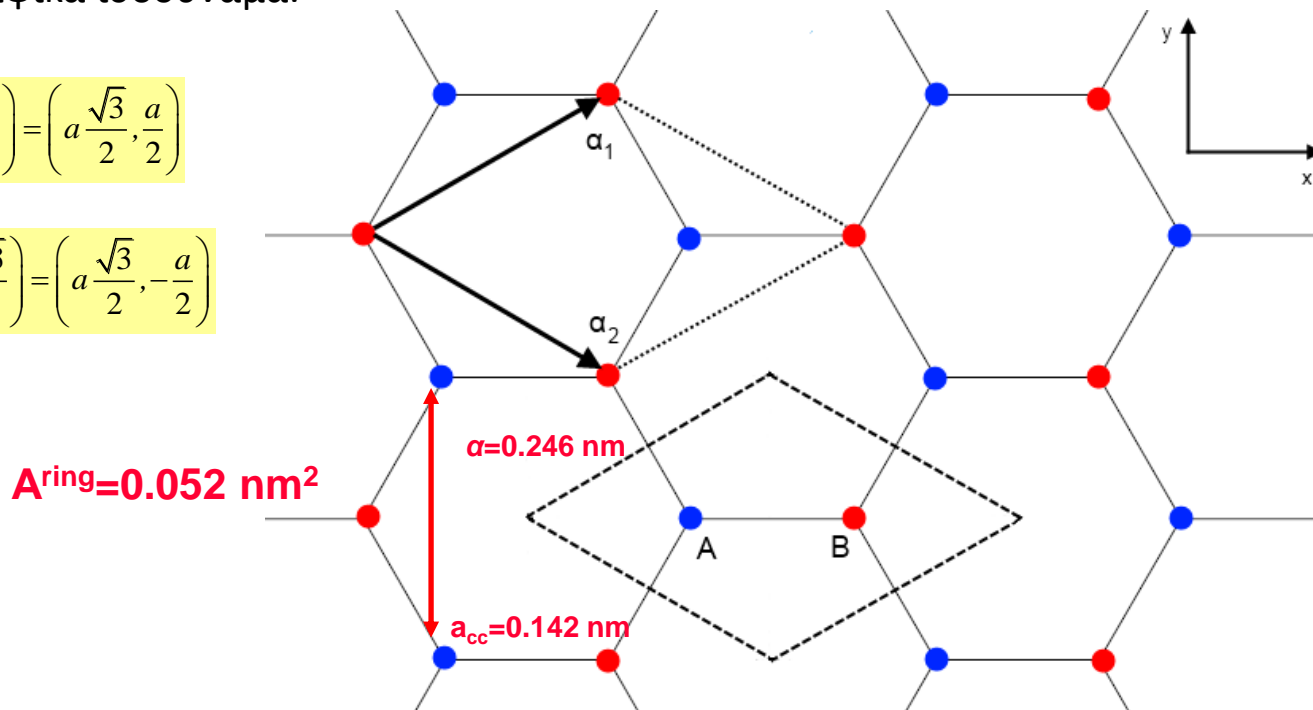
➡ In fact, the term “graphene” grew out of the chemistry of GICs as the need for language to describe the decoupled layers became apparent. The term graphene was first coined by Boehm et al. in 1986 [H. P. Boehm, R. Setton, E. Stumpp, *Carbon* 24, 241 (1986)]

Κρυσταλλική Δομή του Γραφενίου

– Η κρυσταλλική δομή του γραφενίου παρουσιάζει εξαγωνική συμμετρία και περιγράφεται από ένα εξαγωνικό δισδιάστατο πλέγμα Bravais με βάση δύο ατόμων άνθρακα A και B, τα οποία δεν είναι κρυσταλλογραφικά ισοδύναμα.

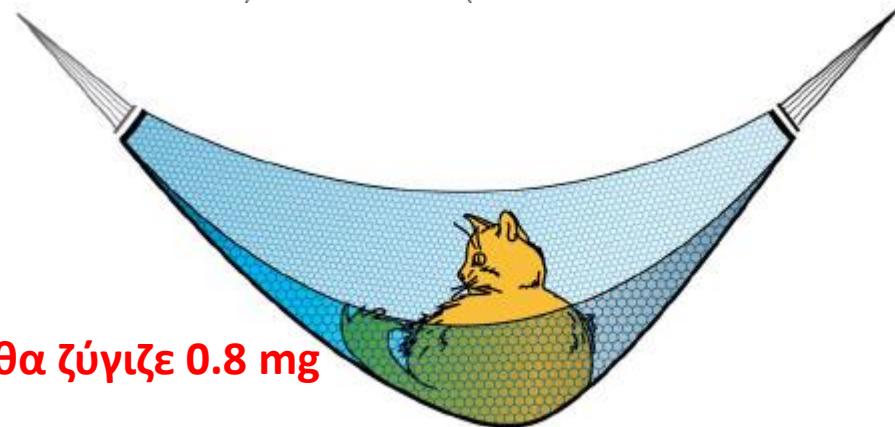
$$\alpha_1 = \left(\frac{3a_{cc}}{2}, a_{cc} \frac{\sqrt{3}}{2} \right) = \left(a \frac{\sqrt{3}}{2}, \frac{a}{2} \right)$$

$$\alpha_2 = \left(\frac{3a_{cc}}{2}, -a_{cc} \frac{\sqrt{3}}{2} \right) = \left(a \frac{\sqrt{3}}{2}, -\frac{a}{2} \right)$$



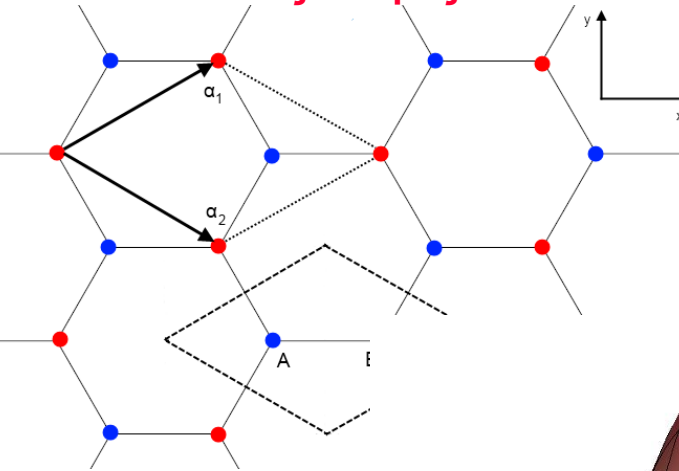
$$\rho = \frac{2 \times 12 \times 1.66 \times 10^{-27} \text{ kg}}{0.052 \times 10^{-18} \text{ m}^2} \approx 0.8 \frac{\text{mg}}{\text{m}^2}$$

– Μια υποθετική αιώρα 1m² από γραφένιο θα ζύγιζε 0.8 mg



Κρυσταλλική και Ηλεκτρονική Δομή του Γραφενίου

«Ευθύς» Χώρος

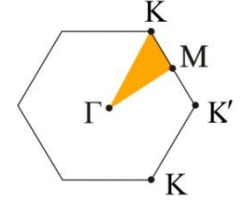
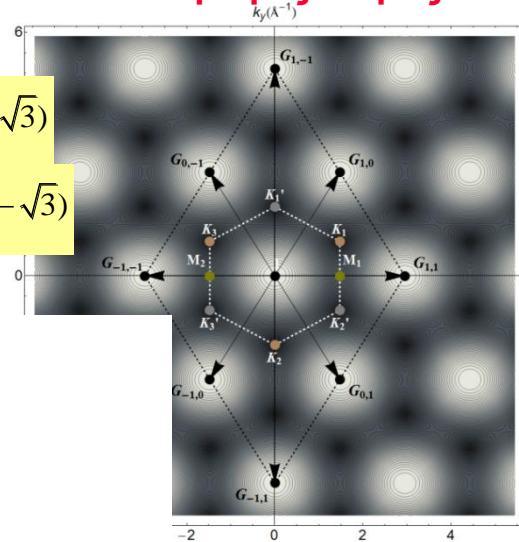


$$\mathbf{G}_{hk} = h\mathbf{b}_1 + k\mathbf{b}_2$$

$$\mathbf{b}_1 = \mathbf{G}_{10} = \frac{2\pi}{3a_{cc}}(1, \sqrt{3})$$

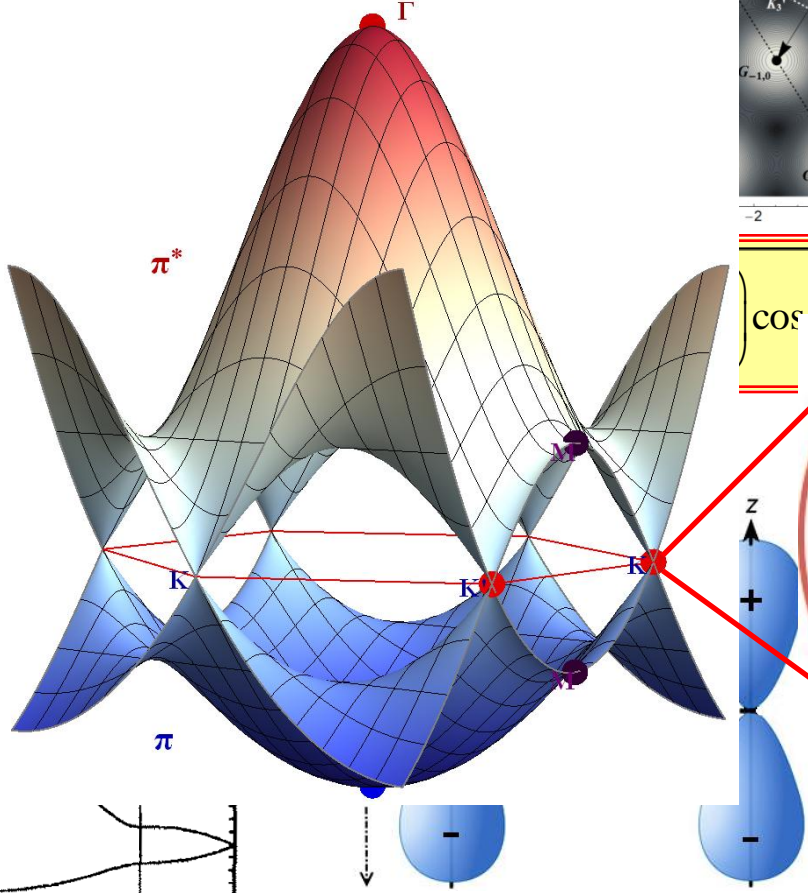
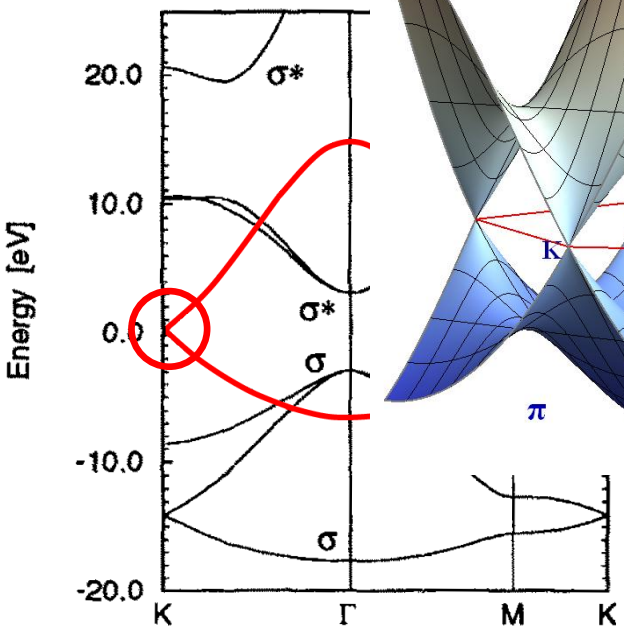
$$\mathbf{b}_2 = \mathbf{G}_{01} = \frac{2\pi}{3a_{cc}}(1, -\sqrt{3})$$

Αντίστροφος Χώρος



– If the A, B sites had different atoms such as B and N the energy dispersion would show an energy between π and π^* states ($E_g = 3.5\text{eV} = \epsilon_{2p}(B) - \epsilon_{2p}(N)$)

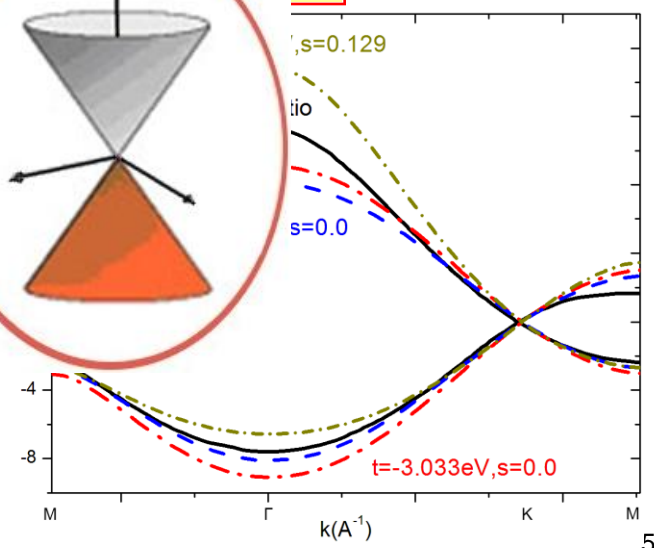
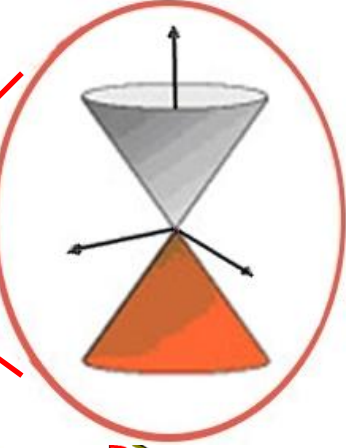
Tight Binding approx



$$E_{\pm}(k) = \pm \hbar \cdot v_F \cdot k$$

$$\left(\cos\left(\frac{k_x a \sqrt{3}}{2}\right) + 1 + \cos\left(\frac{k_y a}{2}\right) \right)^2$$

$$v_F = \frac{3t \cdot a_{cc}}{2\hbar} \approx 10^6 \text{ m/s}$$

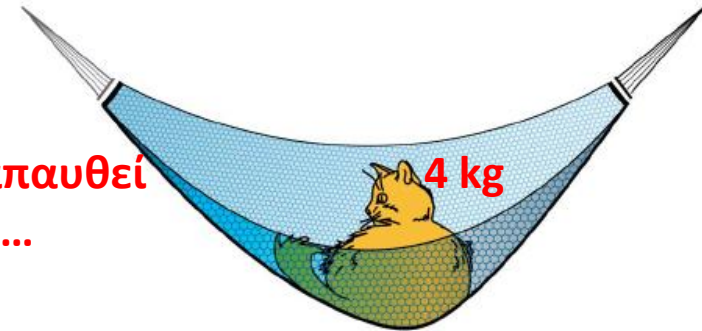


Graphene properties

Αντοχή θραύσης του γραφενίου ($\sigma_{2D} \sim 42 \text{N/m}$). {Παρακάτω δικά μας αποτελέσματα}

- Θεωρώντας το πάχος του γραφενίου ως 0.335nm η αντοχή θραύσης είναι $\sigma_{\text{eff}} \sim 130 \text{GPa}$.
- Για ένα υποθετικό μονοατομικό υμένιο Fe ($250\text{-}1200 \text{MPa}$) η αντοχή θραύσης είναι $\sigma_{2D} \sim 0.084\text{-}0.4 \text{N/m}$.
- Το γραφένιο είναι 100 φορές πιο ανθεκτικό από τον Fe.

Στην υποθετική μας αιώρα (1m^2) θα μπορούσε να αναπαυθεί μια γάτα βάρους $\sim 4 \text{kg}$ χωρίς να συμβεί κάποιο ατύχημα...



Ηλεκτρική αγωγιμότητα του γραφενίου.

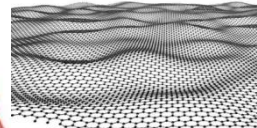
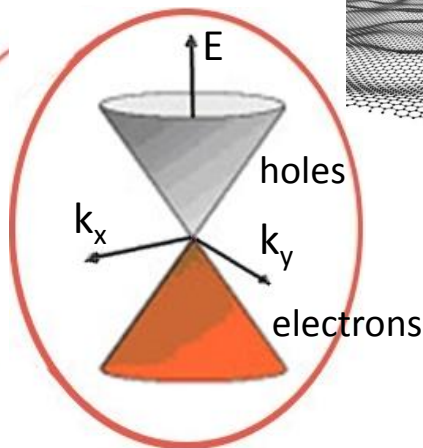
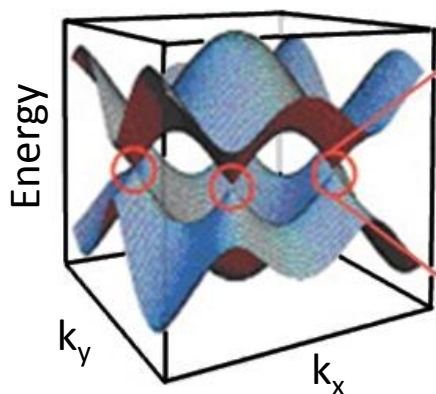
- Η ευκινησία του γραφενίου είναι $200,000 \text{cm}^2 \text{V}^{-1} \text{s}^{-1}$ για $n = 10^{12} \text{cm}^{-2}$. Η 2D αγωγιμότητα του γραφενίου δίνεται από $\sigma = en\mu$. Η 2D ειδική αντίσταση του γραφενίου προκύπτει 31Ω .
- Θεωρώντας το πάχος του γραφενίου ως 0.335nm η "bulk" αγωγιμότητα του γραφενίου είναι $0.96 \times 10^6 \Omega^{-1} \text{cm}^{-1}$ λίγο μεγαλύτερη του Cu ($0.6 \times 10^6 \Omega^{-1} \text{cm}^{-1}$).

Θερμική αγωγιμότητα του γραφενίου ($\sim 5000 \text{Wm}^{-1} \text{K}^{-1}$).

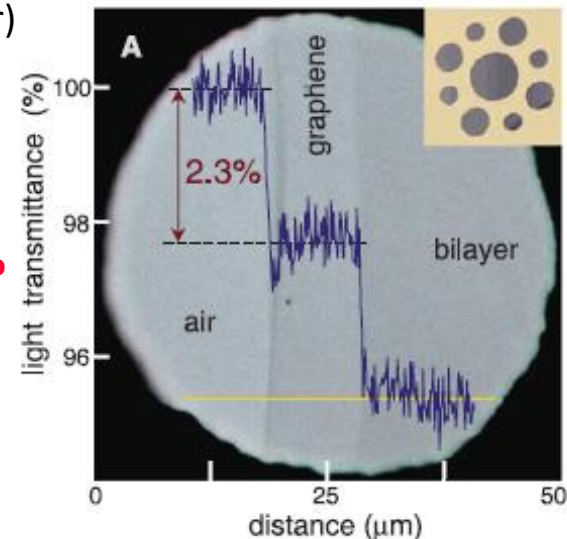
- Οφείλεται στα φωνόνια και έχει 10 φορές μεγαλύτερη από αυτή του Cu σε $T = 300 \text{K}$ $\sim 400 \text{Wm}^{-1} \text{K}^{-1}$).

Graphene properties

- Perfect crystal. Not perfectly flat, stabilized by intrinsic ripples (nm order)
- gapless semiconductor

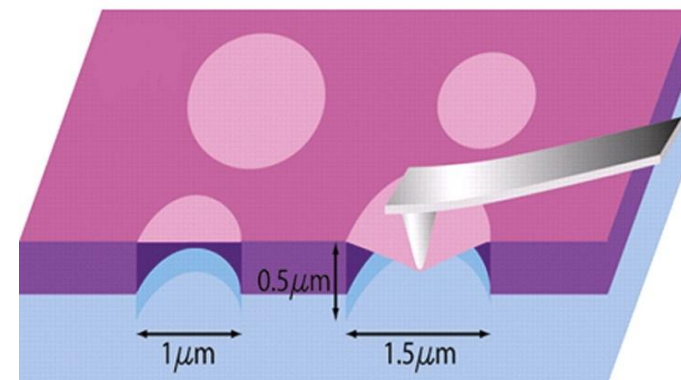


$$\pi\alpha = 2.3\%$$



The opacity of suspended graphene is defined solely by the fine structure $\alpha = e^2/hc = 1/137$ Universal parameter, does not depend on materials parameters [Science 320, 1308 (2008)].

- high e mobility ($\sim 10^5 \text{ cm}^2\text{V}^{-1}\text{s}^{-1}$ at $T=300\text{K}$) and resilience to high current densities ($\sim 10^8 \text{ A/cm}^2$) [Nat. Nanotechnol. 3, 491 (2008)]
- ballistic transport even at room temperature [Nat. Mater. 6, 183 (2007)]
- Superior thermal conductivity ($\sim 5 \times 10^3 \text{ Wm}^{-1}\text{K}^{-1}$ at $T=300\text{K}$) [Nano Lett. 8, 902 (2008)]
- Extreme strength ($\sim 130 \text{ GPa}$) and modulus ($\sim 1\text{TPa}$). [Science 321, 385 (2008)]
- Each graphene layer absorbs $\pi\alpha$ ($\approx 2.3\%$) of the incident light [Science 320, 1308 (2008)]
- Novel quantum Hall physics [Nature 438, 197 (2005)]
- and much more ...



Measurement of the mechanical properties of monolayer graphene suspended over open holes onto SiO_2 substrate using AFM nanoindentation [Science 321, 385 (2008)].

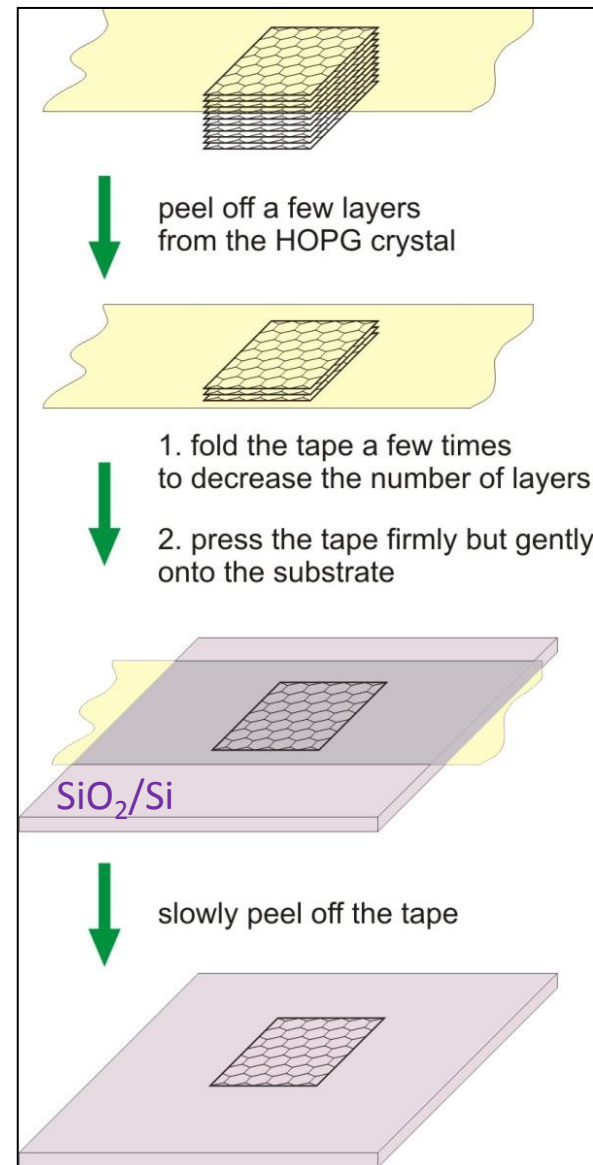
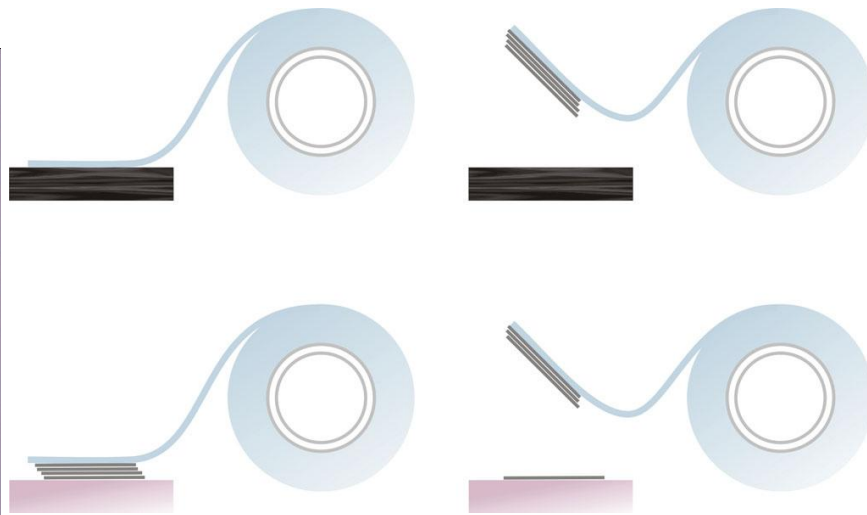
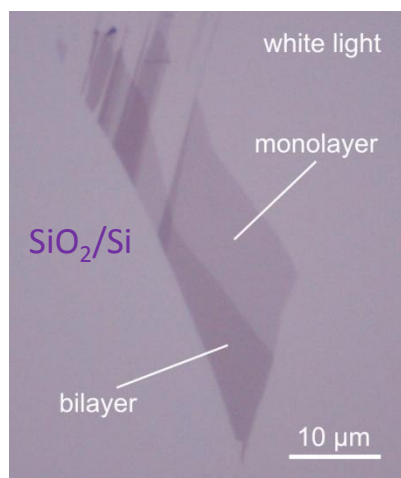
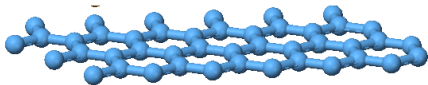
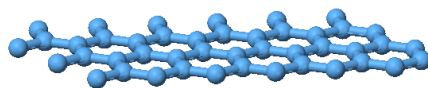
Graphene production (1/2)

I. Μηχανική αποφλοίωση (Scotch tape method)

- Ενέργεια αλληλεπίδρασης van der Waals energy: 2 eV/nm^2
- Απαιτούμενη δύναμη αποφλοίωσης $\sim 300 \text{ nN/mm}^2$

- Επαρκεί η κοινή κολλητική ταινία
- Κατάλληλο υπόστρωμα για δημιουργία αντίθεσης (δηλ. $\text{SiO}_2(300\text{nm})/\text{Si}$ or $\text{SU8}/\text{PMMA}$)

- Παραγωγή γραφενίου χωρίς ατέλειες με επιφάνεια
- μερικές εκατοντάδες μm^2



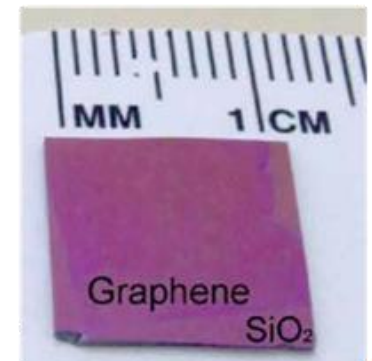
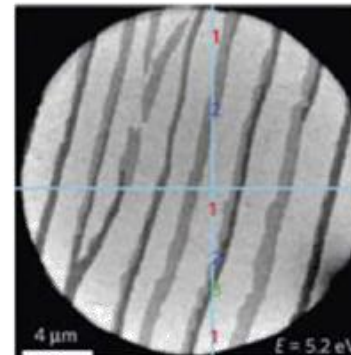
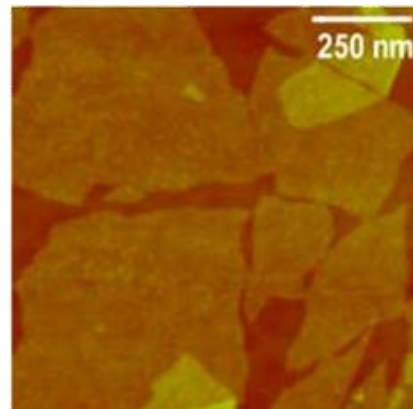
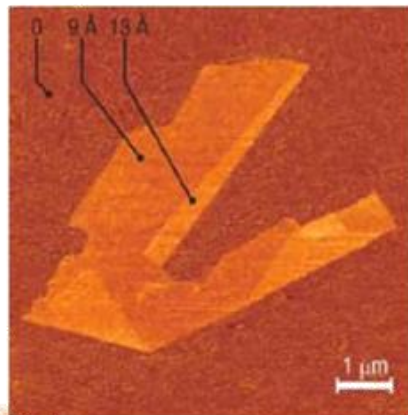
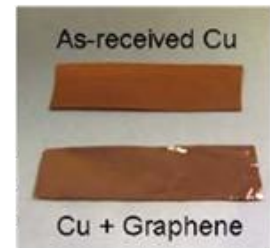
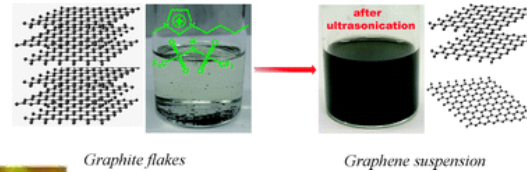
Carefully scan SiO_2 surface with optical microscope (see below) ₈

Graphene production: Overview

Method	Micromechanical exfoliation of graphite	Reduction of graphene oxide	CVD or PE-CVD growth on metal substrates	Desorption* of Si from SiC	Direct** exfoliation of graphite
Quality	Good	Not pristine graphene	Good	Good	'Good'
Size	10~100 μm	nm to μm	∞	SiC wafer size	nm to μm
Transfer	Yes	Yes	Yes (Ni and Cu)	No	Yes
Scalability	No	Yes	Yes	Yes	Yes

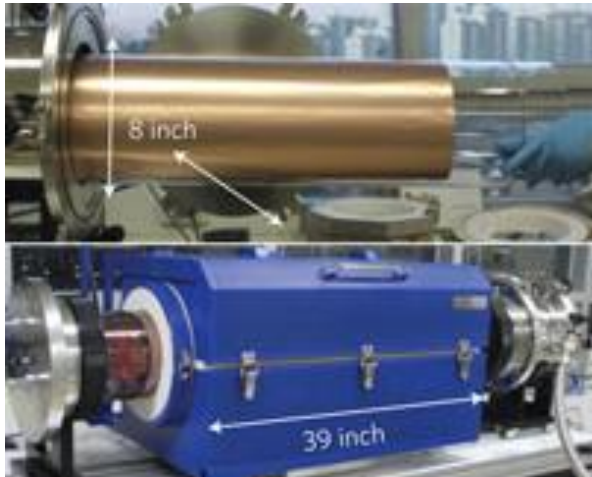
*epitaxial growth
>1300 °C Si evaporation

** tip sonication of natural graphite in aqueous or polar organic media

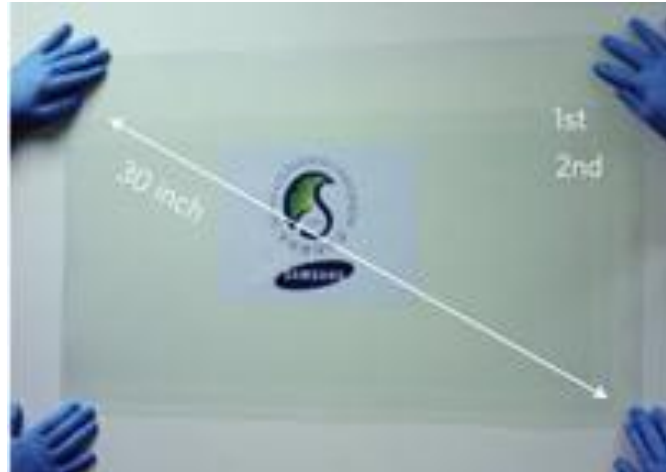


Graphene production (2/2)

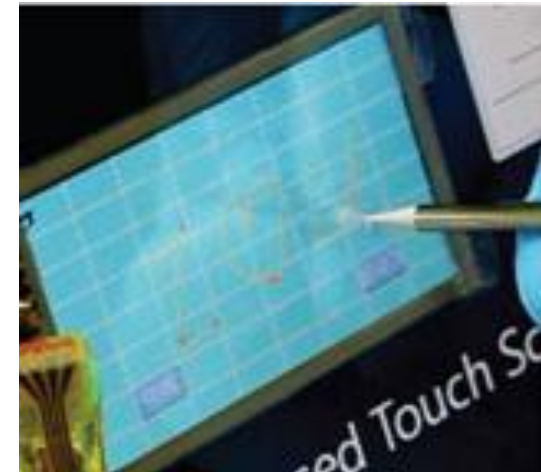
Bae et al., *Nature Nanotech.* 5, 574 (2010)



CVD reactor for graphene production on Cu substrates.



Transparent ultra large-area graphene film transferred on a 35-inch PET sheet.



Graphene-based touch-screen panel connected to a PC with control software.

II. Epitaxial growth by CVD

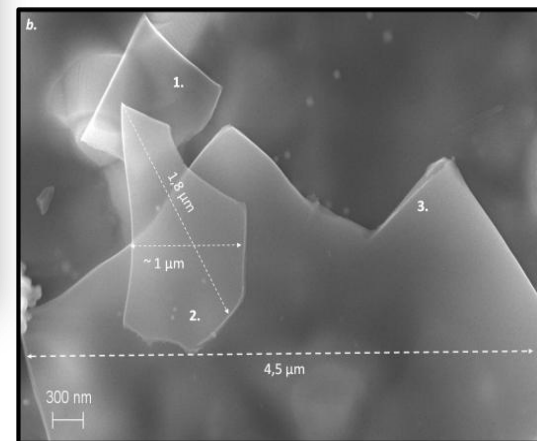
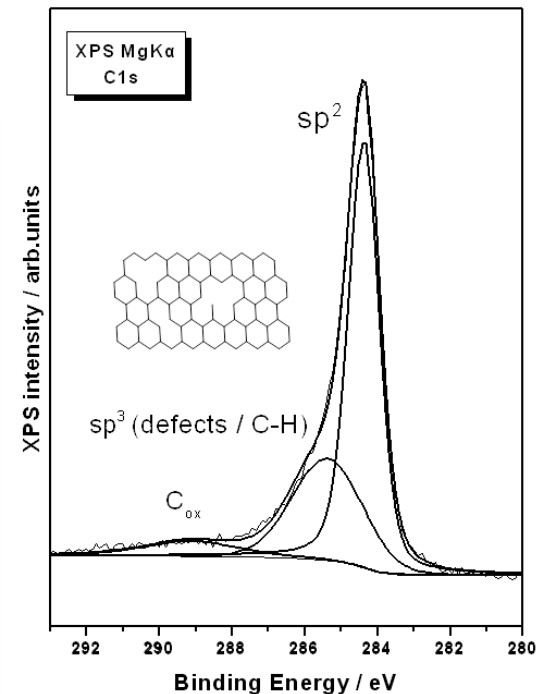
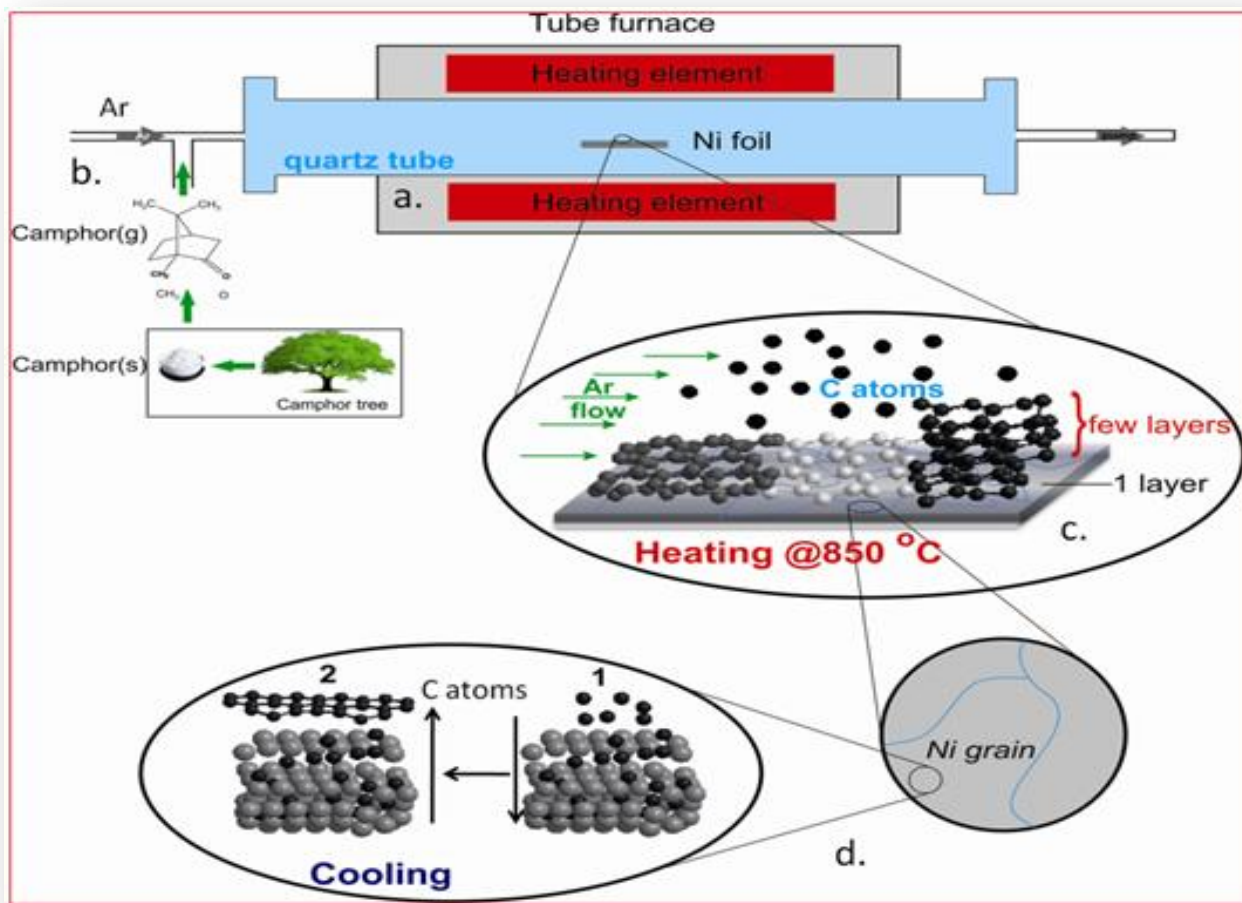
- Development of methods capable of producing large and defect-free monolayers.
- Different substrates – Cu, Ni, Pt, Ru, Ir, TiC, TaC.
- Formation of graphene either by catalytic decomposition of the hydrocarbon gas at the substrate (e.g. Cu), or by dissolution of carbon in the substrate and precipitation of graphene layers upon cooling (e.g. Ni).
- CVD on centimeter-scale Cu substrates opening a new route to large-scale production of high quality graphene films for practical applications. Also, the combination with standard lithographic methods, might be suitable for chip fabrication.

III. Epitaxial growth on SiC

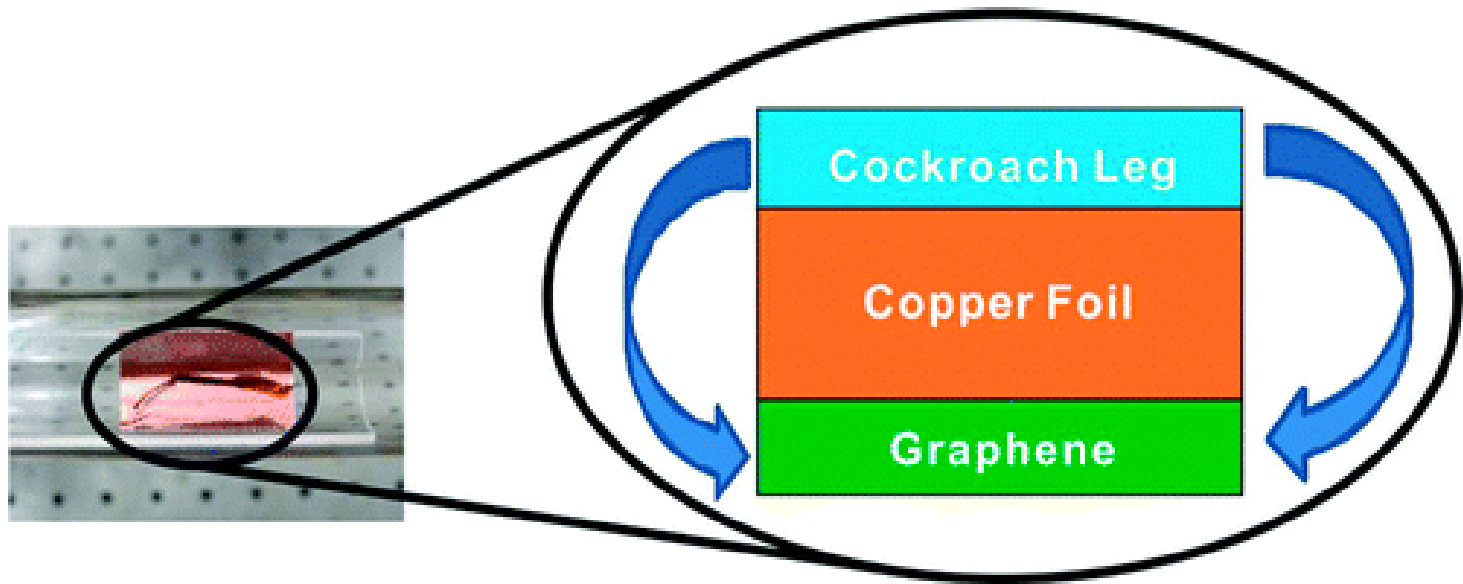
IV. Chemical Exfoliation (e.g. GO reduction)

V. Unzipping carbon nanotubes

CVD Production from Camphor



Growth of Graphene from Food, Insects, and Waste



Cockroach leg before conversion to graphene

Cross view of the growth of graphene on the backside of the Cu foil

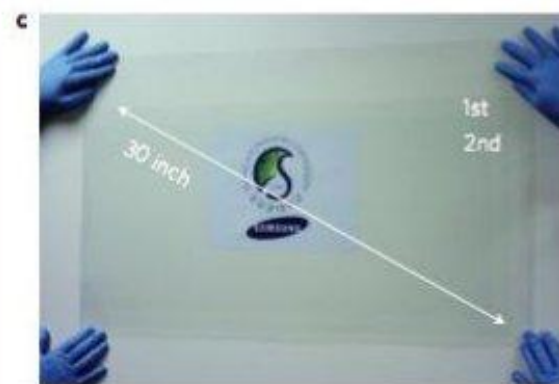
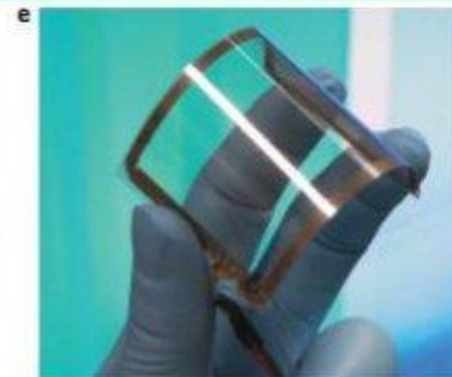
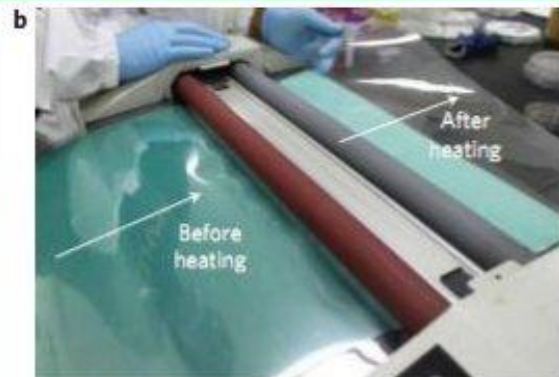
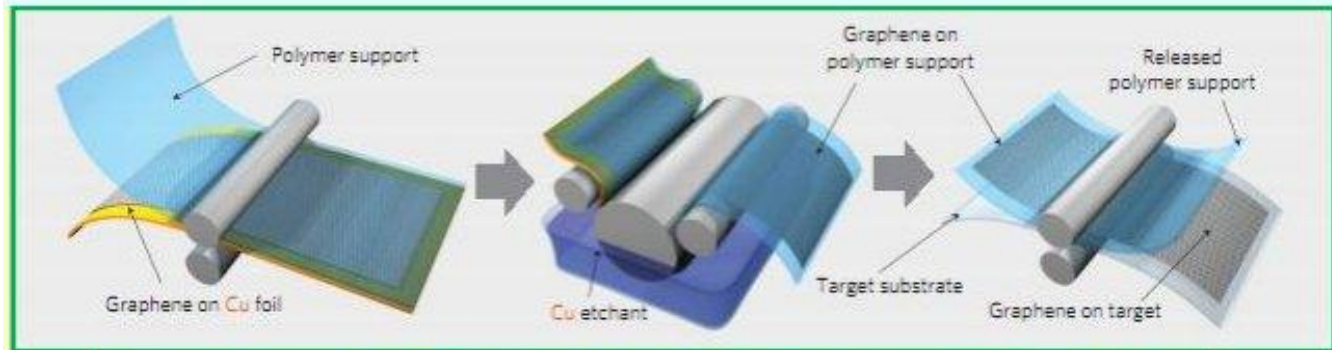
Other precursor materials for graphene production
cookies, chocolate, grass, plastics, roaches, and dog feces

Μεταφορά γραφενίου

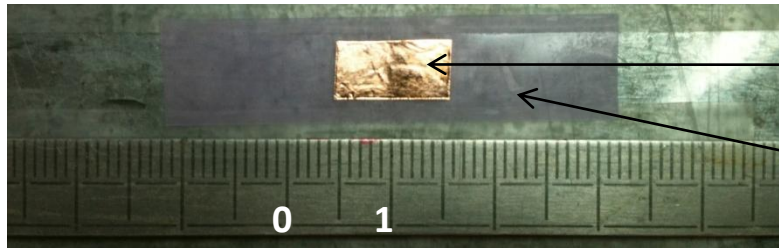
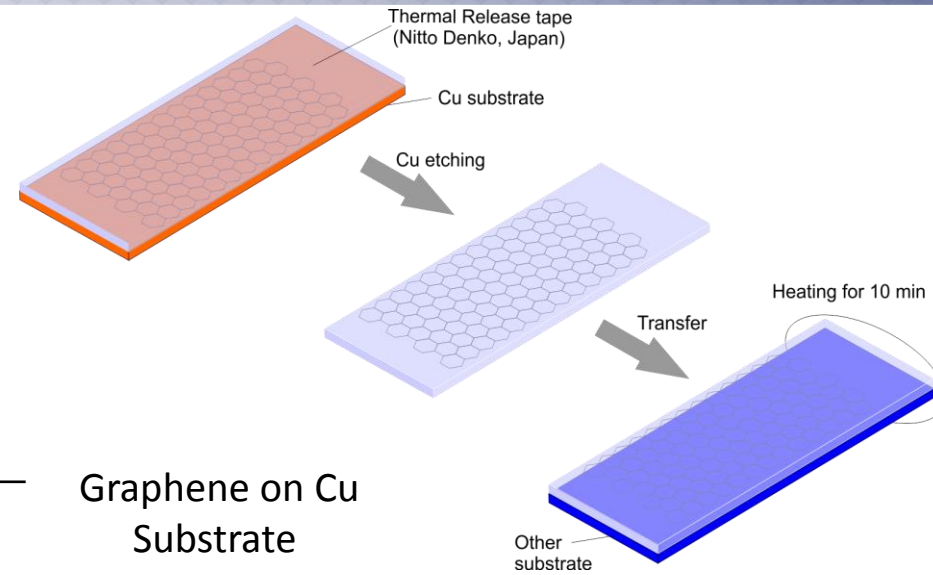
Επικόλληση
γραφενίου σε
πολυμερές
υποστήριξης

Απομάκρυνση
χαλκού-
στέγνωμα

Μεταφορά στο
πολυμερές-
στόχο με
ταυτόχρονη
ξήρανση

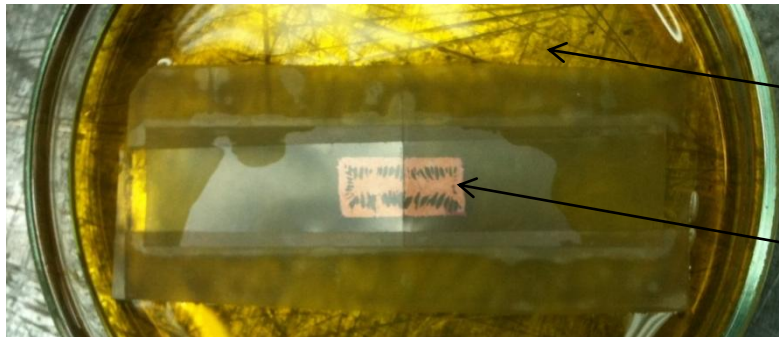


Μεταφορά γραφενίου σε εργαστηριακή κλίμακα



Graphene on Cu Substrate

Thermal release tape



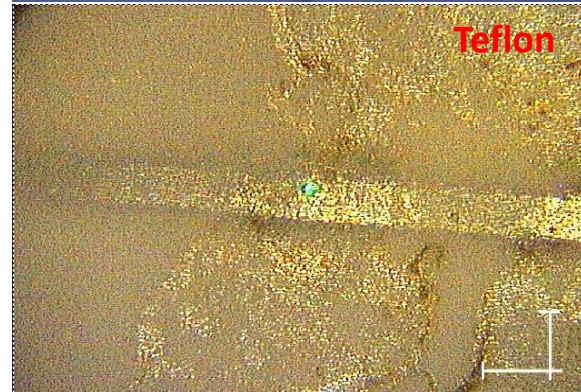
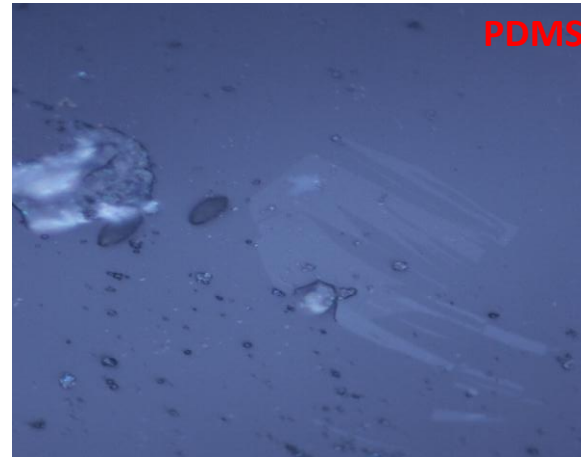
Cu etchant

Partly etched Cu



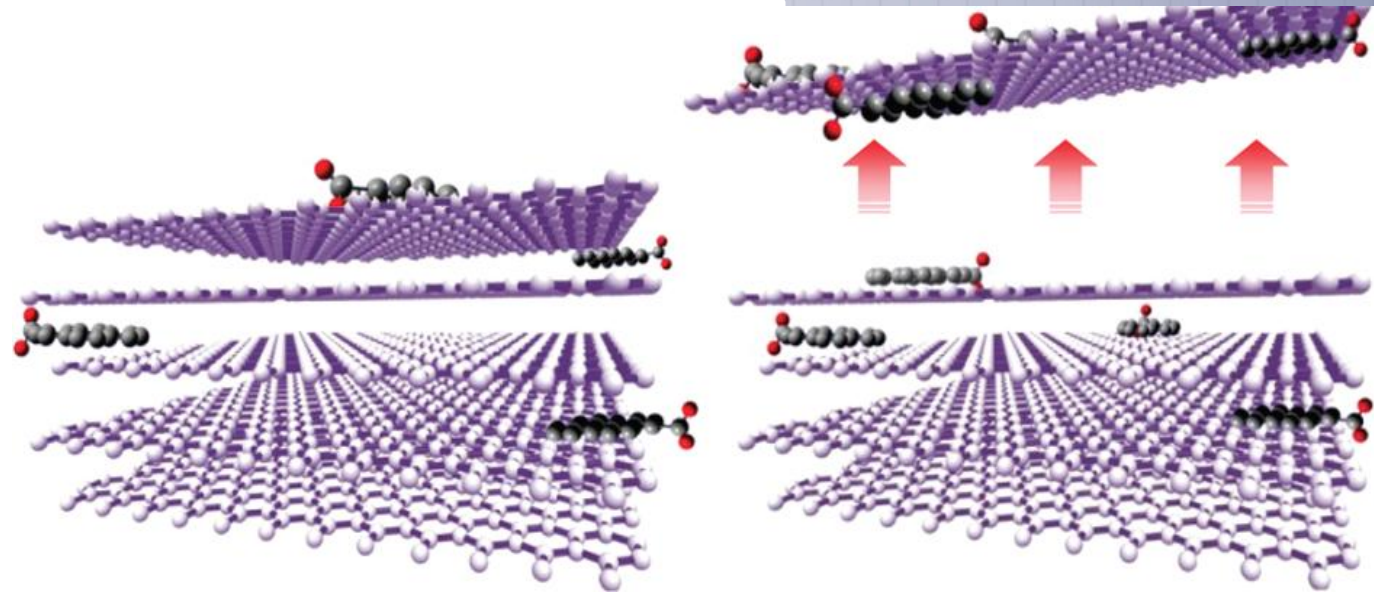
In a few minutes etching has been completed

Graphene on various substrates

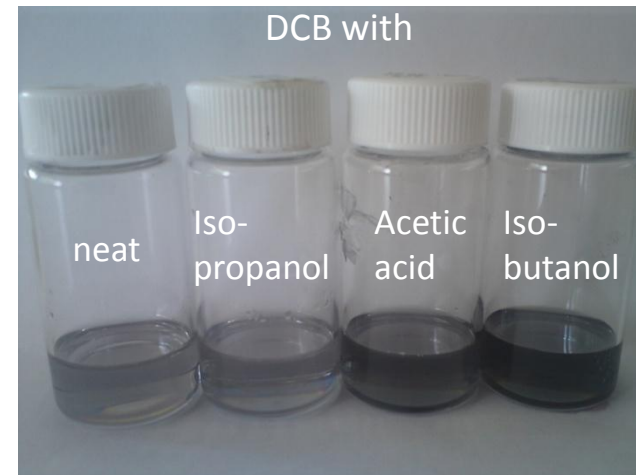
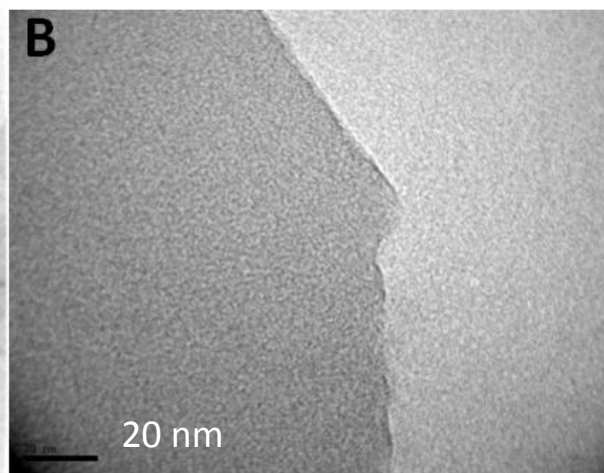
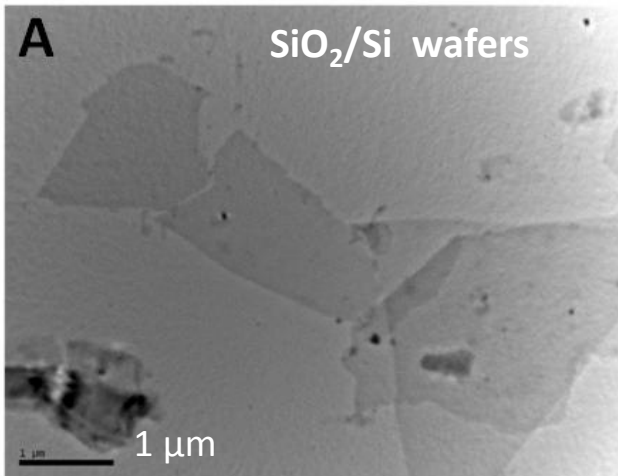


↳ Ιδιαίτερο ενδιαφέρον για εφαρμογές παρουσιάζει η μελέτη της αλληλεπίδρασης του γραφενίου με διαφορετικά υποστρώματα π.χ. πολυμερικά και μεταλλικά.

Exfoliation in Binary Solvents

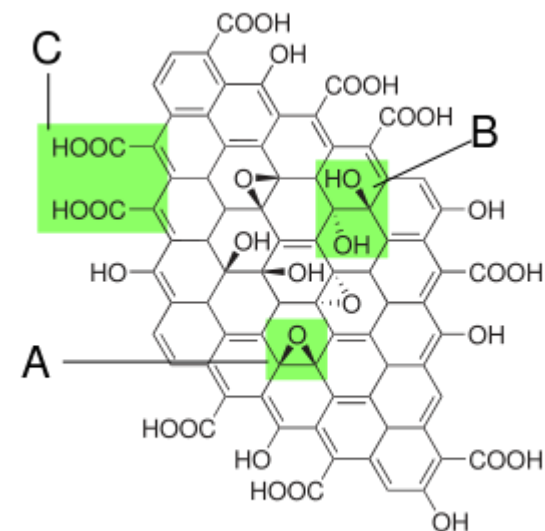


Certain solvent mixtures work better than the neat components



*Tasis et al , Chemistry of Materials, 2012 (*in press*)

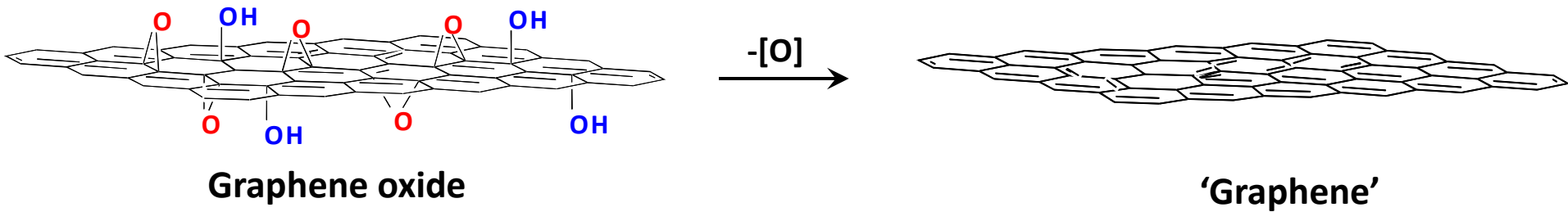
Graphite Oxide and its 'exfoliation' to yield 'graphene oxide platelets' thus a colloidal dispersion



Graphite oxide exfoliated/suspended in water as individual platelets of 'graphene oxide'

Exfoliation/Reduction Approach

- Graphene oxide sheets are not electrically conductive
- Reduction (de-oxygenation) can be employed to partially restore the graphene network



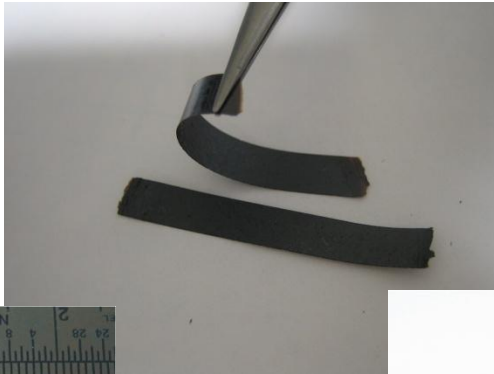
Hydrazine \longrightarrow



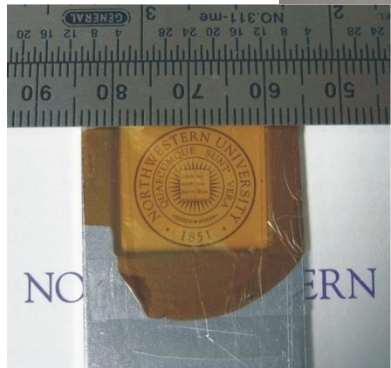
Reduction of graphene oxide with, e.g., hydrazine

'Graphene oxide paper'

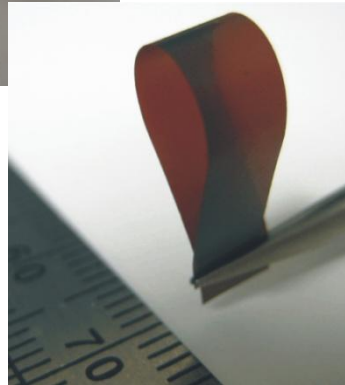
- Prepared by filtering a GO dispersion
 - Forms a layered film that can be peeled away from filter
- Sheets interact through van der Waals interactions and hydrogen bonding
 - Very large surface area



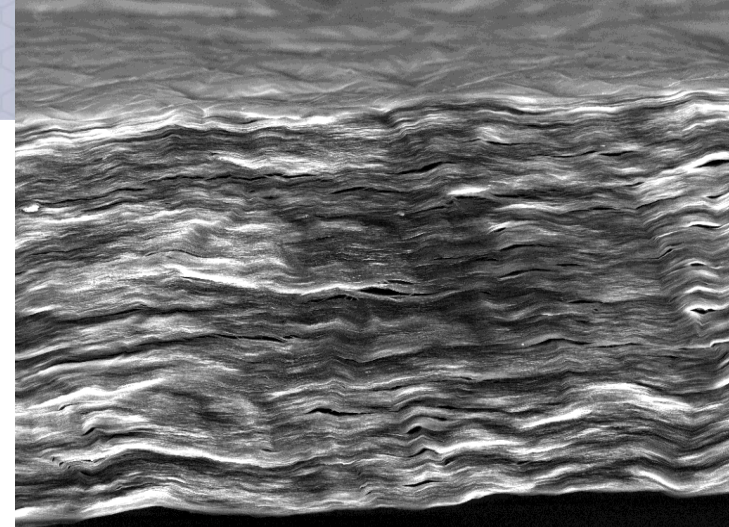
~20 μm thick



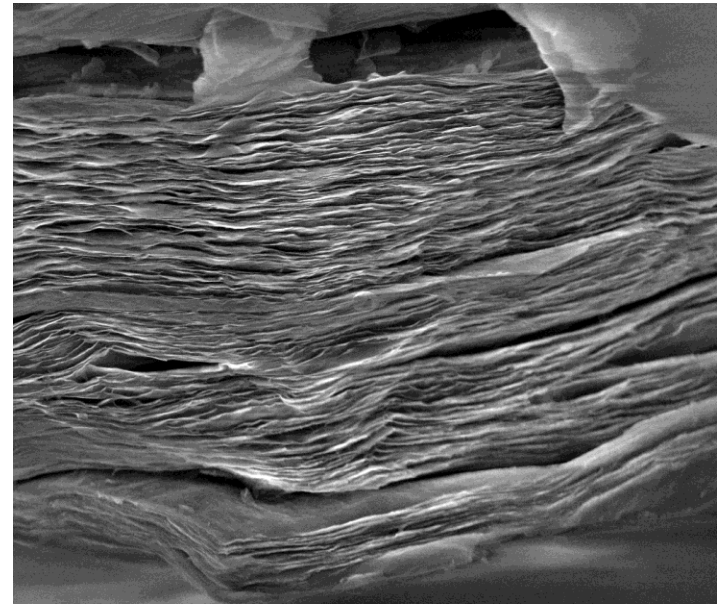
~1 μm thick



~5 μm thick



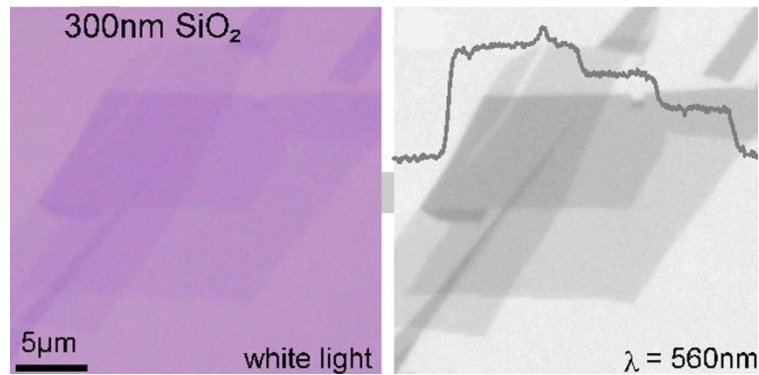
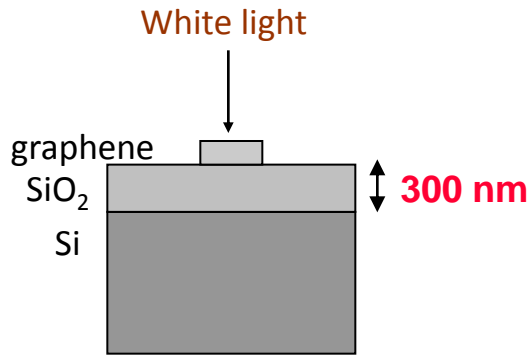
det	HV	mag	WD	pressure	Lens Mode	10 μm
Helix	8.50 kV	8 000 x	3.5 mm	0.378 Torr	Immersion	by D. Dikn



det	HV	mag	WD	pressure	Lens Mode	4 μm
Helix	5.00 kV	25 000 x	4.3 mm	0.378 Torr	Immersion	by D. Dikn

“Visibility” of Graphene

– optical microscopy (hard work but effective)



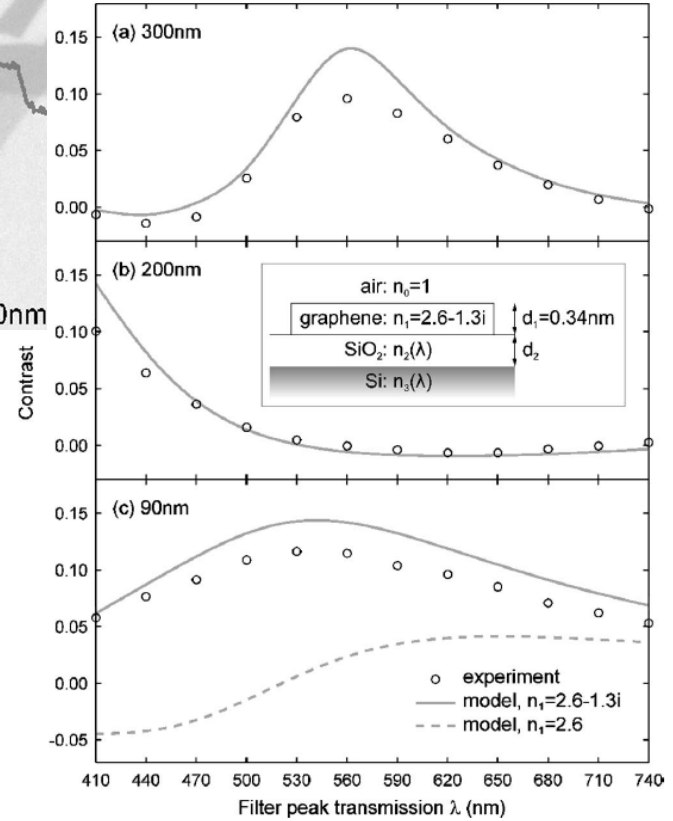
[Blake et al, *APL* 91, 063124(2007)]

Fresnel Theory

$$I(n_1) = \left| \frac{r_1 e^{i(\Phi_1 + \Phi_2)} + r_2 e^{-i(\Phi_1 - \Phi_2)} + r_3 e^{-i(\Phi_1 + \Phi_2)} + r_1 r_2 r_3 e^{i(\Phi_1 - \Phi_2)}}{e^{i(\Phi_1 + \Phi_2)} + r_1 r_2 e^{-i(\Phi_1 - \Phi_2)} + r_1 r_3 e^{-i(\Phi_1 + \Phi_2)} + r_2 r_3 e^{i(\Phi_1 - \Phi_2)}} \right|^2$$

$$r_1 = \frac{n_o - n_1}{n_o + n_1} \quad r_2 = \frac{n_1 - n_2}{n_1 + n_2} \quad r_3 = \frac{n_2 - n_3}{n_2 + n_3} \quad \Phi_1 = 2\pi n_1 \frac{d_1}{\lambda} \quad \Phi_2 = 2\pi n_2 \frac{d_2}{\lambda}$$

$$\text{Contrast} = \frac{I(n_1 = 1) - I(n_1)}{I(n_1 = 1)}$$

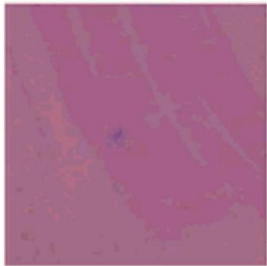


👉 **The contrast can be maximized for any SiO₂ thickness by using narrow band filters!**

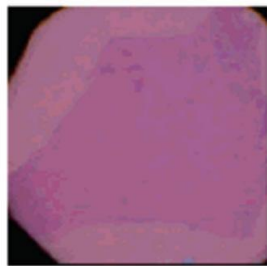
- Electron microscopy SEM, TEM (very low throughput)
- AFM (very low throughput)
- Raman (powerful)

Ανίχνευση του γραφενίου

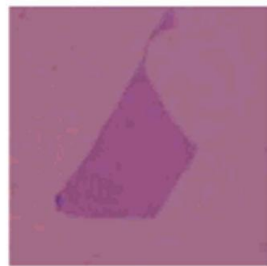
Γραφένιο σε Si/SiO₂



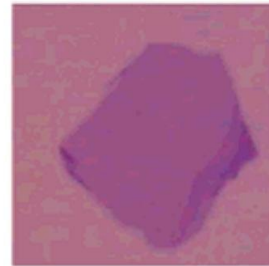
1 layer



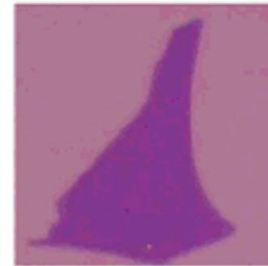
2 layers



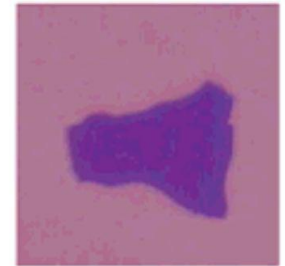
3 layers



4 layers



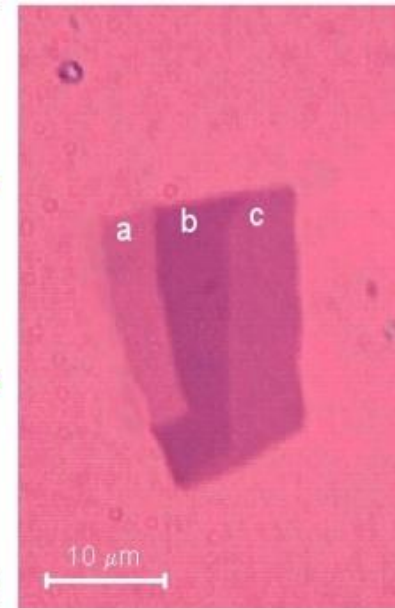
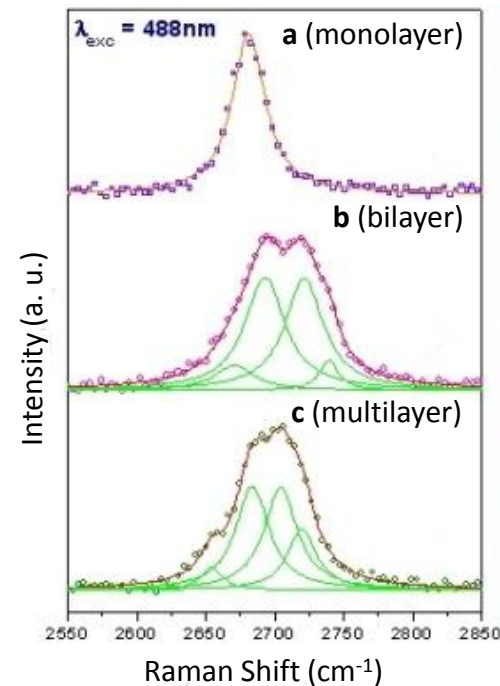
7 layers



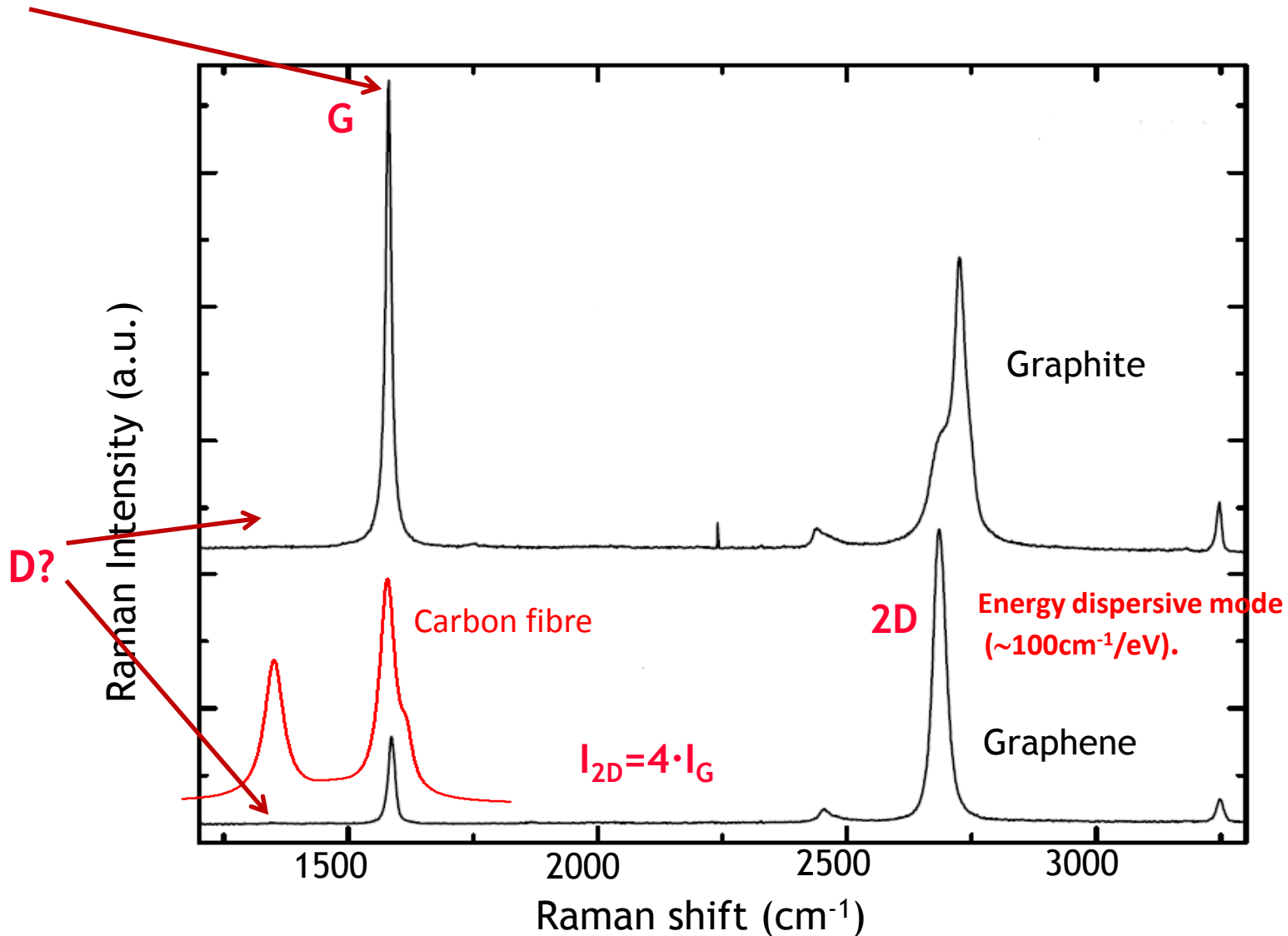
9 layers

RS a unique characterization tool for Nanomaterials

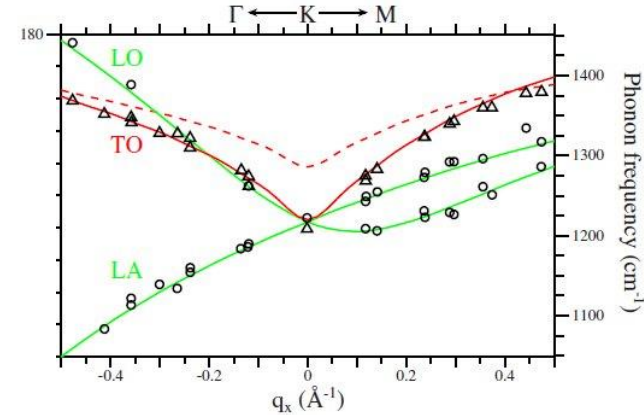
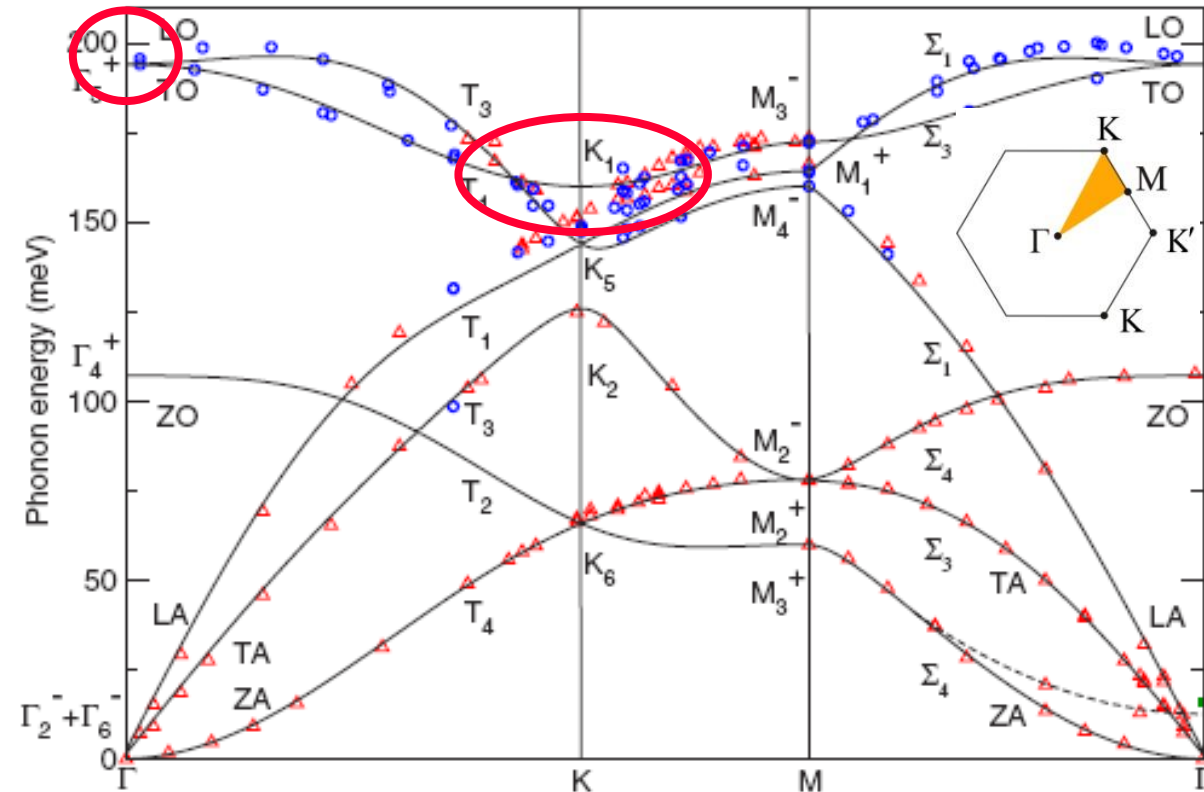
- Non destructive, high throughput, quick and substrate independent
- can identify the number of layers in a sample
- Evolution of Raman lines is directly connected to electronic structure
- can determine the amount of doping and the presence of disorder
- can determine the crystallographic orientation of graphene (polarisation measurements)
- study graphene's edges and ribbons
- quantify anharmonic process and thermal conductivity
- revealed novel physics such as Kohn anomalies and the breakdown of Born-Oppenheimer approximation
- have successfully partnered with first principles calculations to provide microscopic insight and understanding



Typical Raman spectra ($\lambda_{\text{exc}}=514.5 \text{ nm}$)



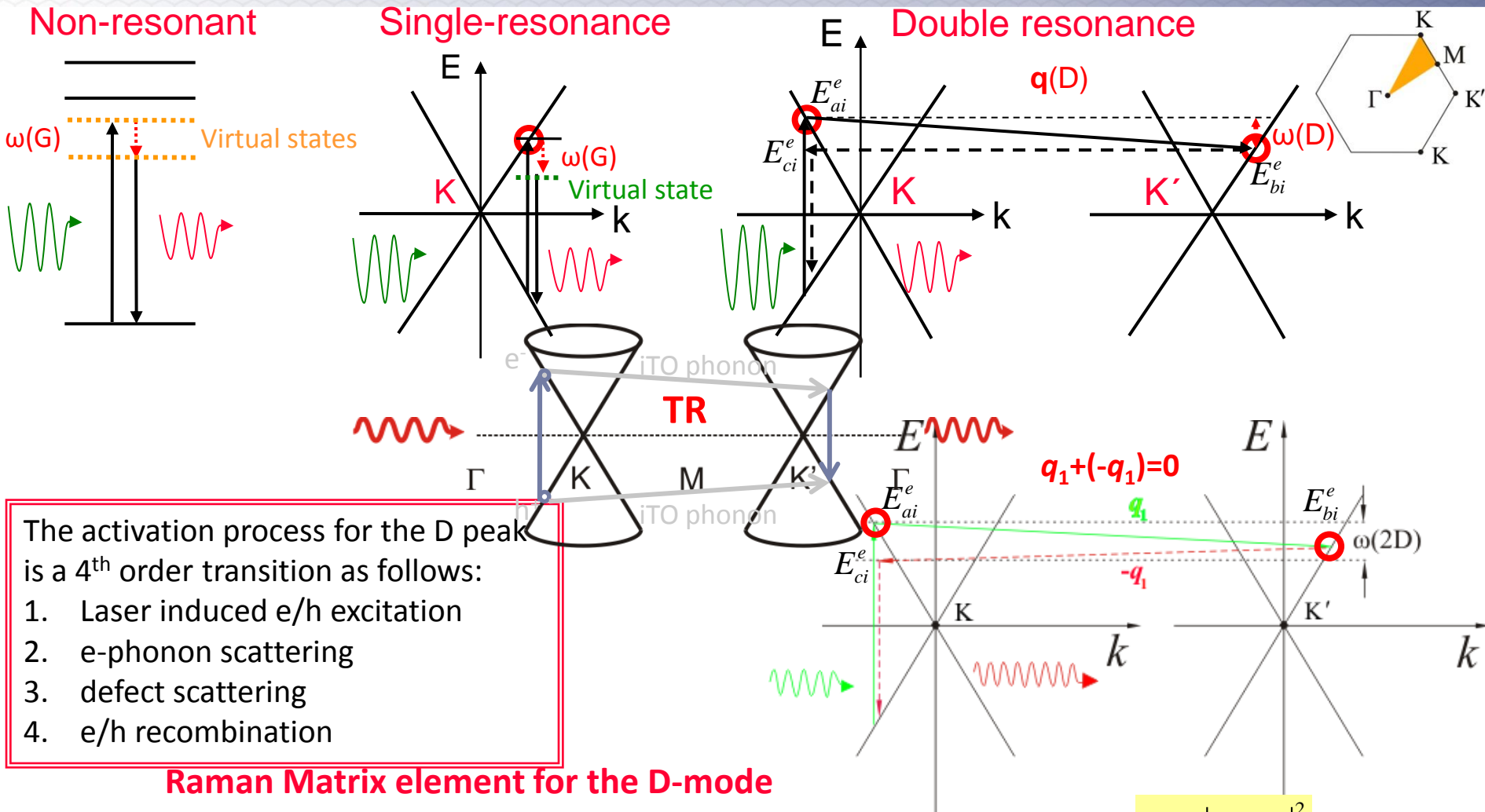
Phonon Dispersion Curves of Graphite



[Grüneis PRB 80, 085423 (2009)]

- The proper inclusion of the electron-electron correlation (through the GW approach) in the calculation of the EPC is crucial to obtain a good agreement with the experiment. GW calculations are in almost perfect agreement with measurements while DFT calculations severely underestimate the phonon slope of the TO branch and thus the EPC at K and overestimate the phonon energy.
- It is thus impossible to derive the phonon branches at Γ and K by force constant approaches based on a finite number of force constants.

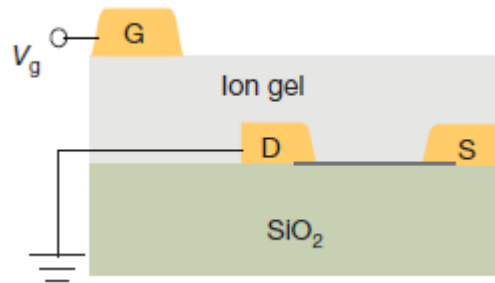
Double Resonance Mechanism for D and 2D modes



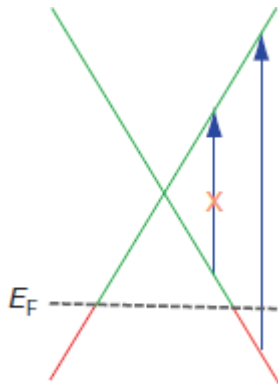
$$K_{2f,10} = \sum_{a,b,c} \frac{M_{fc} M_{cb} M_{ba} M_{ai}}{(E_{laser} - E_{ai}^e - i\gamma)(E_{laser} - \hbar\omega_{ph} - E_{bi}^e - i\gamma)(E_{laser} - \hbar\omega_{ph} - E_{ci}^e - i\gamma)} + \sum_{a,b,c} \frac{M_{fc} M_{cb} M_{ba} M_{ai}}{(E_{laser} - E_{ai}^e - i\gamma)(E_{laser} - E_{bi}^e - i\gamma)(E_{laser} - \hbar\omega_{ph} - E_{ci}^e - i\gamma)}$$

M_{xy} : is the matrix element for the scattering over electr. states x, y.
 E_{xy} : is the energy difference between electronic states x,y.

Quantum Interference between graphene Raman pathways

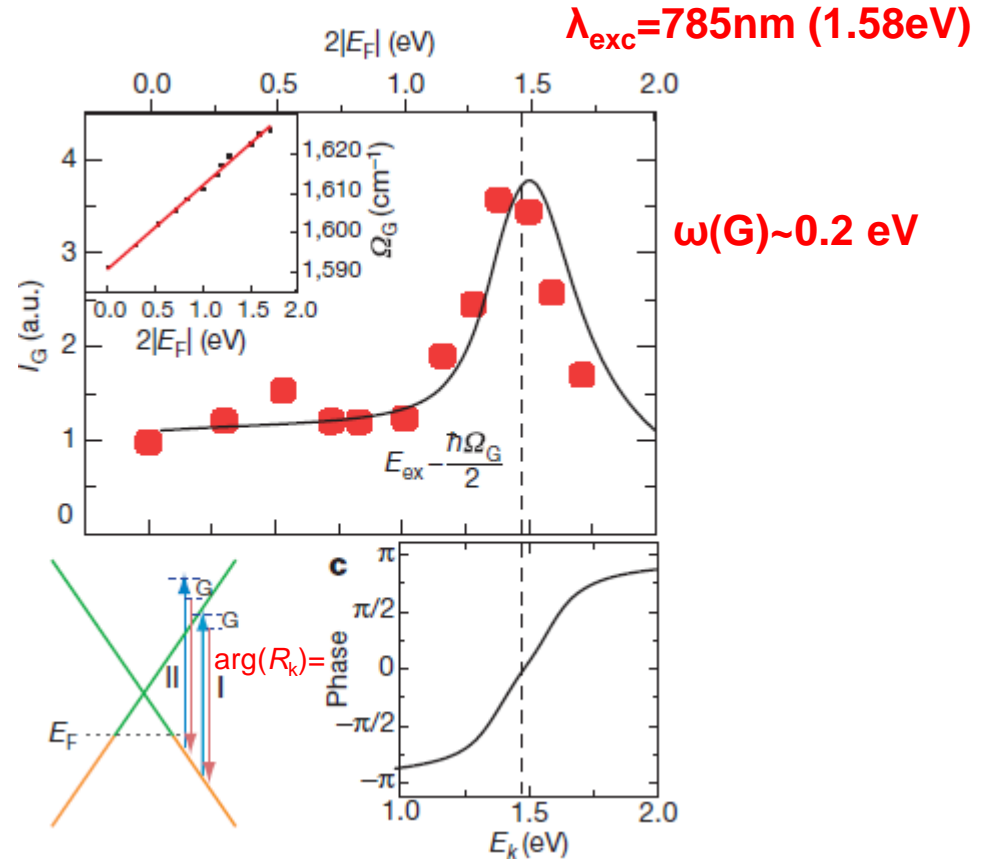


$$2E_F = 1.8 \text{ eV} \rightarrow n = 6 \times 10^{13} \text{ cm}^{-2}$$



$$I(G) = \sum_k C_k R_k$$

$$R_k = \sum_k \frac{1}{(E_{laser} - E_k - i\gamma)(E_{laser} - \hbar\omega_G - E_k - i\gamma)}$$



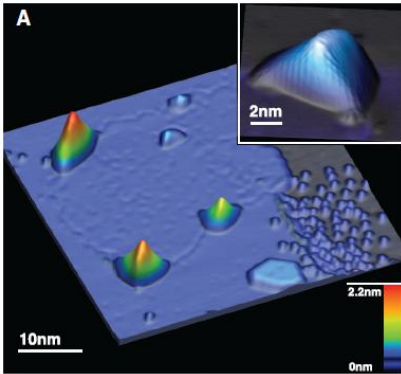
Chi-Fan Chen et al, Nature 471, 617 (2011)

☞ This study reveals quantum interference between different Raman pathways in graphene: when some of the pathways are blocked, the one-phonon Raman intensity does not diminish, as commonly expected, but increases dramatically!!

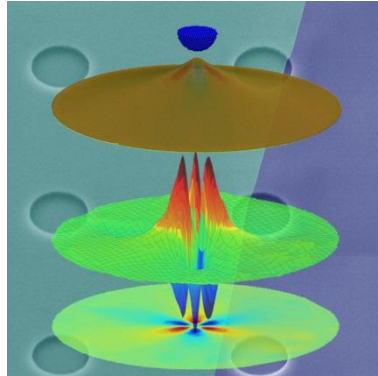
Why strain in graphene?

- Can significantly affect device performance (e.g. to improve carrier mobility as in the s-silicon microelectronic technology).
- “Strain engineering” electronics by patterning not graphene, but the substrate on which it rests.

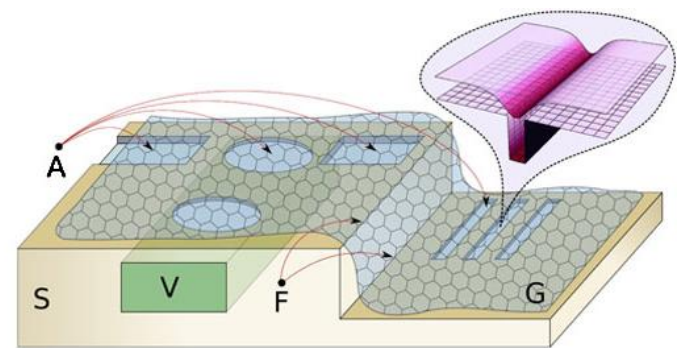
Graphene nanobubbles



Graphene drumheads



Strain engineering



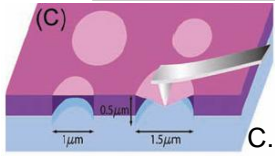
Levy et al., *Science* **329**, 544 (2010); Klimov et al. *Science* **336**, 1557 (2012)

[V. M. Pereira, *PRL* 103, 046801 (2009)]

- Certain configurations of strain induce strong gauge fields that effectively act as a uniform magnetic field exceeding 300 T.
- Strained superlattices can be used to open significant energy gaps in graphene’s electronic spectrum [F. Guinea et al, *Nature Physics* (2010)].
- Revealing the physics of high strains in graphene (high deformation/breaking of C-C bonds, trace the interatomic potentials etc).
- To quantify the amount of uniaxial or biaxial strain, providing a fundamental tool for graphene-based nanoelectronics and nano/microelectronic mechanical systems.
- Stress/ strain sensing, stress transfer efficiency in graphene based nanocomposites

Thus, the precise determination and monitoring of stress and/or strain is a key requirement for many graphene applications

Efforts to apply strain in graphene

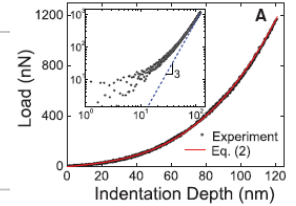


AFM nanoindentation

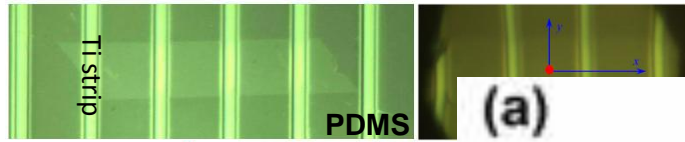
C. Lee, *et al.*, *Science* **321**, 385 (2008)

$$F = \sigma_0^{2D} (\pi a) \left(\frac{\delta}{a}\right) + E^{2D} (q^3 a) \left(\frac{\delta}{a}\right)^3$$

E = 1.0 TPa, Fracture strength = 130 GPa



Bending of the substrate (PDMS) & Raman



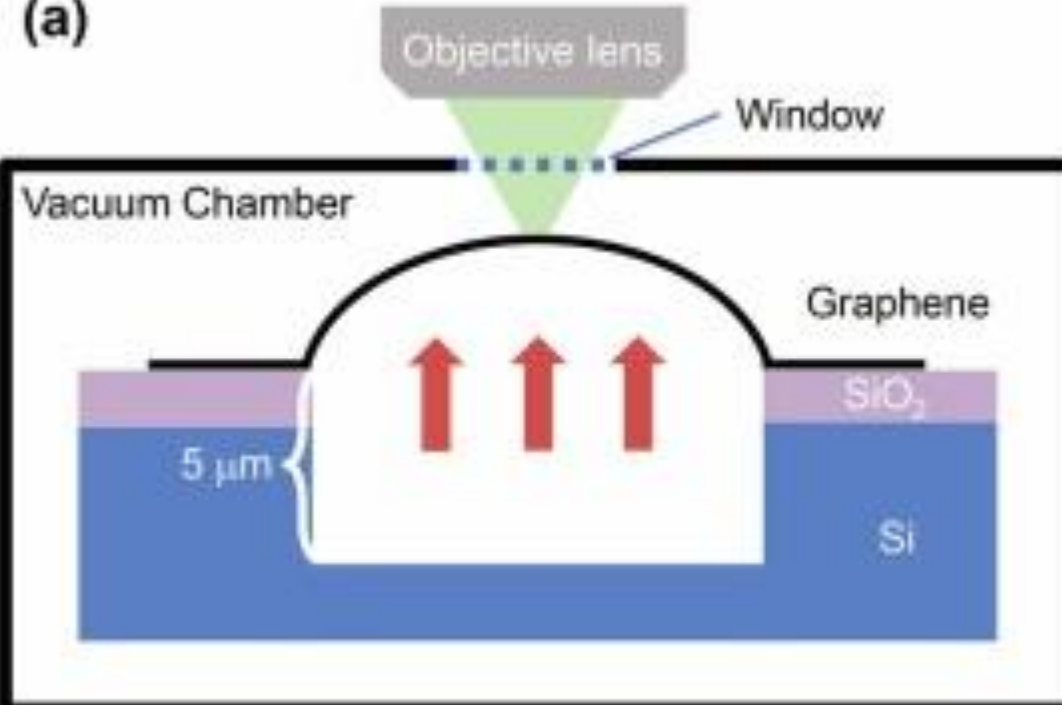
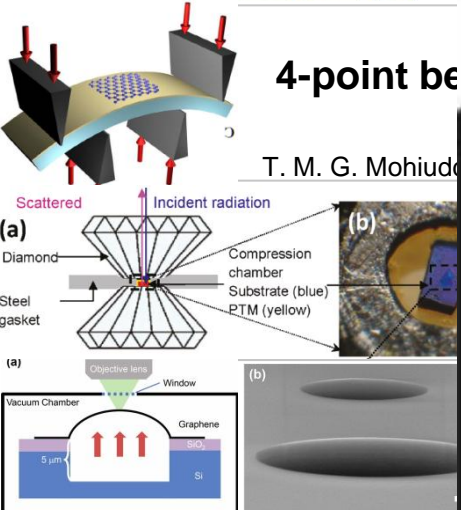
$$\frac{\partial \omega_{G^+}}{\partial \varepsilon} = -12.5 \text{ cm}^{-1}/\%$$

$$\frac{\partial \omega_{G^-}}{\partial \varepsilon} = -5.6 \text{ cm}^{-1}/\%$$

$$\frac{\partial \omega_{2D}}{\partial \varepsilon} = -21.0 \text{ cm}^{-1}/\%$$

4-point bending

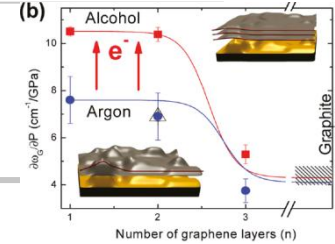
T. M. G. Mohiud



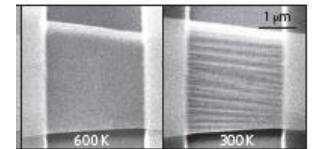
$$\frac{\partial \omega_{G^+}}{\partial \varepsilon} \sim -10.8 \text{ cm}^{-1}/\%$$

$$\frac{\partial \omega_{G^-}}{\partial \varepsilon} \sim -31.7 \text{ cm}^{-1}/\%$$

$$\frac{\partial \omega_{2D}}{\partial \varepsilon} \sim -64 \text{ cm}^{-1}/\%$$



= 2.4 TPa!!!

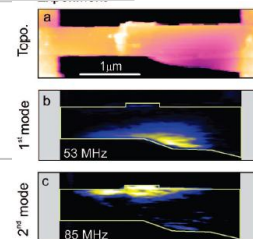
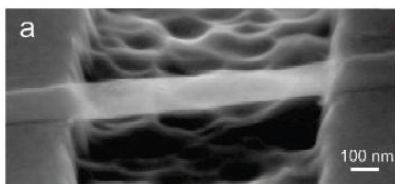
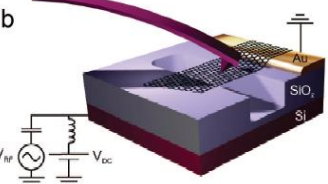


W. Bao, *et al.*, *Nat Nano* **4**, 562 (2009)

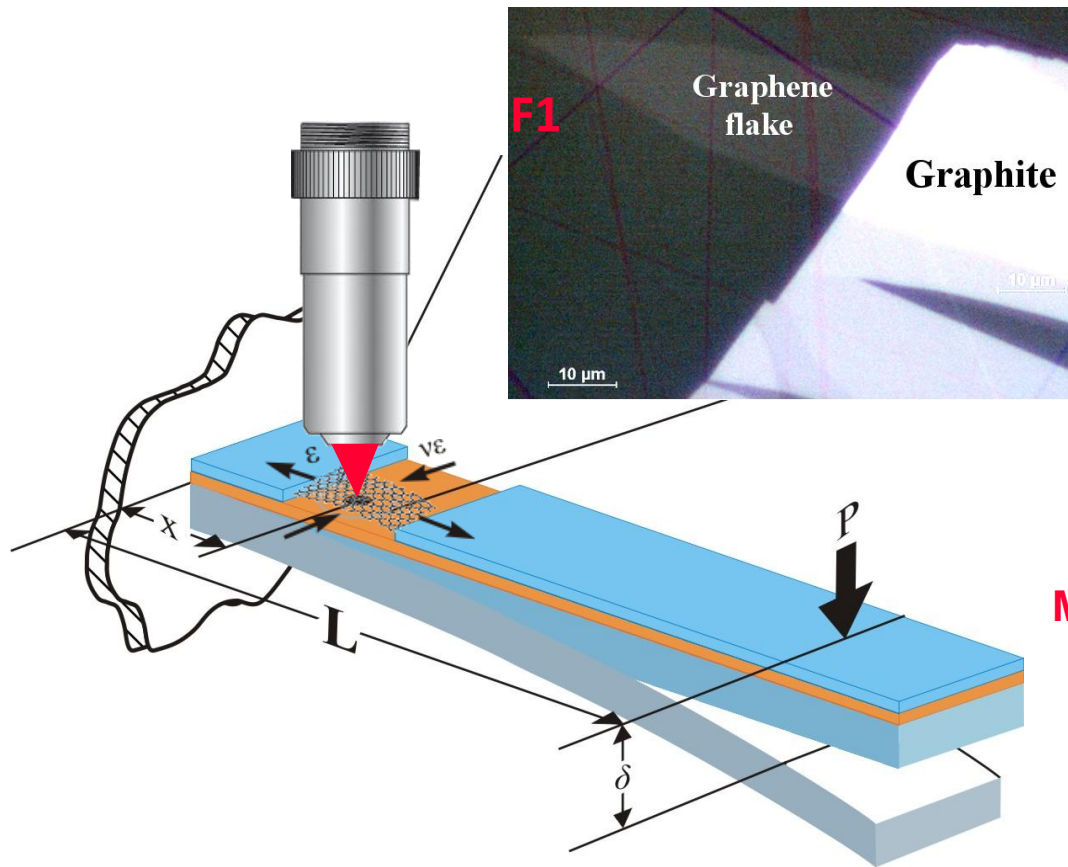
Imaging of a vibrating graphene beam using SPM

Graphene resonator with local buckling

Garcia-Sanchez, *et al.*, *Nano Lett.*, **8**, 1399 (2008)



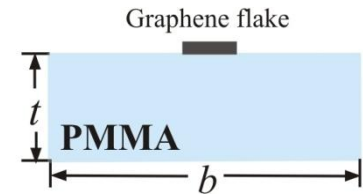
Experimental set-up for application of uniaxial strain



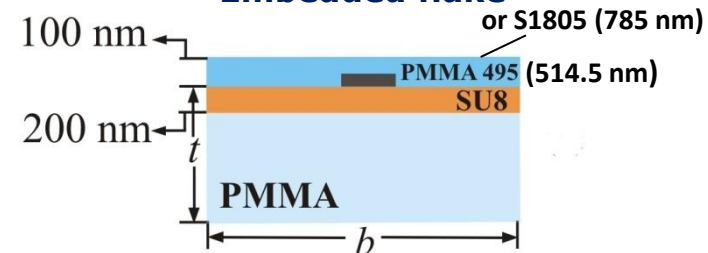
Materials & Geometry

- SU8 photo resist epoxy-based polymer
- PMMA beam substrate (2.9x12.0x70) mm³
- $x = 10.44$ mm
- $L = 70$ mm

Bare (just attached) flake



Embedded flake



Mechanical strain at the top of the beam

$$\varepsilon(x) = \frac{3t\delta}{2L^2} \left(1 - \frac{x}{L} \right)$$

δ : deflection of the beam neutral axis

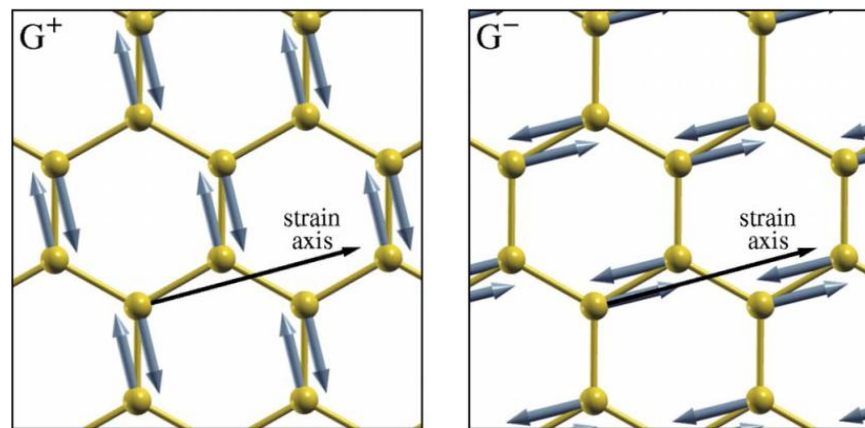
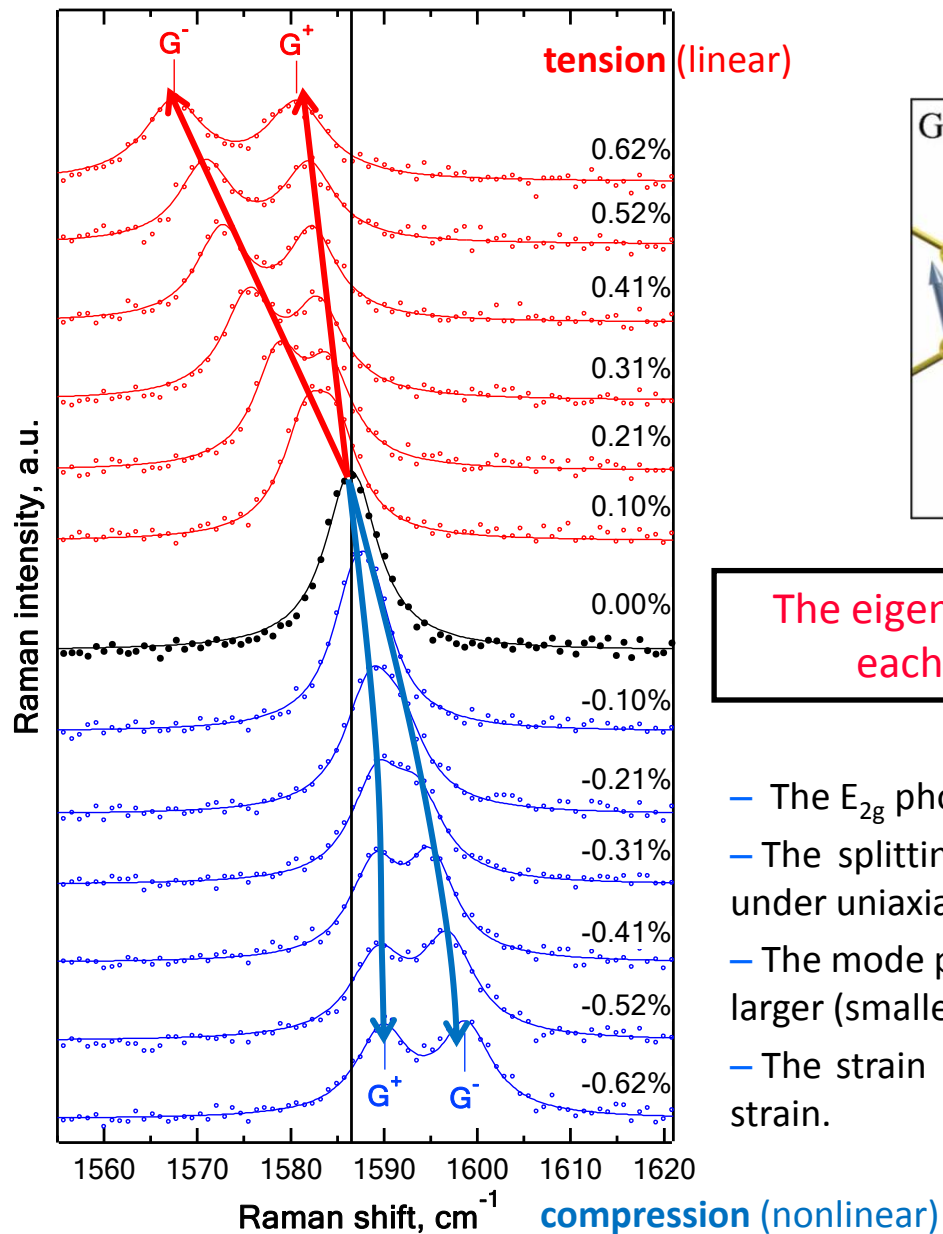
L : span of the beam

t : beam thickness

The method is valid for:

- $L \gg 10\delta_{\max}$
- $-1.5\% < \varepsilon < 1.5\%$

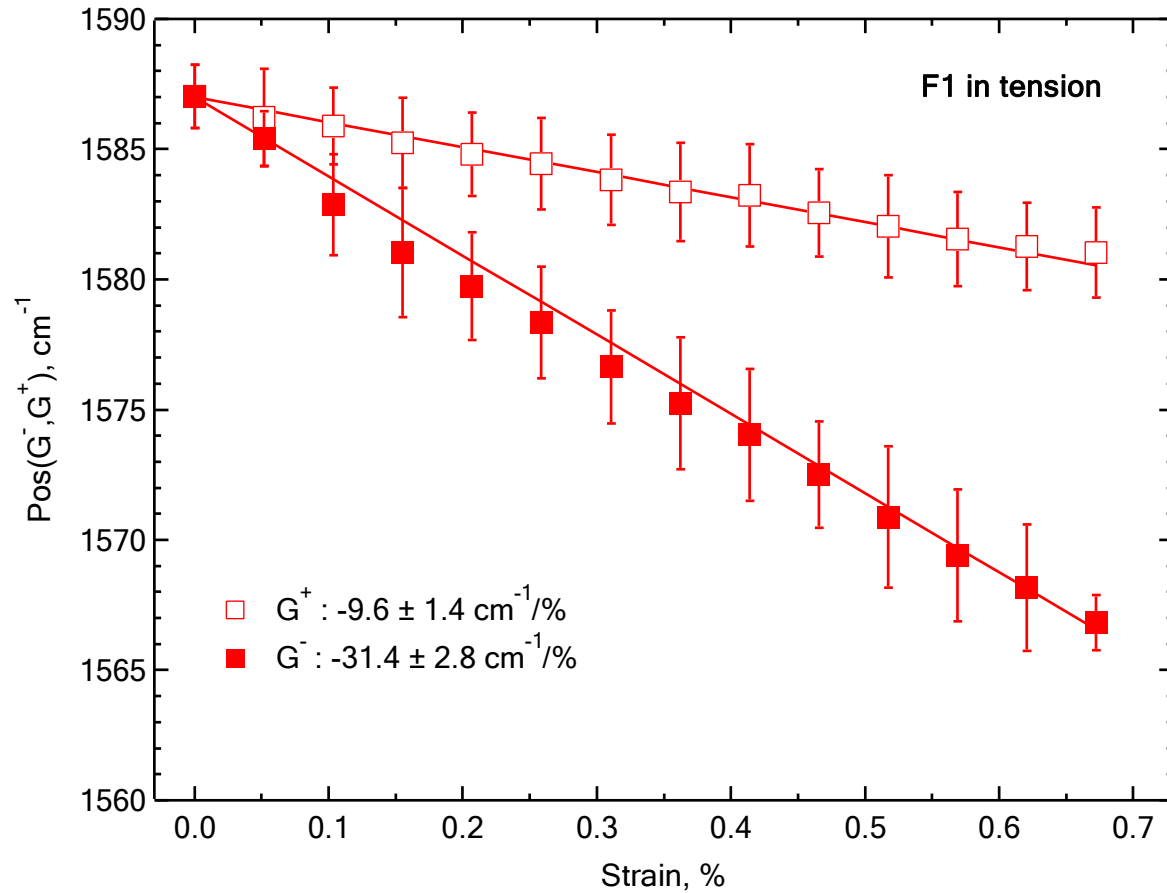
SLG - G mode vs strain ($\lambda_{exc}=785\text{ nm}$)



The eigenvectors of G^+ and G^- modes are perpendicular to each other with G^- polarized along the strain axis

- The E_{2g} phonon at $\sim 1580\text{cm}^{-1}$ is doubly degenerate.
- The splitting is caused by lifting up the mode degeneracy is lifted under uniaxial strain and the E_{2g} splits into distinct components.
- The mode parallel (perpendicular) to the strain direction undergoes a larger (smaller) shift and is therefore entitled G^- (G^+).
- The strain rate of the G^- and G^+ is independent on the direction of strain.

G^+ , G^- sensitivity rates for embedded graphene ($\lambda_{exc}=785nm$)



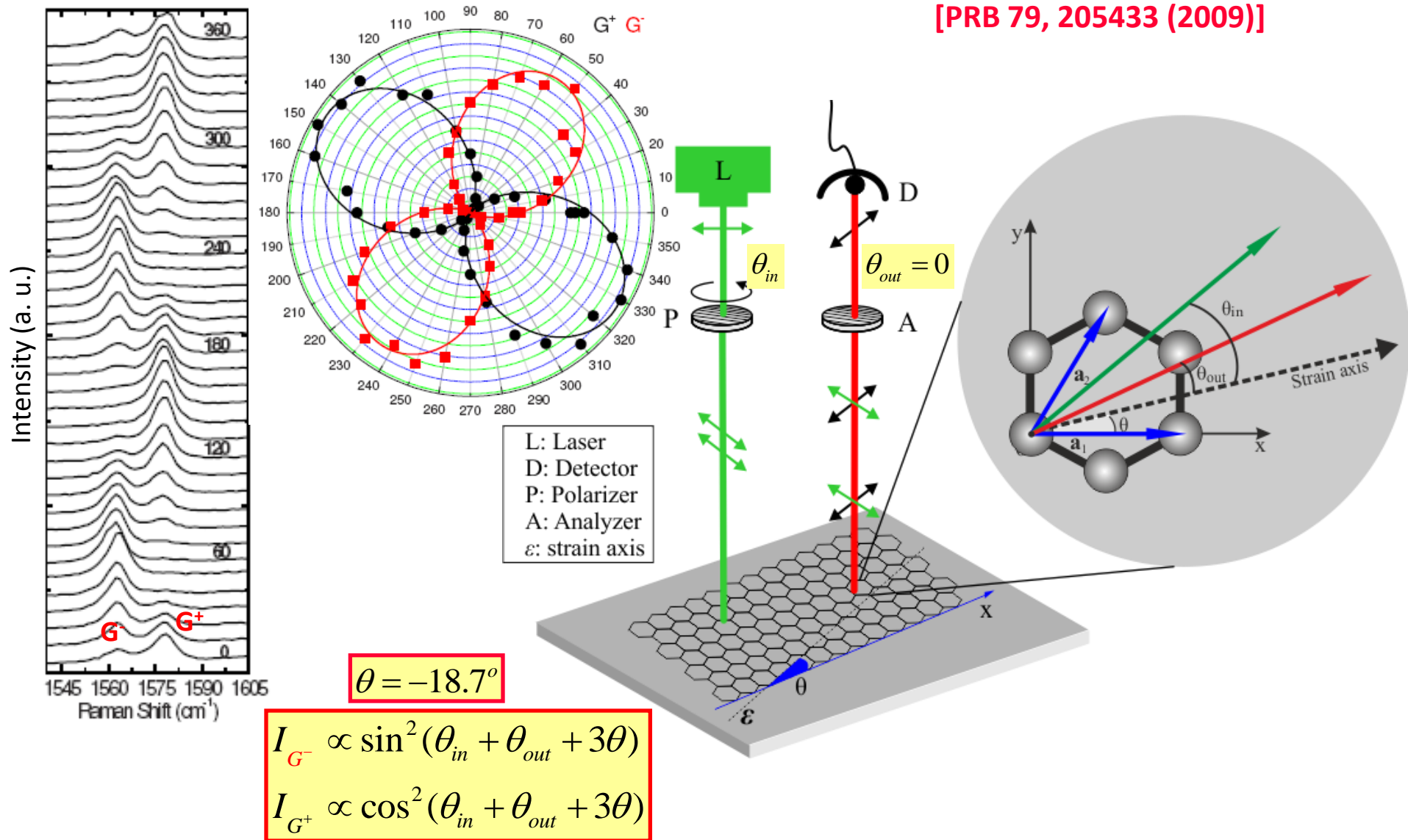
$$\partial\omega_{G^-} / \partial\varepsilon = -31.4 \text{ cm}^{-1}/\%$$

$$\partial\omega_{G^+} / \partial\varepsilon = -9.6 \text{ cm}^{-1}/\%$$

[ACS-NANO 4, 3131 (2010)]

Determination of graphene's crystallographic orientation

[PRB 79, 205433 (2009)]



Polarized Raman Spectroscopy: A purely optical method for the determination of the crystallographic orientation of graphene.

Phonon deformation potentials of graphene – G band

For graphene the vibrational decomposition at $\mathbf{q}=\mathbf{0}$ yields

$$\Gamma_{vib}^{Graphene} = A_{2u} + E_{1u} + B_{2g} + E_{2g}$$

$$(D_{6h}^1) \quad (P6/mmm)$$

$$\sum_{\beta} K_{\alpha\beta} u_{\beta} = \bar{m} \omega^2 u_{\alpha} \quad (1)$$

S. Ganesan *al.*, *Annals in Physics* 56, 556 (1970)

where ω is the phonon frequency in the presence of strain, m is the reduced mass of the two carbon atoms in the unit cell, u_i is the i -th component of the relative displacement of the two carbon atoms and $K_{\alpha\beta}$ are the elements of the force constant of the E_{2g} modes.



$$K_{\alpha\beta} = K_{\alpha\beta}^{(0)} + \sum_{lm} \frac{\partial K_{\alpha\beta}}{\partial \varepsilon_{lm}} \varepsilon_{lm}$$

is the strain tensor

(2)

$K_{\alpha\beta lm}$ are the elements of a 4th order tensor (symmetric in its first and second pair of indices). Represents the change in the spring constant of the E_{2g} mode due to the applied strain ε_{lm} . **PHONON DEFORMATION POTENTIALS.**

$$K_{\alpha\beta}^{(0)} = \bar{m} \omega_0^2 \delta_{\alpha\beta}$$

is the spring constant in the absence of strain) and ω_0 the Raman frequency of the unstrained crystal

(1), (2) \Rightarrow

$$\sum_{\beta} K_{\alpha\beta}^{(0)} u_{\beta} + \sum_{\beta lm} \frac{\partial K_{\alpha\beta}}{\partial \varepsilon_{lm}} \varepsilon_{lm} u_{\beta} = \bar{m} \omega^2 u_{\alpha}$$

$$\sum_{\beta lm} \frac{1}{\bar{m}} K_{\alpha\beta lm} \varepsilon_{lm} u_{\beta} = (\omega^2 - \omega_0^2) u_{\alpha}$$

Phonon deformation potentials of graphene – E_{2g} or G band

$$\sum_{\beta lm} \tilde{K}_{\alpha\beta lm} \varepsilon_{lm} u_{\beta} = (\omega^2 - \omega_0^2) u_{\alpha} \quad (3)$$

$\tilde{K}_{\alpha\beta lm} = \frac{1}{\bar{m}} K_{\alpha\beta lm}$ has only 3 nonzero components due to the hexagonal symmetry of graphene

$$\tilde{K}_{1122} = B$$

$$\tilde{K}_{1111} = \tilde{K}_{2222} = A$$

$$\tilde{K}_{1212} = \frac{1}{2}(A - B)$$

From the dynamical equations (3) a secular equation can be obtained

$$\begin{vmatrix} \tilde{K}_{1111}\varepsilon_{11} + \tilde{K}_{1122}\varepsilon_{22} - \lambda & \tilde{K}_{1212}\varepsilon_{12} + \tilde{K}_{1221}\varepsilon_{21} \\ \tilde{K}_{2112}\varepsilon_{12} + \tilde{K}_{2121}\varepsilon_{21} & \tilde{K}_{2211}\varepsilon_{11} + \tilde{K}_{2222}\varepsilon_{22} - \lambda \end{vmatrix} = 0$$

or equivalently

$$\begin{vmatrix} A\varepsilon_{xx} + B\varepsilon_{yy} - \lambda & (A - B)\varepsilon_{xy} \\ (A - B)\varepsilon_{xy} & B\varepsilon_{xx} + A\varepsilon_{yy} - \lambda \end{vmatrix} = 0$$

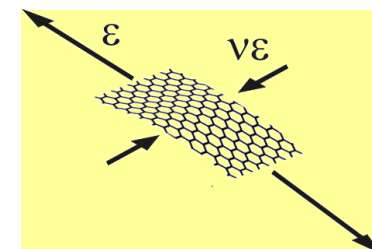
where

$$\lambda = (\omega^2 - \omega_0^2) = 2\omega_0\Delta\omega$$

Phonon deformation potentials of graphene – G band

The secular equation for the E_{2g} or G mode of graphene under strain is given by:

$$\begin{vmatrix} A\varepsilon_{xx} + B\varepsilon_{yy} - \lambda & (A-B)\varepsilon_{xy} \\ (A-B)\varepsilon_{xy} & B\varepsilon_{xx} + A\varepsilon_{yy} - \lambda \end{vmatrix} = 0$$



$$\begin{aligned} \varepsilon_{xx} &= \varepsilon, \\ \varepsilon_{yy} &= -\nu\varepsilon, \\ \varepsilon_{xy} &= 0 \end{aligned}$$

Solving analytically and ignoring terms higher than ε^2 the frequency values for uniaxial strain in x direction is given by:

$$\frac{\partial\omega_{G^+}}{\partial\varepsilon} = \frac{\omega_{G^+} - \omega_o}{\varepsilon} = \frac{B - \nu A}{2\omega_o}$$

$$\frac{\partial\omega_{G^-}}{\partial\varepsilon} = \frac{\omega_{G^-} - \omega_o}{\varepsilon} = \frac{A - \nu B}{2\omega_o}$$

$$A = \frac{2\omega_o \left(\frac{\partial\omega_{G^-}}{\partial\varepsilon} + \nu \frac{\partial\omega_{G^+}}{\partial\varepsilon} \right)}{1 - \nu^2}$$

$$B = 2\omega_o \frac{\partial\omega_{G^+}}{\partial\varepsilon} + \nu A$$

using $\nu=0.33$ (Matrix) AND $\frac{\partial\omega_{G^-}}{\partial\varepsilon} = -31.4 \text{ cm}^{-1}/\%$
 $\frac{\partial\omega_{G^+}}{\partial\varepsilon} = -9.6 \text{ cm}^{-1}/\%$



Phonon deformation potential coefficients:

$$A = -1.23 \times 10^7 \text{ cm}^{-2}$$

$$B = -7.16 \times 10^6 \text{ cm}^{-2}$$

Extracted shift rates for graphene in air ($\lambda=785$ nm)

$$\frac{\partial\omega_{G^+}}{\partial\varepsilon} = \frac{B - \nu A}{2\omega_o}$$

$$\frac{\partial\omega_{G^-}}{\partial\varepsilon} = \frac{A - \nu B}{2\omega_o}$$

$$A = -1.23 \times 10^7 \text{ cm}^{-2}$$

$$B = -7.16 \times 10^6 \text{ cm}^{-2}$$

$$\nu = 0.13 \text{ (for graphene)}$$



Strain rates for **graphene in air**

$$\frac{\partial\omega_{G^-}}{\partial\varepsilon} = -36.0 \text{ cm}^{-1}/\%$$

$$\frac{\partial\omega_{G^+}}{\partial\varepsilon} = -17.5 \text{ cm}^{-1}/\%$$

First Principles calculations:

$$\frac{\partial\omega_{G^-}}{\partial\varepsilon} = -34.0 \text{ cm}^{-1}/\%$$

$$\frac{\partial\omega_{G^+}}{\partial\varepsilon} = -14.5 \text{ cm}^{-1}/\%$$

[ACS-NANO 4, 3131 (2010)]

[PRB 80, 205410 (2009)]

Obtained values for important thermomechanical parameters:

Grüneisen parameter

$$\gamma_G = -\frac{1}{\omega_G} \frac{\partial\omega_G^h}{\partial\varepsilon_h} = -\frac{A+B}{4\omega_G^2} = 2.07$$

Shear deformation potential

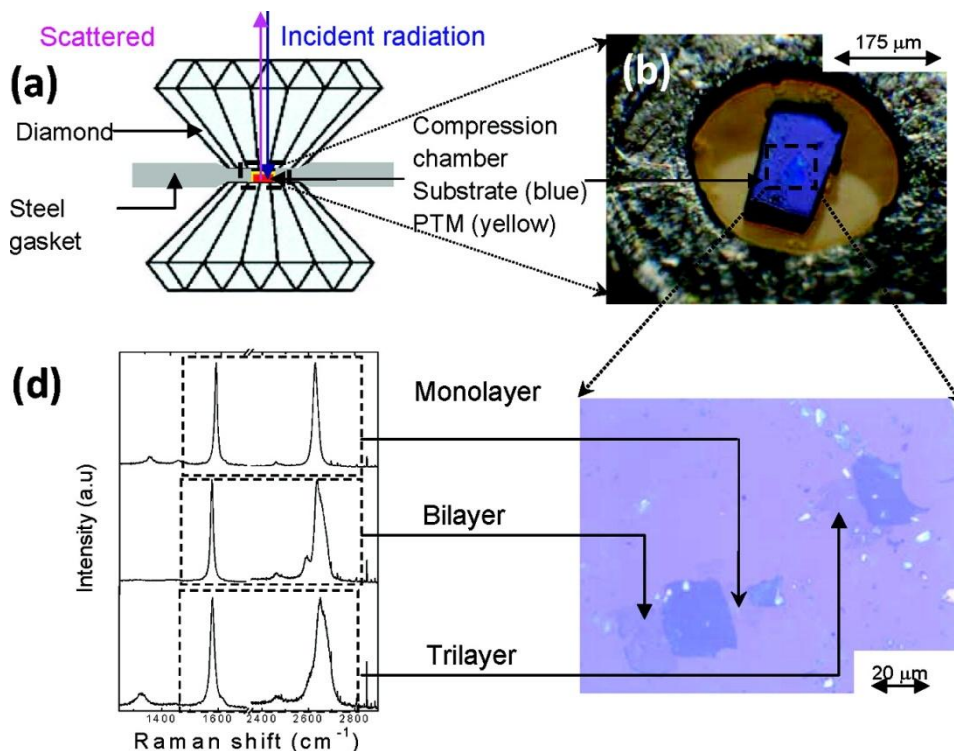
$$\beta_G = -\frac{1}{\omega_G} \frac{\partial\omega_G^s}{\partial\varepsilon_s} = \frac{A-B}{2\omega_G^2} = 0.97$$

Biaxial or hydrostatic pressure on graphene: an estimation

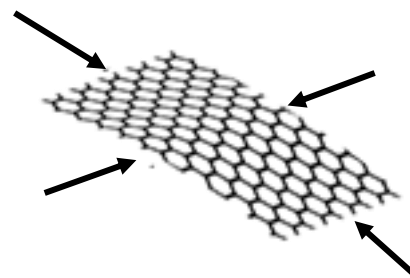
For biaxial stress in graphene, the resulting strains are given by

$$\varepsilon_{xx} = \varepsilon_{yy} = \varepsilon = (S_{11} + S_{12})\sigma = 0.82 \times 10^{-3} \text{ GPa}^{-1} \sigma (\text{GPa})$$

From the analysis earlier we obtain:



Nicolle et al, Nano Letters 11, 3564 (2011)

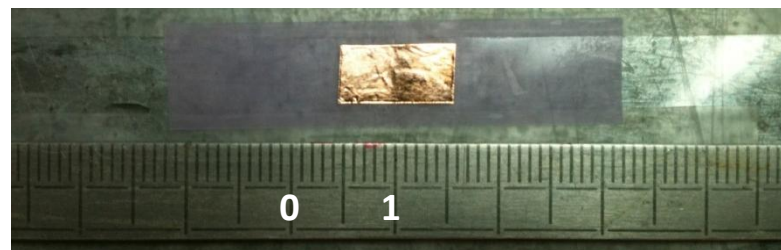
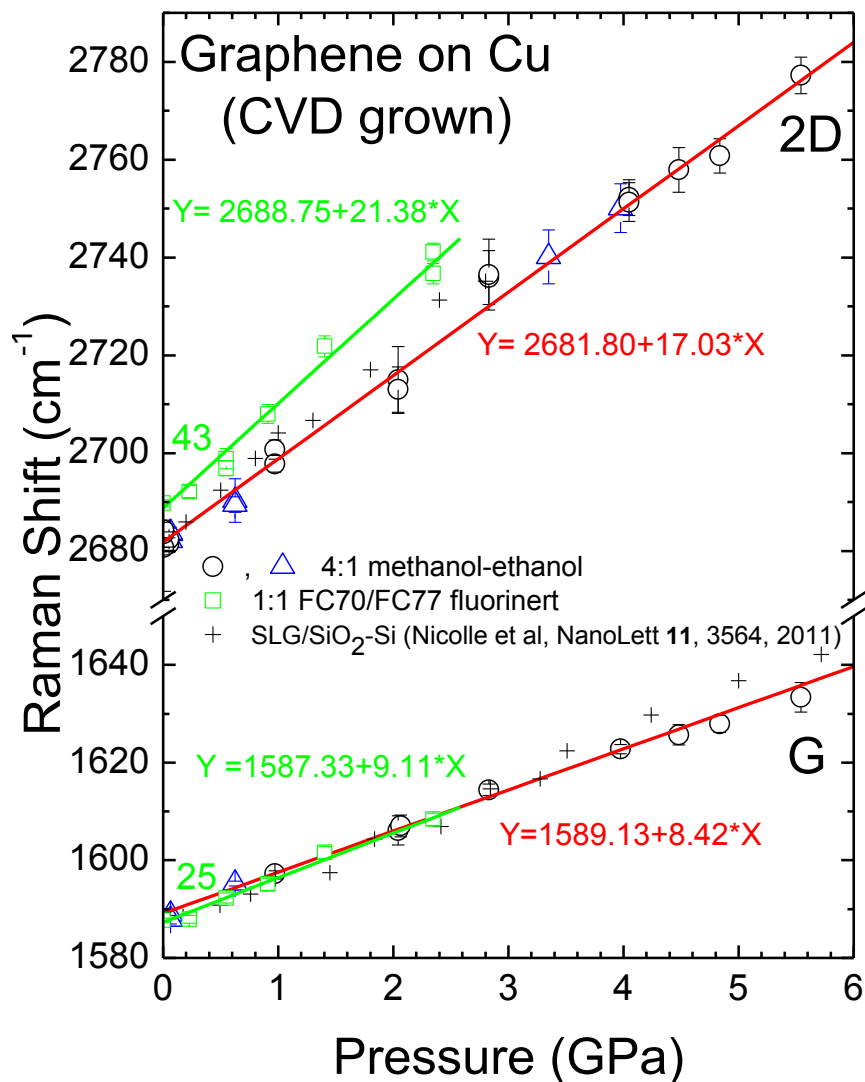


$$\frac{\partial \omega_G}{\partial \varepsilon} = \frac{(A+B)}{2\omega_0} \approx 61.3 \text{ cm}^{-1} / \%$$

$$\frac{\partial \omega_G}{\partial \sigma} = \frac{\partial \omega_G}{\partial \varepsilon} \cdot \frac{\partial \varepsilon}{\partial \sigma} = 5.0 \text{ cm}^{-1} / \text{GPa}$$

- ☑ The extracted values are both in nice agreement with the experiments. High pressure Raman data shows pressure slopes ranging between 5-10 cm⁻¹/GPa depending on the sample and the pressure transmitting medium.

Preliminary high pressure data on supported CVD grown SLG

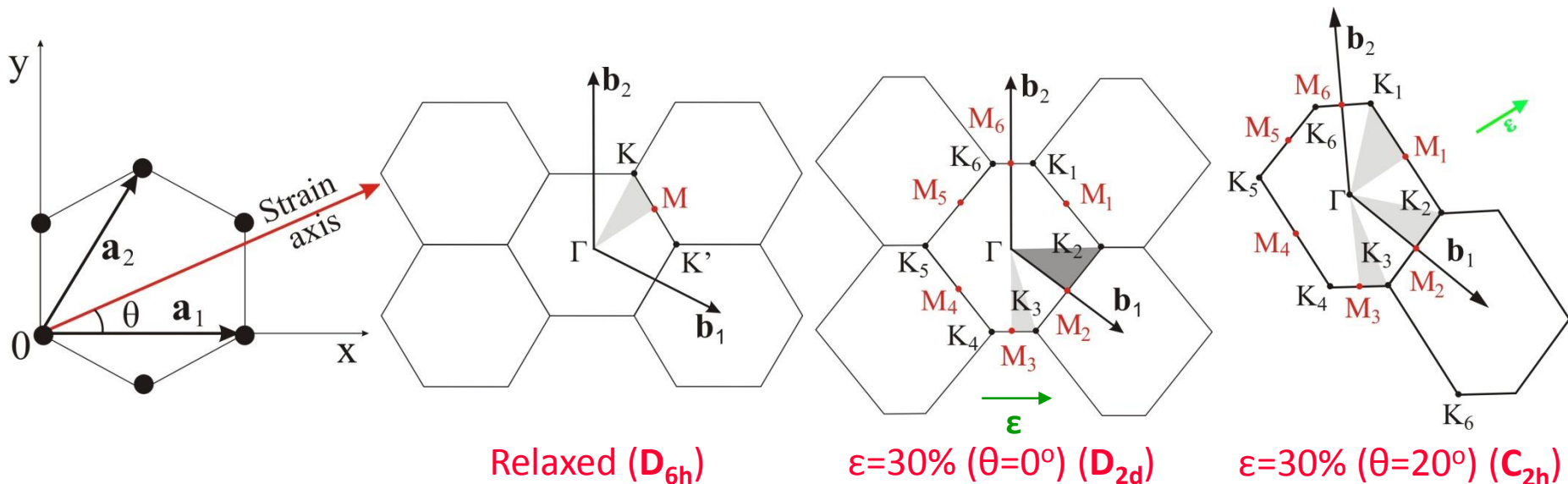


- Similar pressure rates of both the G and 2D Raman bands for two different pressure transmitting media (polar and non-polar).
- Pressure-induced charge transfer effects do not contribute considerably in the pressure response of graphene.
- In biaxial experiments, the adhesion properties of graphene with the substrates seems to play an important role and should be further investigated.

$$\frac{\partial \omega_G}{\partial P} \sim 9 \text{ cm}^{-1}/\%$$

$$\frac{\partial \omega_{2D}}{\partial P} \sim 19 \text{ cm}^{-1}/\%$$

First principles calculations on graphene - Basics



– Calculations were performed with the QUANTUM ESPRESSO (plane wave basis, RRKJ pseudopotentials and GGA). The dynamical matrices were calculated using the implemented linear response theory

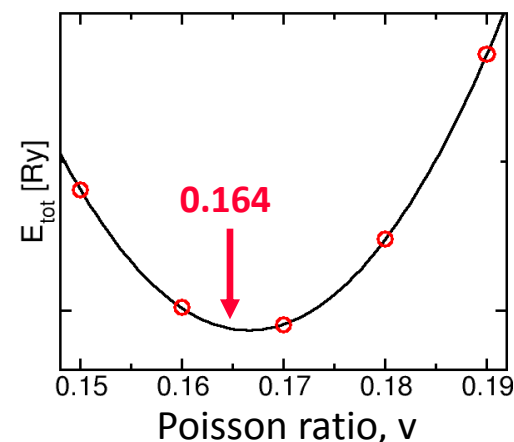
– Tensile strain along the x- axis (zig-zag direction) can be expressed by the strain tensor

$$\tilde{\epsilon} = \begin{pmatrix} \epsilon & 0 \\ 0 & -\nu\epsilon \end{pmatrix}$$

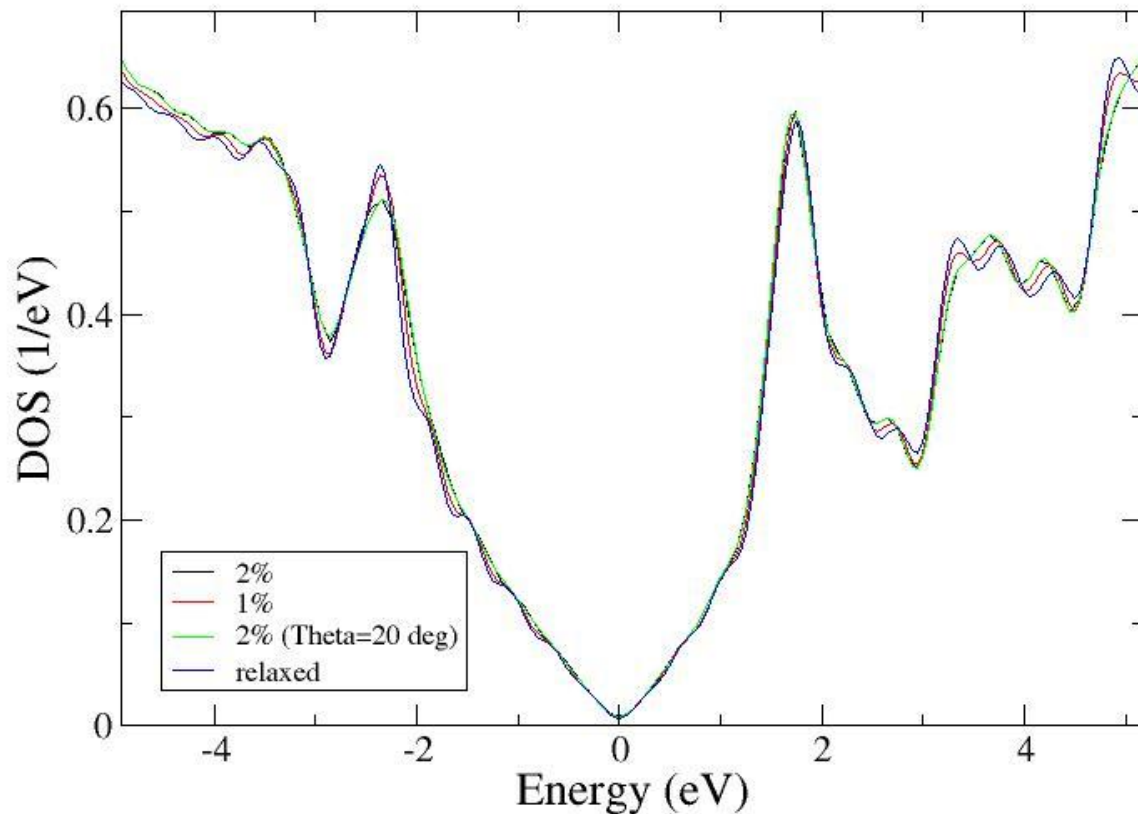
– The strain tensor in arbitrary direction relative to the x0y coordinate system is

$$\tilde{\epsilon} = \mathbf{R}^{-1} \tilde{\epsilon} \mathbf{R} = \begin{pmatrix} \cos^2 \theta - \nu \sin^2 \theta & (1 + \nu) \cos \theta \sin \theta \\ (1 + \nu) \cos \theta \sin \theta & \sin^2 \theta - \nu \cos^2 \theta \end{pmatrix}$$

– After applying a finite amount of strain we relax the coordinates of the basis atoms until the forces are below 0.001Ry/a.u. and minimize the total energy with respect to ν

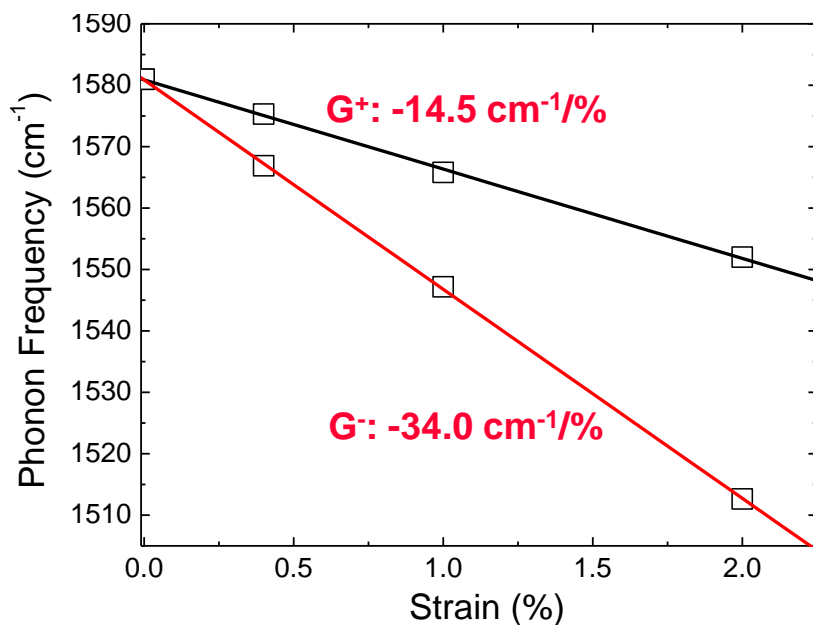
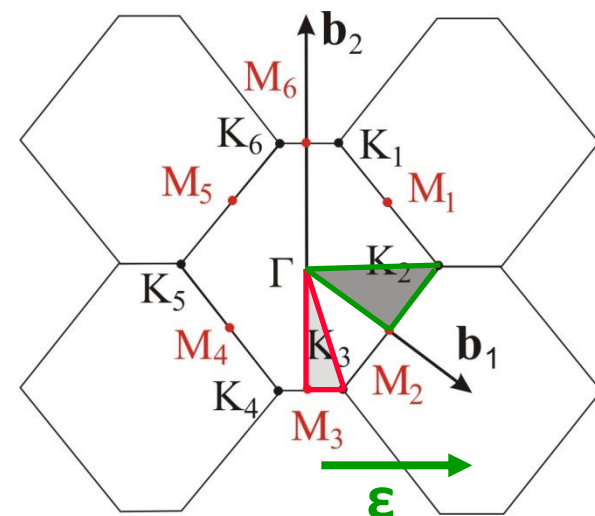
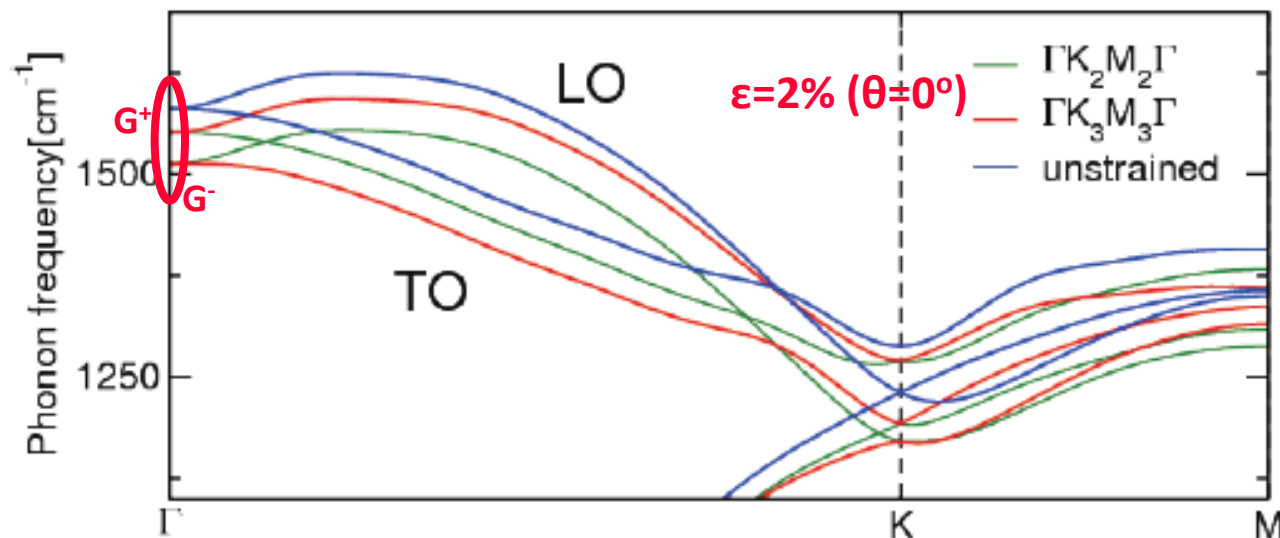


Electronic DOS of relaxed and uniaxially strained graphene



– Graphene is gapless up to $\epsilon=2\%$

G- band for relaxed and strained graphene



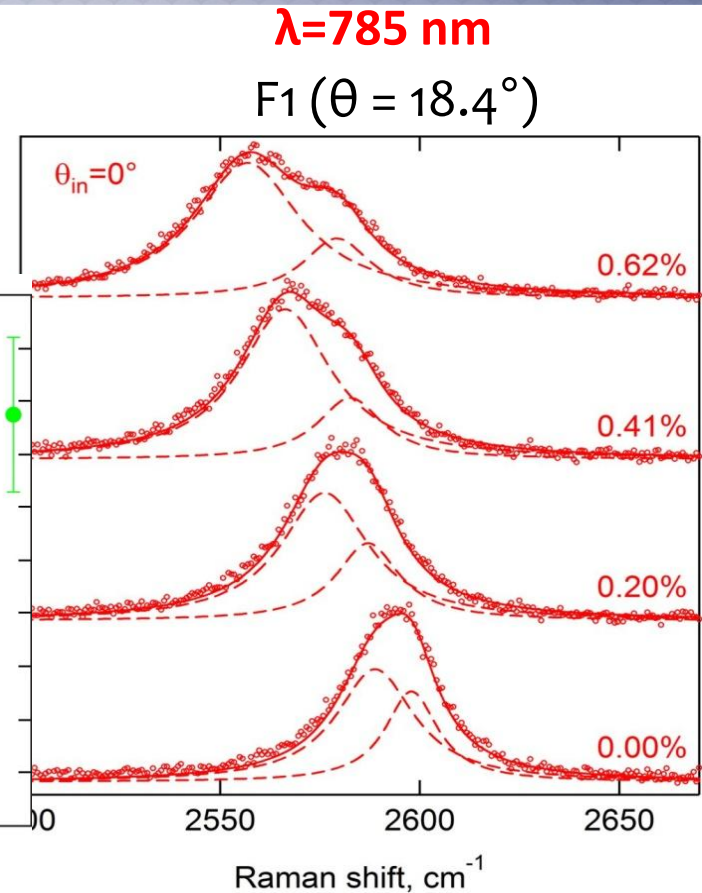
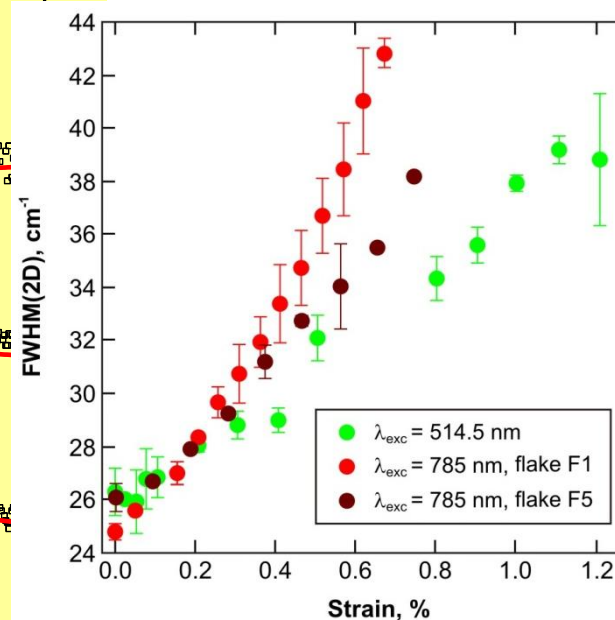
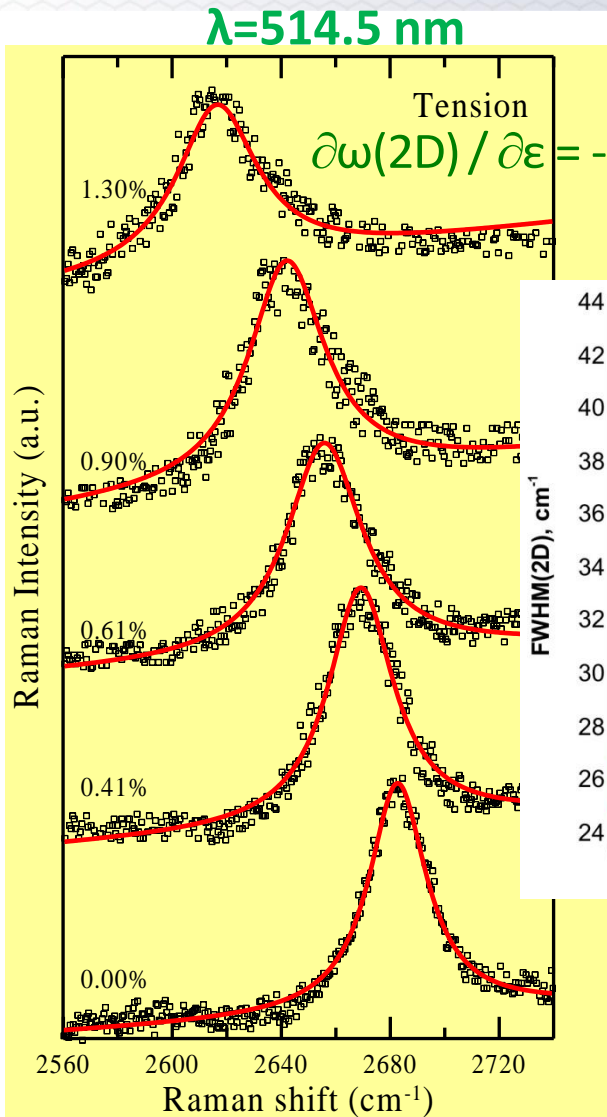
Experiment:

G⁺: -17.5 cm⁻¹/%

G⁻: -36.0 cm⁻¹/%

The strain rate of the G⁻ and G⁺ modes is independent of the direction of strain

SLG- Raman 2D mode splitting



polarization parallel to the strain axis

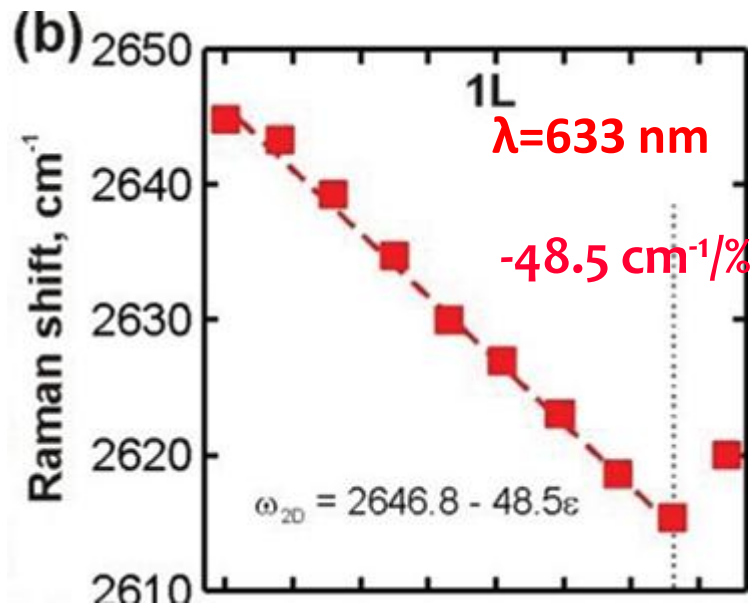
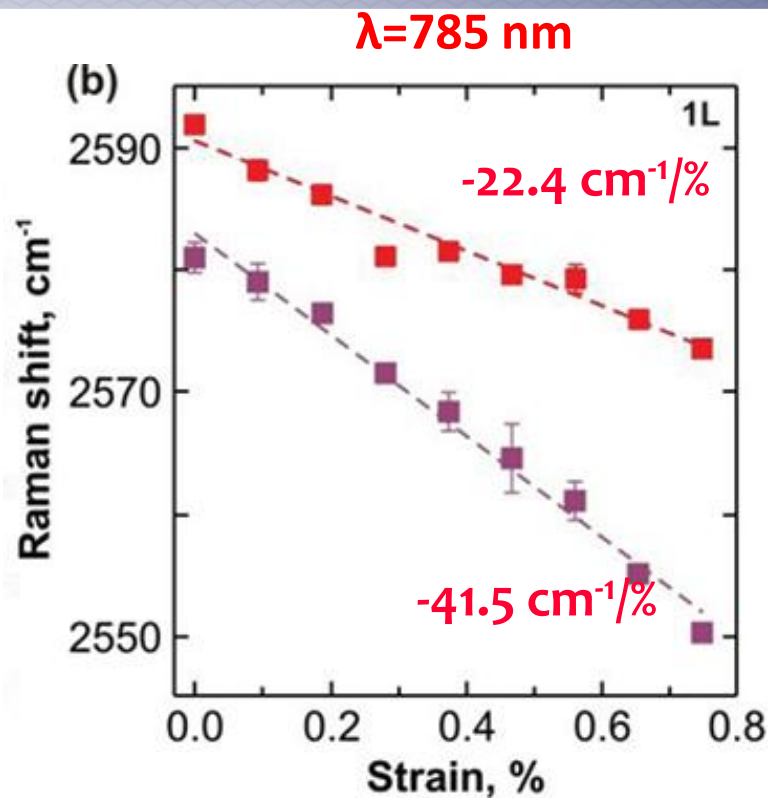
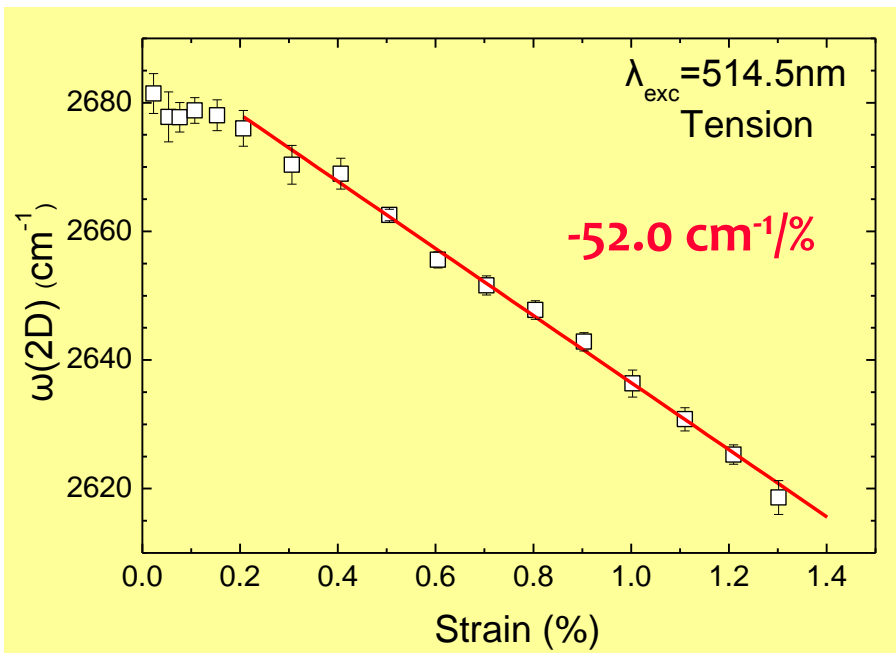
[ACS-NANO 5, 2231 (2011)]

[PRB 80, 205410 (2009)]

🔑 Even with 633 nm a single 2D peak is observed

- ➡ For 785 nm 2 components are clearly present even at zero strain!!!!
- ➡ The 2D mode line-shape strongly depends on the excitation energy.

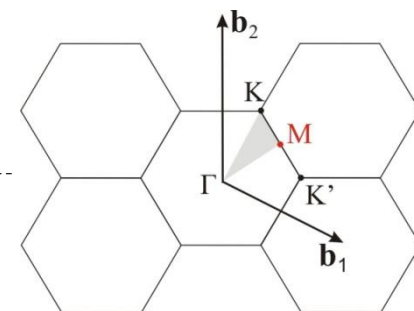
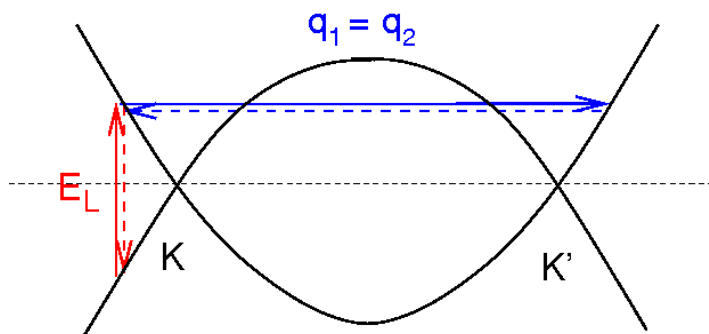
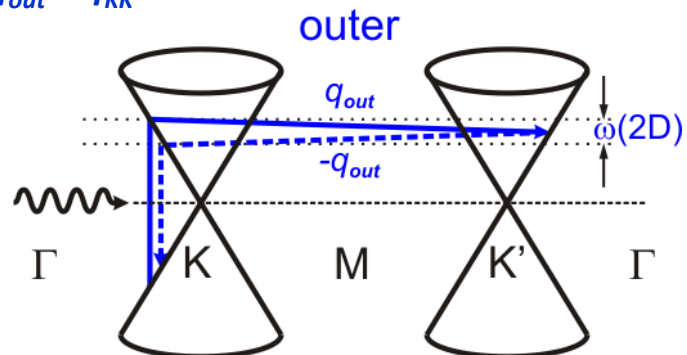
SLG- Raman 2D mode splitting



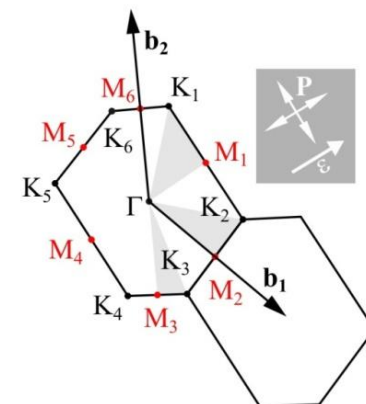
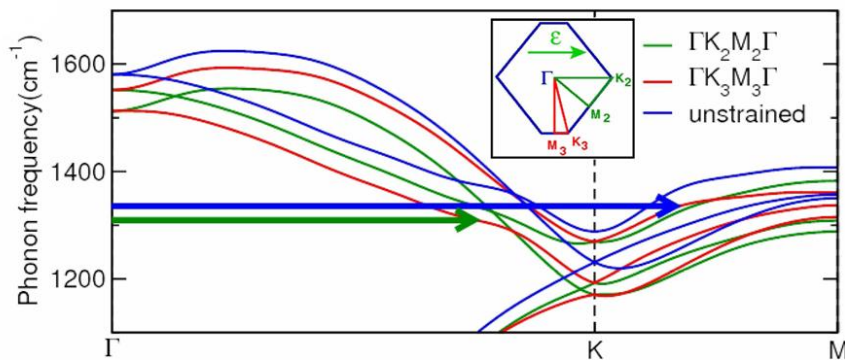
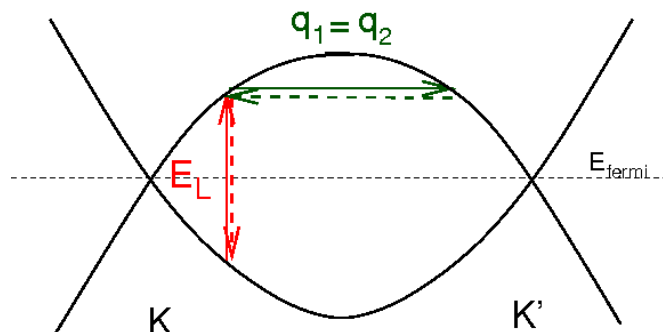
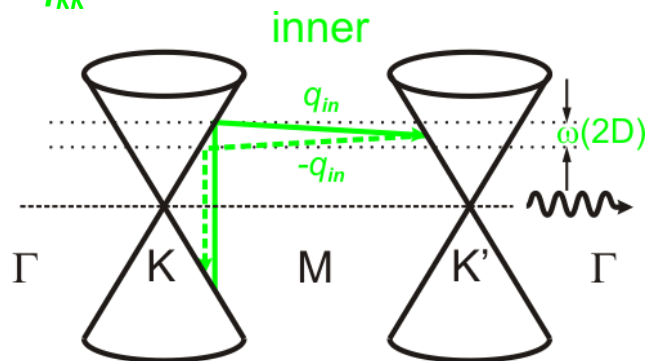
Qualitative explanation of the 2D splitting in SLG ($\lambda=785$ nm)

– Normally, only outer processes are considered due to the trigonal wrapping. First principles calculations shows 2D peak broadening and not splitting for this case.

$q_{out} > q_{KK'}$



$q_{in} < q_{KK'}$

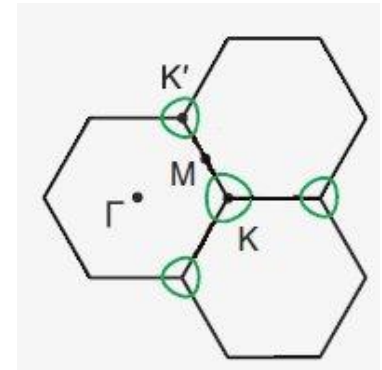
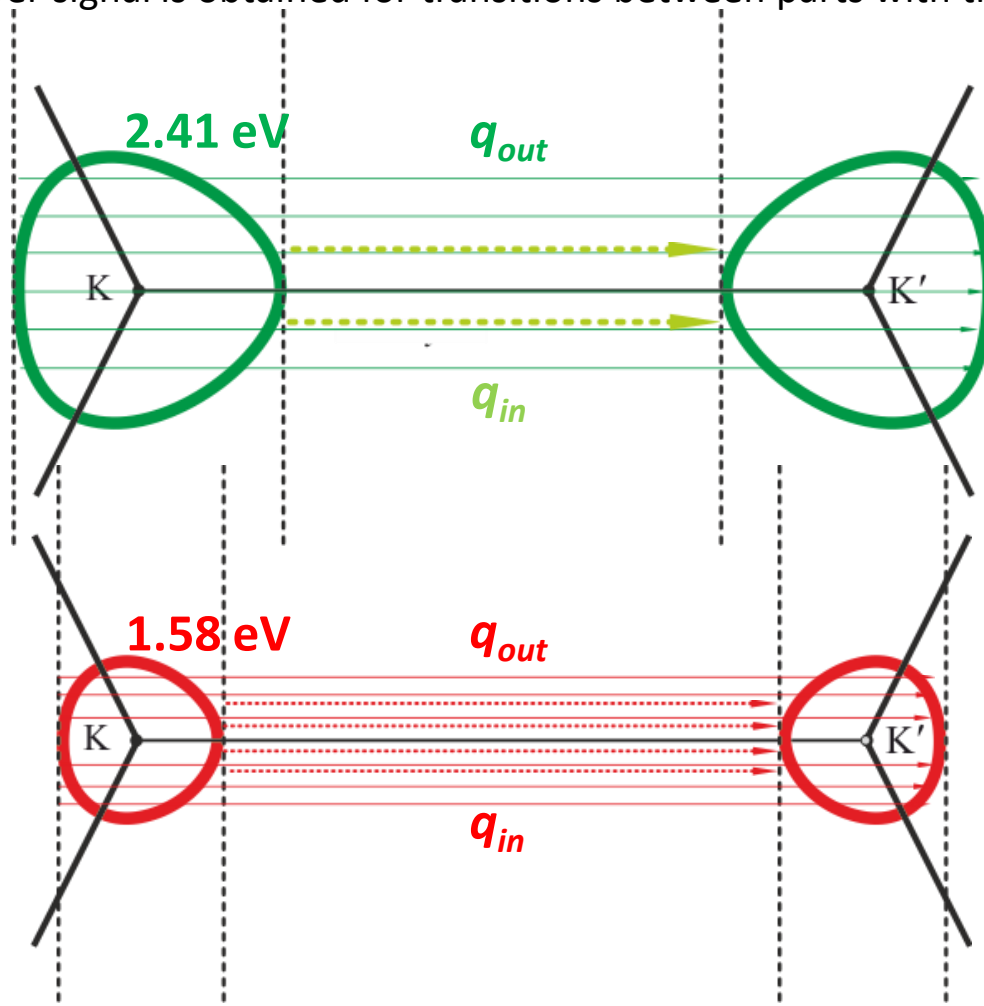
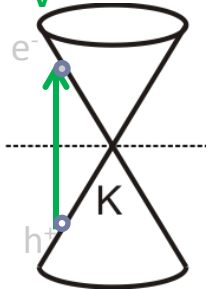


Why for 785nm inner/outer processes must be considered?

Equi-excitation-energy contour plots around the K and K' points of π electrons involved in the scattering process for 2.41eV (=514.5nm) and 1.58eV (=785nm) excitation energies.

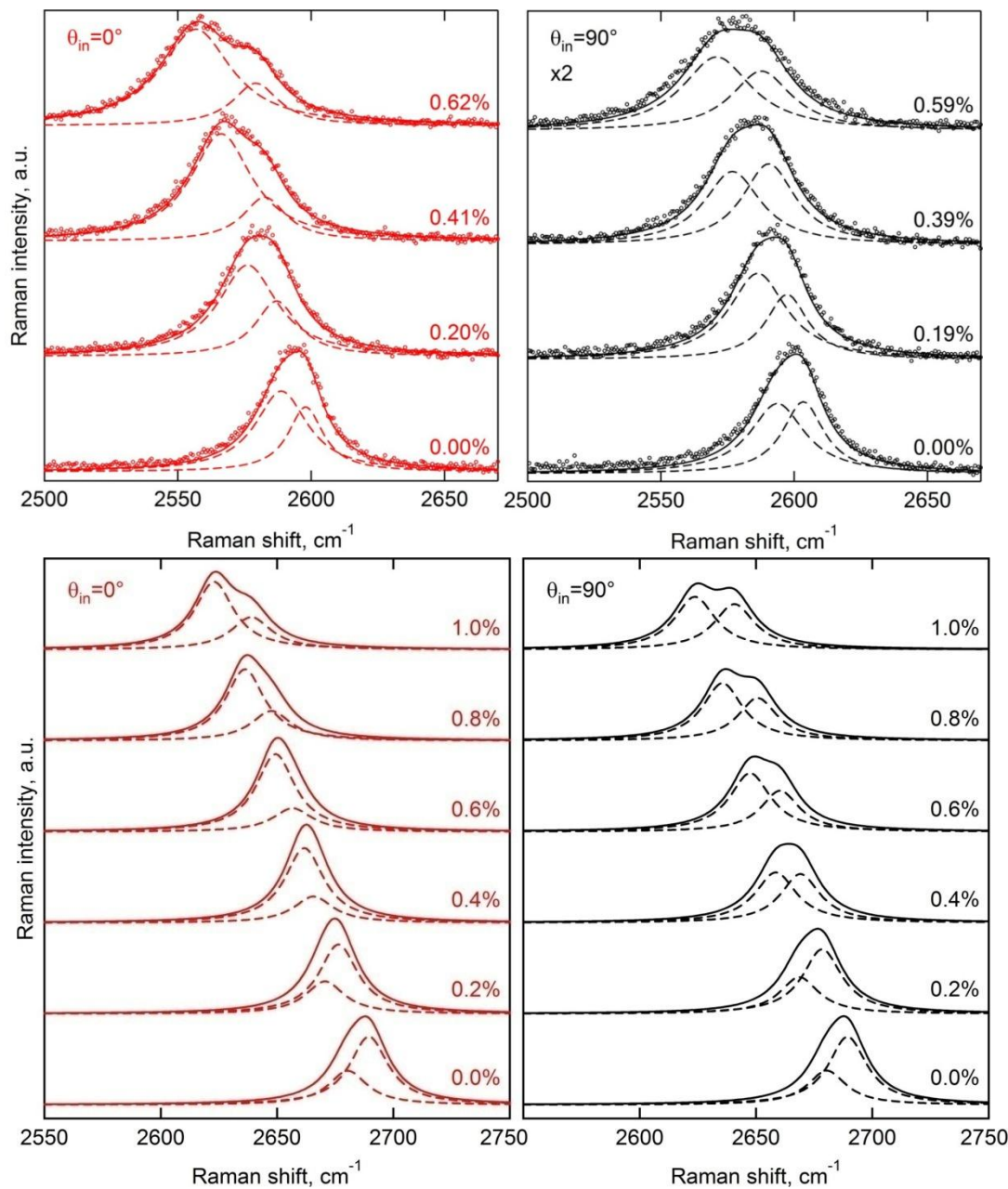
- 2.41eV: the highest Raman intensity occurs for transitions between parallel parts of the contours (outer processes). Much lower signal is obtained for transitions between parts with the highest curvature (inner)

$$E_c - E_v = 2.41 \text{ eV}$$



- 1.57eV: the equi-excitation-energy contours are notably more round and the trigonal wrapping effect weaker. Both inner and outer process give comparable contribution to the Raman intensity.

Simulated Raman spectra for $\theta=20^\circ$ ($\lambda_{exc}=785nm$)

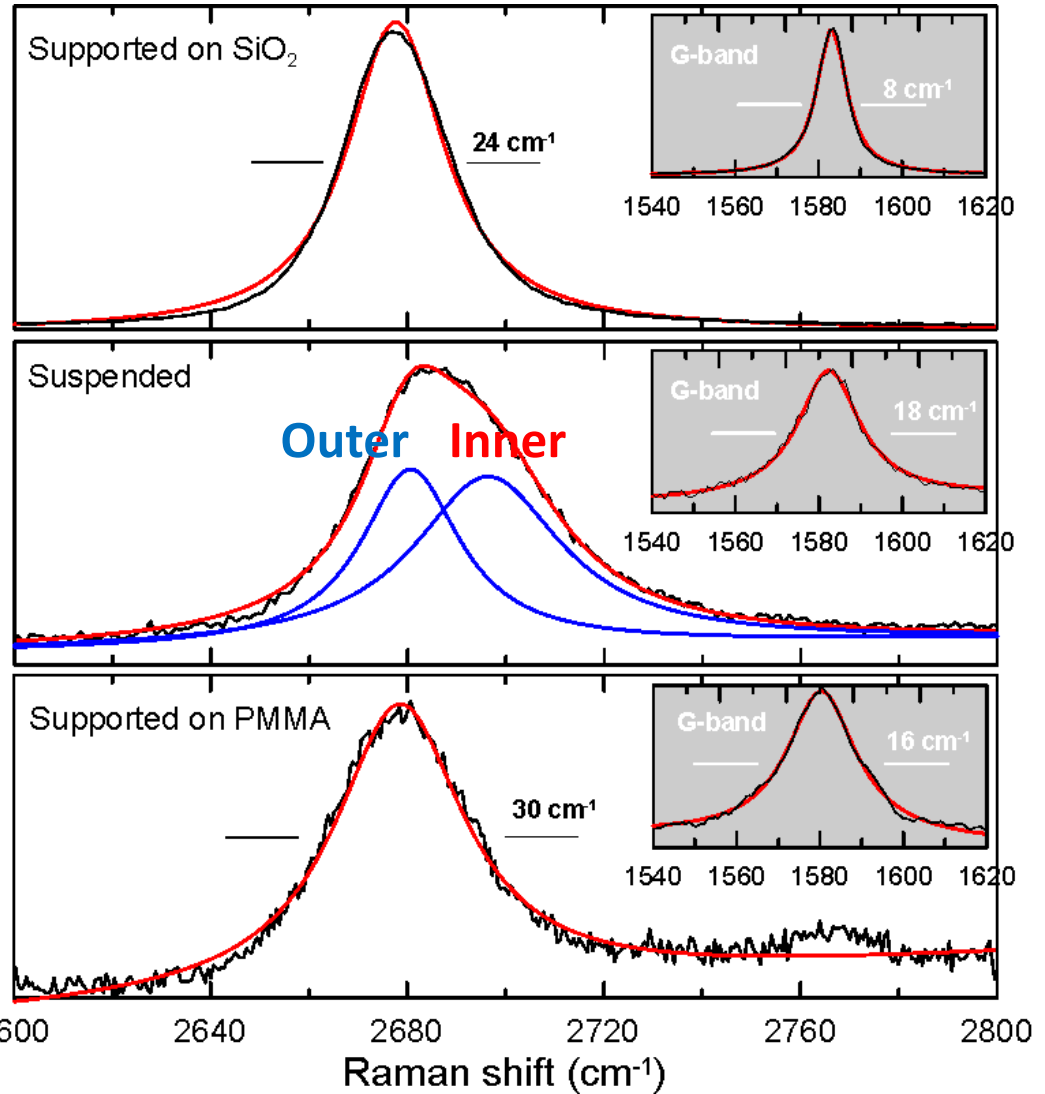
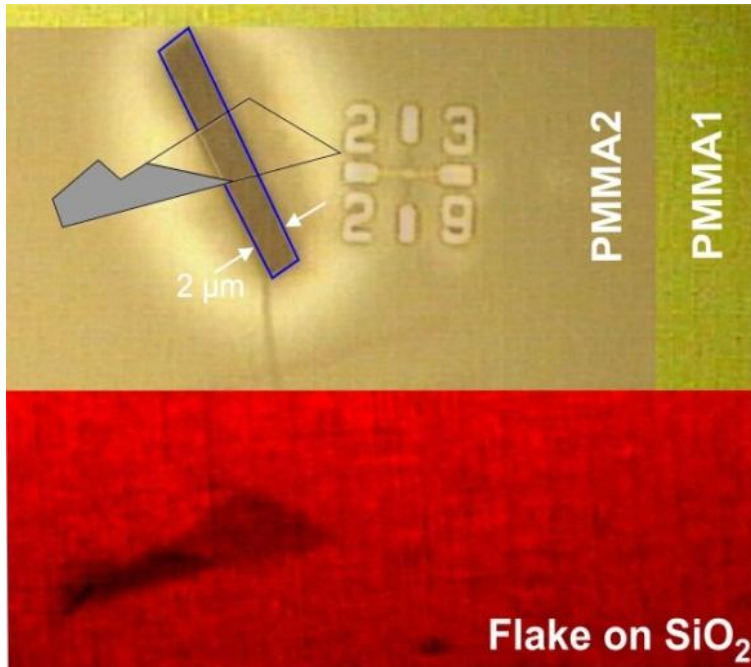


☑ The experimental shift rates for 2.41 eV and 1.58 eV excitations are in excellent agreement with first principles calculations.

[ACS-NANO 5, 2231 (2011)]

Raman spectrum of free standing graphene REVISITED

514.5 nm (2.41 eV)

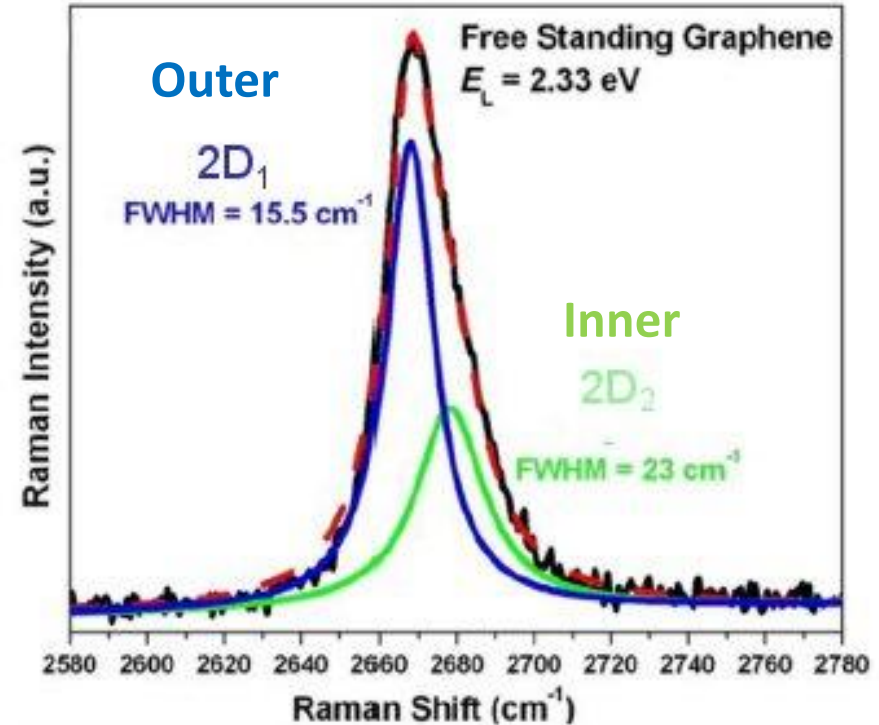
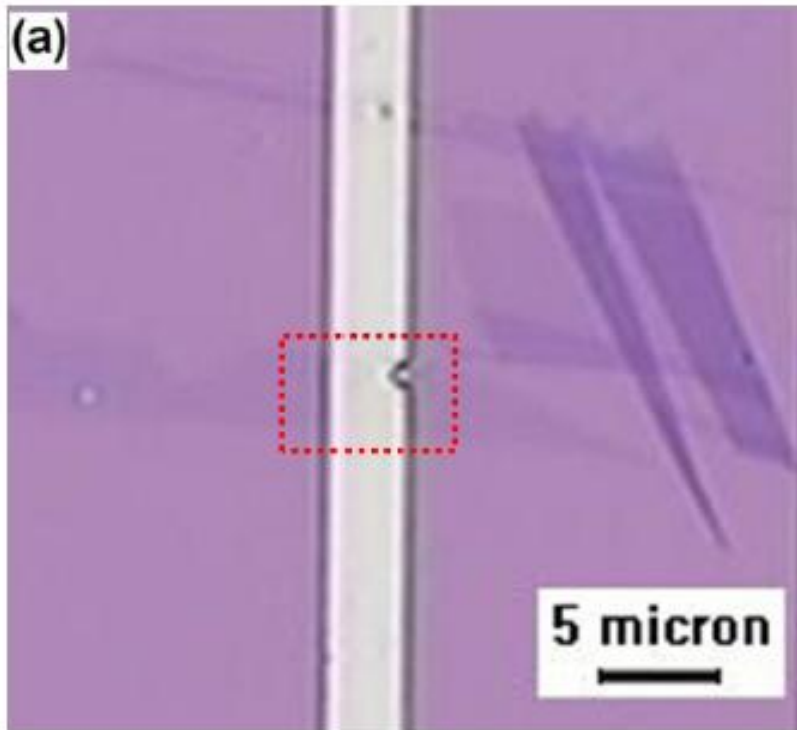


See also: Z. Luo et al, APL 100, 243107 (2012)]

- ❖ The 2D band of free standing graphene is obviously asymmetric while the same peak on SiO₂/Si substrate appears as a broad symmetric peak.
- ❖ Coexistence of both outer and inner processes in the DR Raman signal.

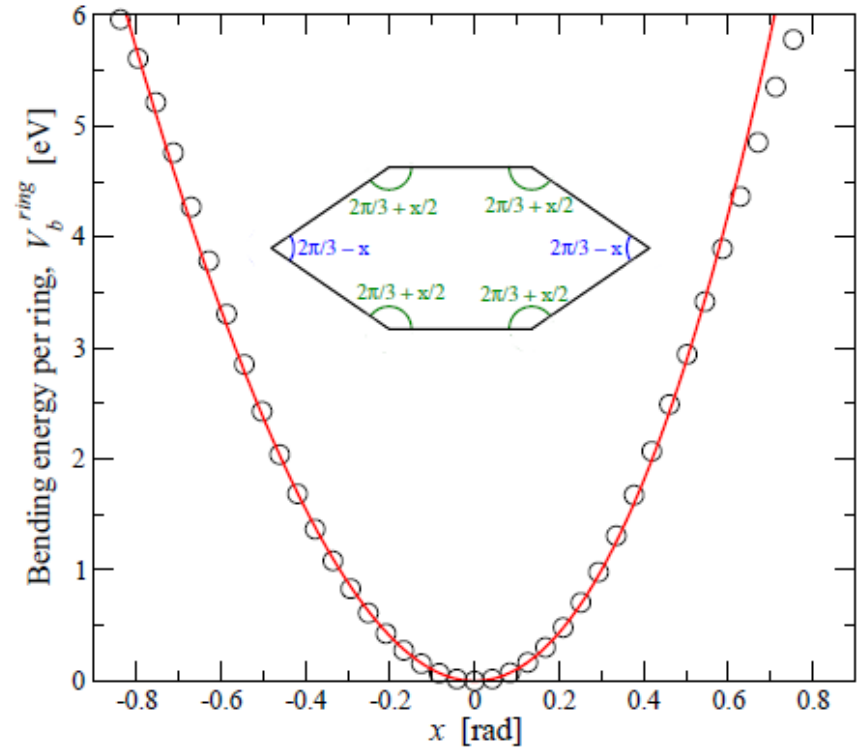
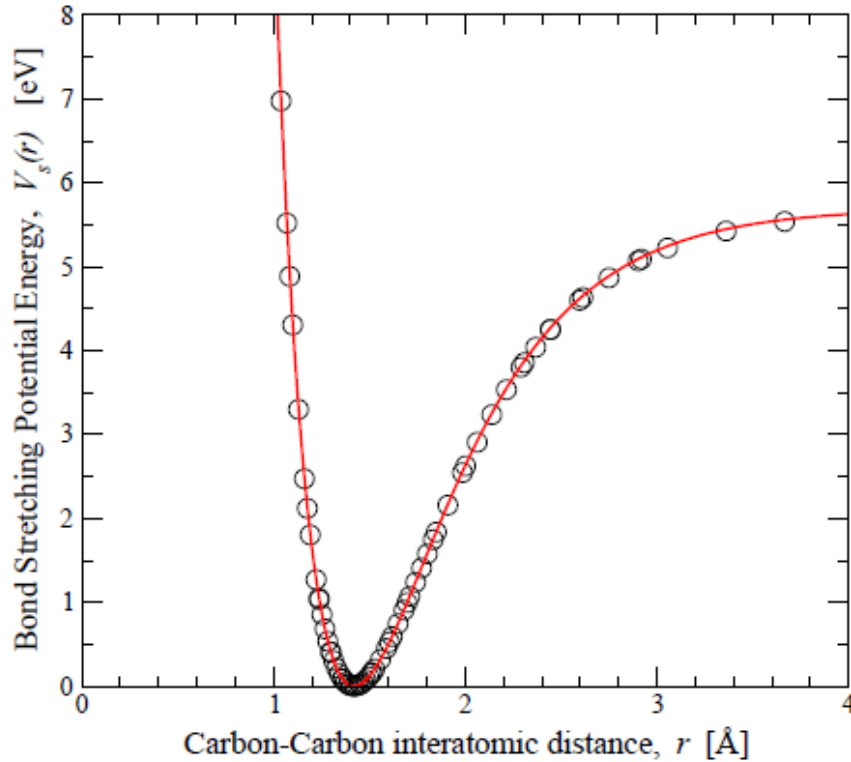
Direct observation of inner/outer processes in free standing graphene

Z. Luo et al, APL 100, 243107 (2012)]



- ❖ The 2D band of free standing graphene is obviously asymmetric while the same peak on SiO₂/Si substrate appears as a broad symmetric peak.
- ❖ Coexistence of both outer and inner processes in the double resonance Raman signal.

Atomistic simulations of graphene's mechanical properties



► $D=5.7\text{eV}$, $\alpha=1.96\text{\AA}^{-1}$, $r_0=1.42\text{\AA}$, $k=7\text{eV/rad}^2$, $k'=4\text{eV/rad}^3$.

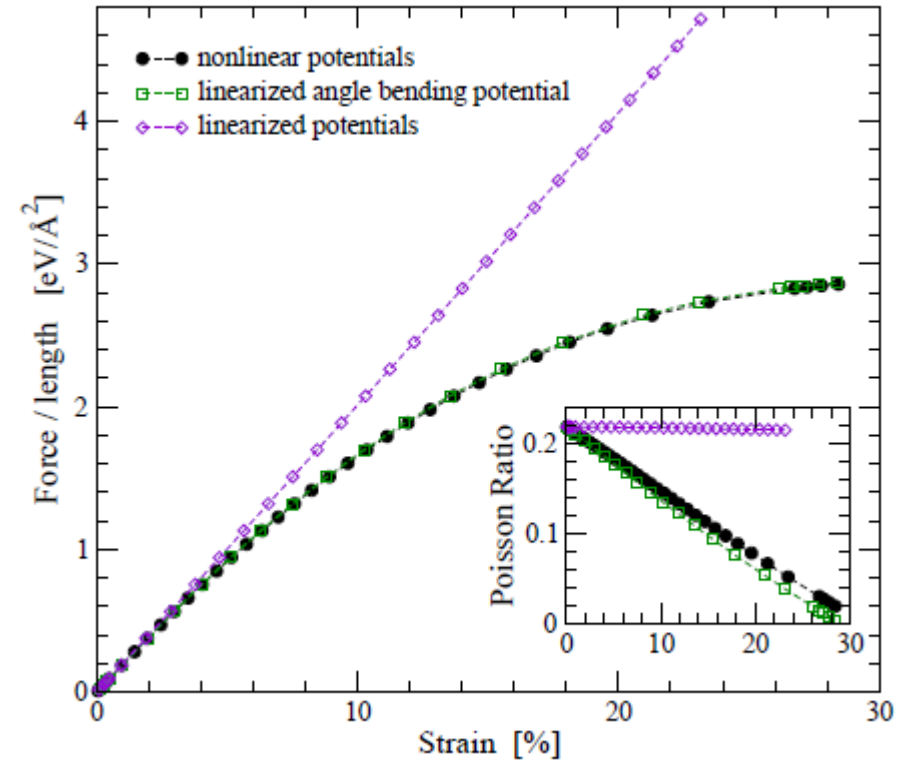
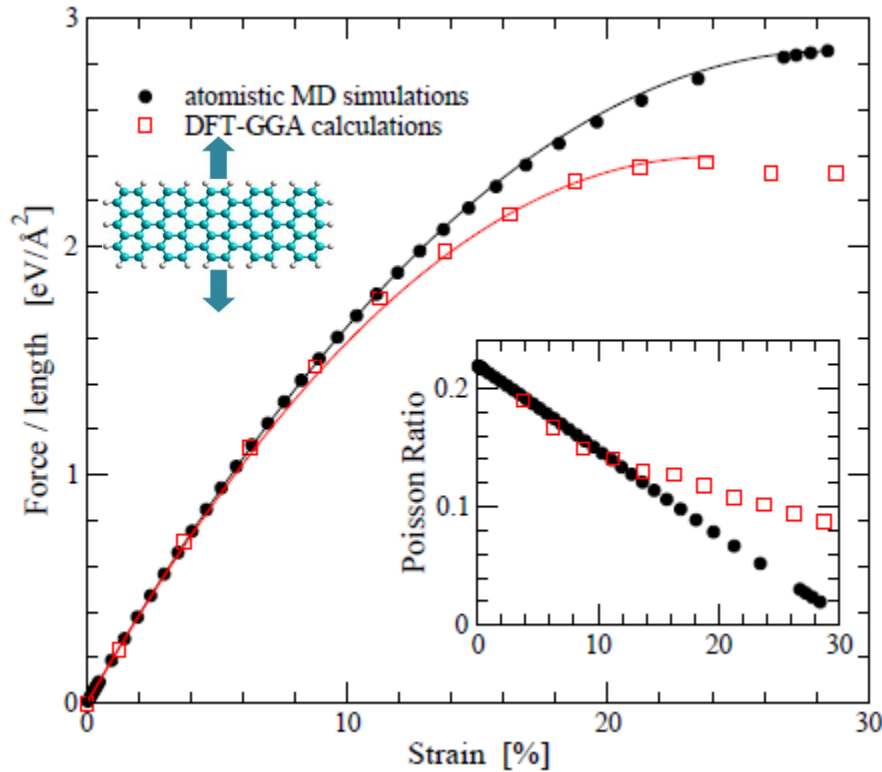
Fitting with analytical expressions

$$V(r) = D \left(e^{-a(r-r_0)} - 1 \right)^2$$

$$V(\varphi) = \frac{k}{2} \left(\varphi - \frac{2\pi}{3} \right)^2 - \frac{k'}{3} \left(\varphi - \frac{2\pi}{3} \right)^3$$

Atomistic simulations of graphene's mechanical properties

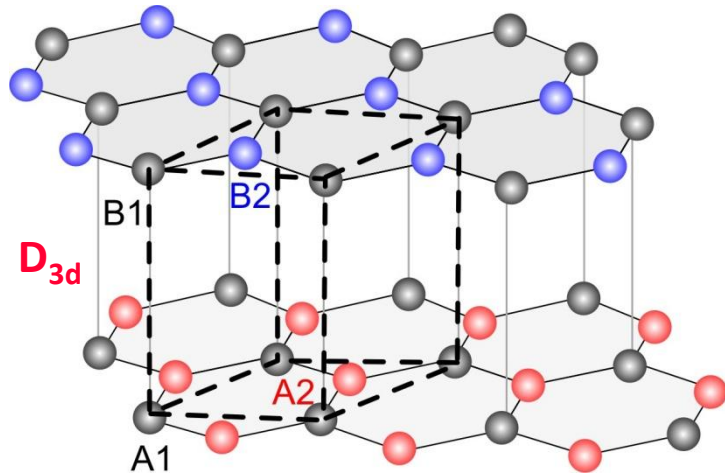
- The mechanical response of graphene is investigated using atomistic MD simulations and DFT calculations.



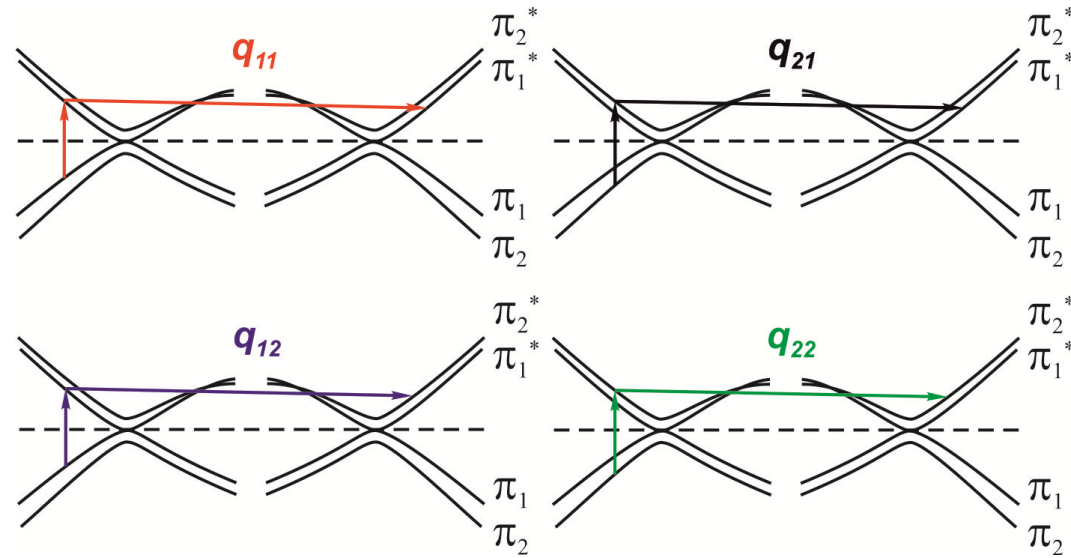
$$E_{2D} = 320 \text{ N/m} \rightarrow E_{\text{eff}} = E_{2D}/0.335\text{nm} = 0.96 \text{ TPa}$$

$$2D \text{ Intrinsic strength: } \sigma_{2D} = 39\text{-}45 \text{ N/m} \rightarrow \sigma_{\text{eff}} = \sigma/0.335\text{nm} = 120\text{-}130 \text{ GPa}$$

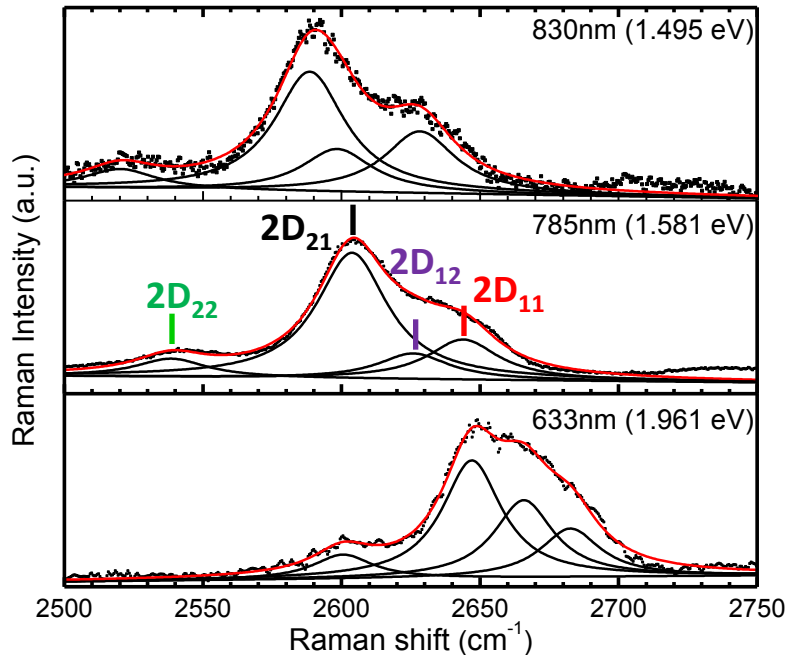
Graphene Bernal-stacked bilayer



– 4 DR processes predicted by group theory

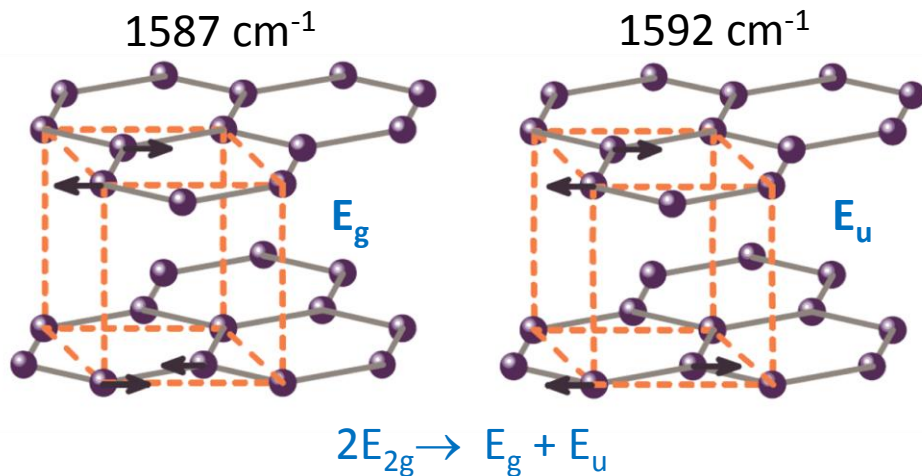


[L. Malard et al, Phys. Rep. 51, 473 (2009)]

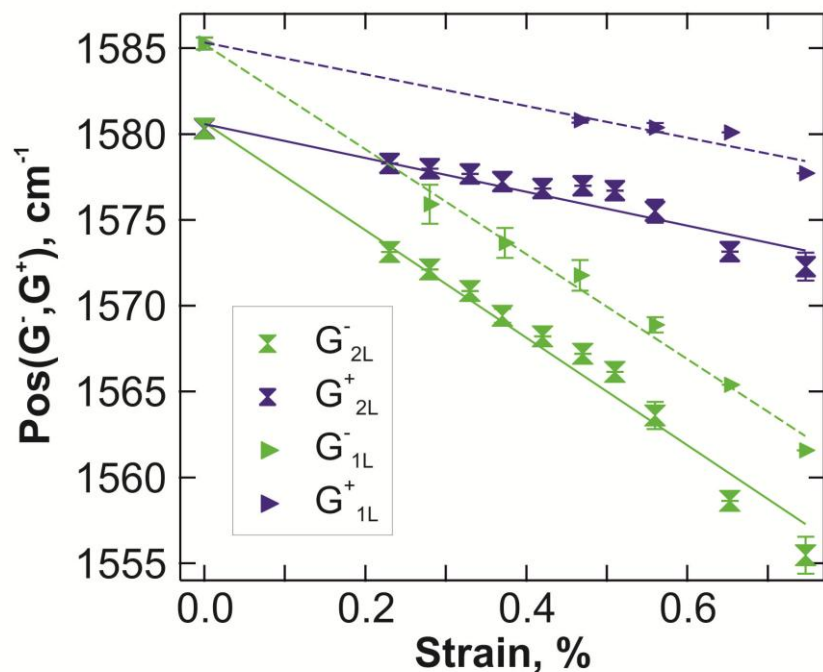
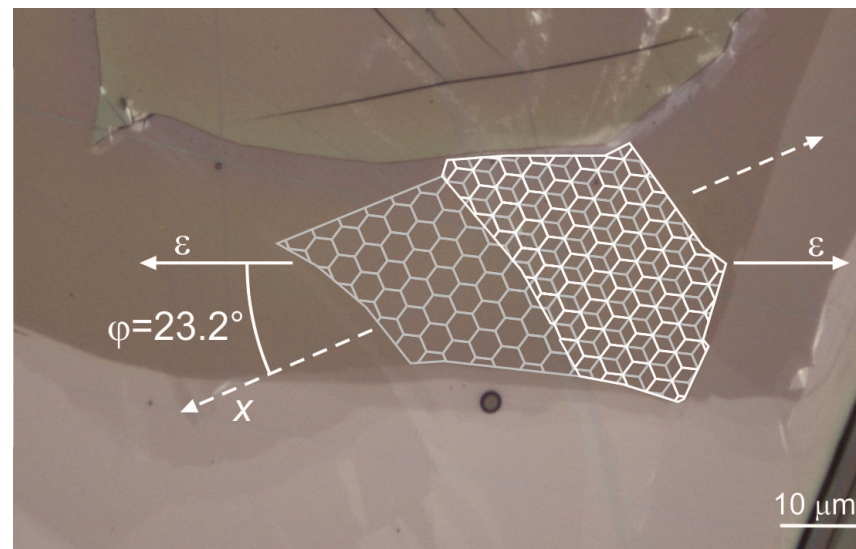


- 2 conduction and 2 valence bands and parabolic dispersion relation near \mathbf{K}/\mathbf{K}' .
- If valence and conduction bands were mirror images of one another then processes 12 and 21 would be degenerate.
- Due to Kohn anomaly at \mathbf{K} the highest (lowest) frequency peak of the 2D is associated with q_{11} (q_{22}).

Embedded 2LG under uniaxial tension – G band



[Yan et al. PRB 77, 125401 (2009)]

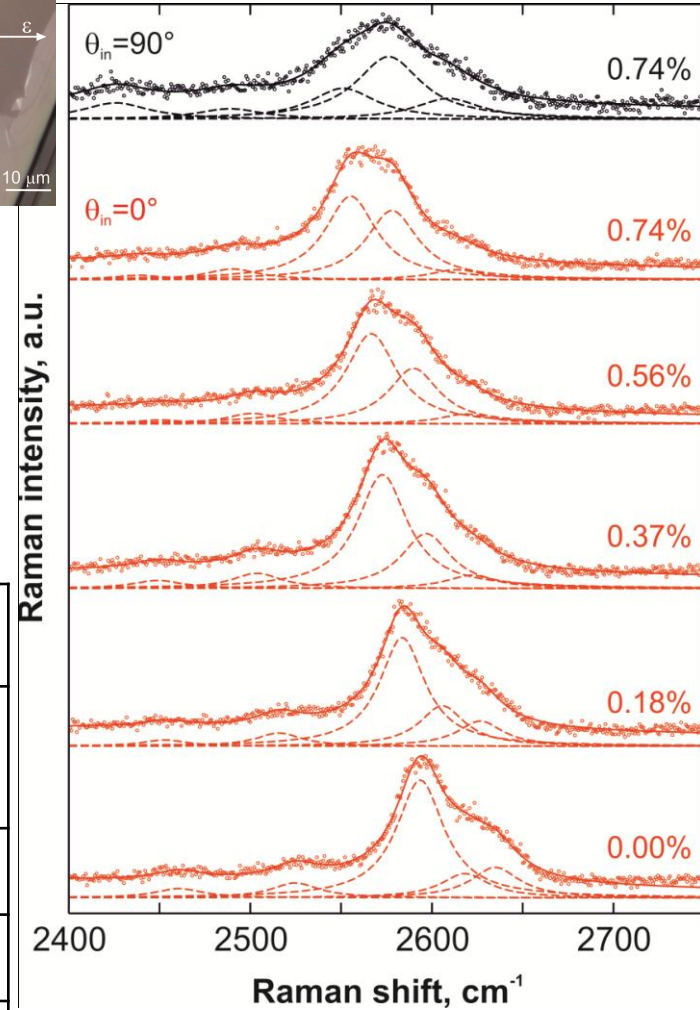
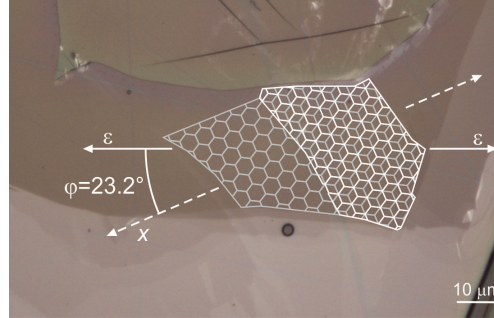
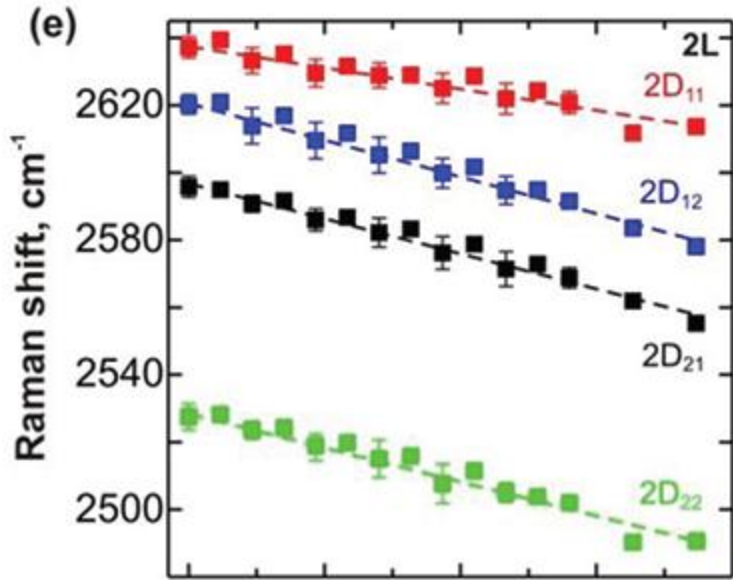


$$\frac{\partial \omega_G^+(2L)}{\partial \epsilon} = -9.9 \pm 4.9 \text{ cm}^{-1} / \%$$

$$\frac{\partial \omega_G^-(2L)}{\partial \epsilon} = -31.3 \pm 5.4 \text{ cm}^{-1} / \%$$

[Nano Letters 12, 687 (2012)]

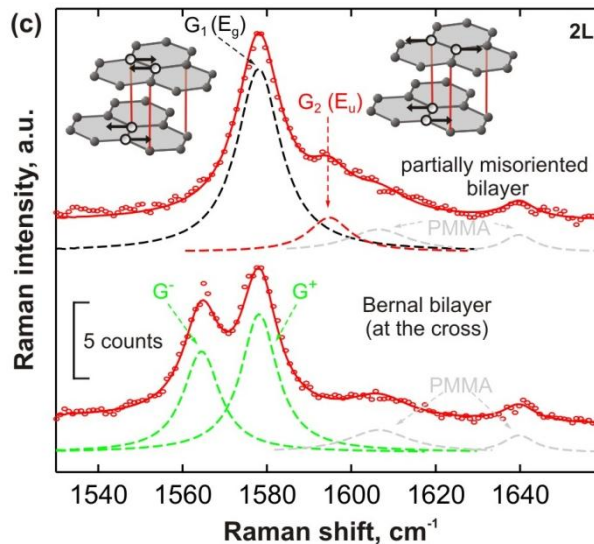
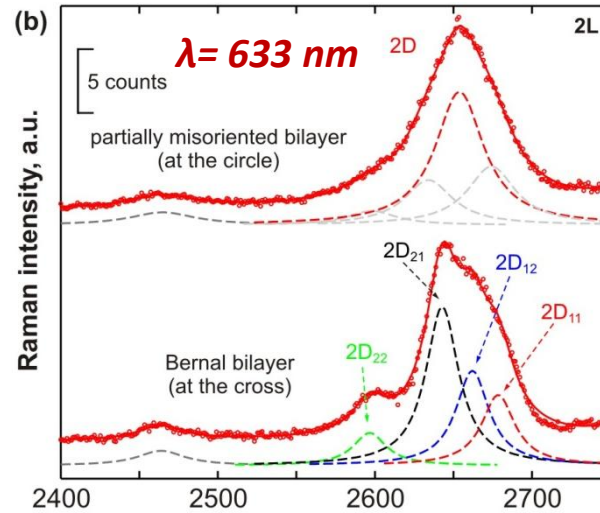
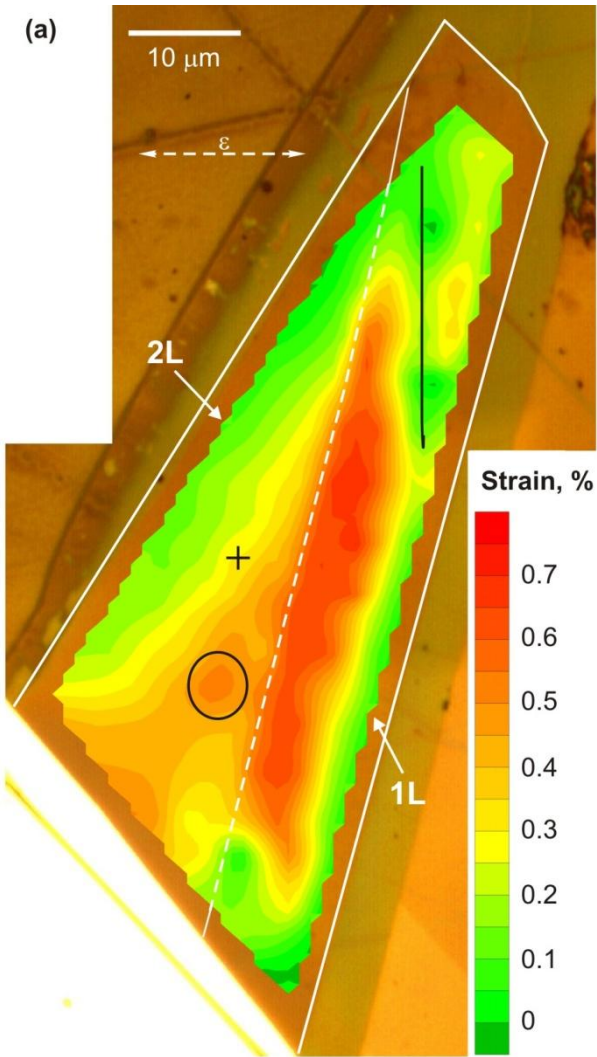
Embedded graphene bilayer under uniaxial tension – 2D band



	$\lambda = 785 \text{ nm}$		$\lambda = 633 \text{ nm}$	
	ω_{2D} [cm ⁻¹]	$\partial\omega_{2D}/\partial\varepsilon$ [cm ⁻¹ /%]	ω_{2D} [cm ⁻¹]	$\partial\omega_{2D}/\partial\varepsilon$ [cm ⁻¹ /%]
2D₁₁	2637.9±2.5	-32.3±6.7	2688.0±2.2	-57.5±7.3
2D₁₂	2621.3±2.7	-55.0±7.0	2671.0±2.5	-57.6±8.4
2D₂₁	2596.8±2.8	-51.7±6.2	2651.0±1.3	-54.8±4.4
2D₂₂	2529.3±2.6	-51.8±6.9	2603.1±1.6	-45.6±5.4

Strain-induced inversion symmetry breaking in 2LG

0.74% nominal strain value

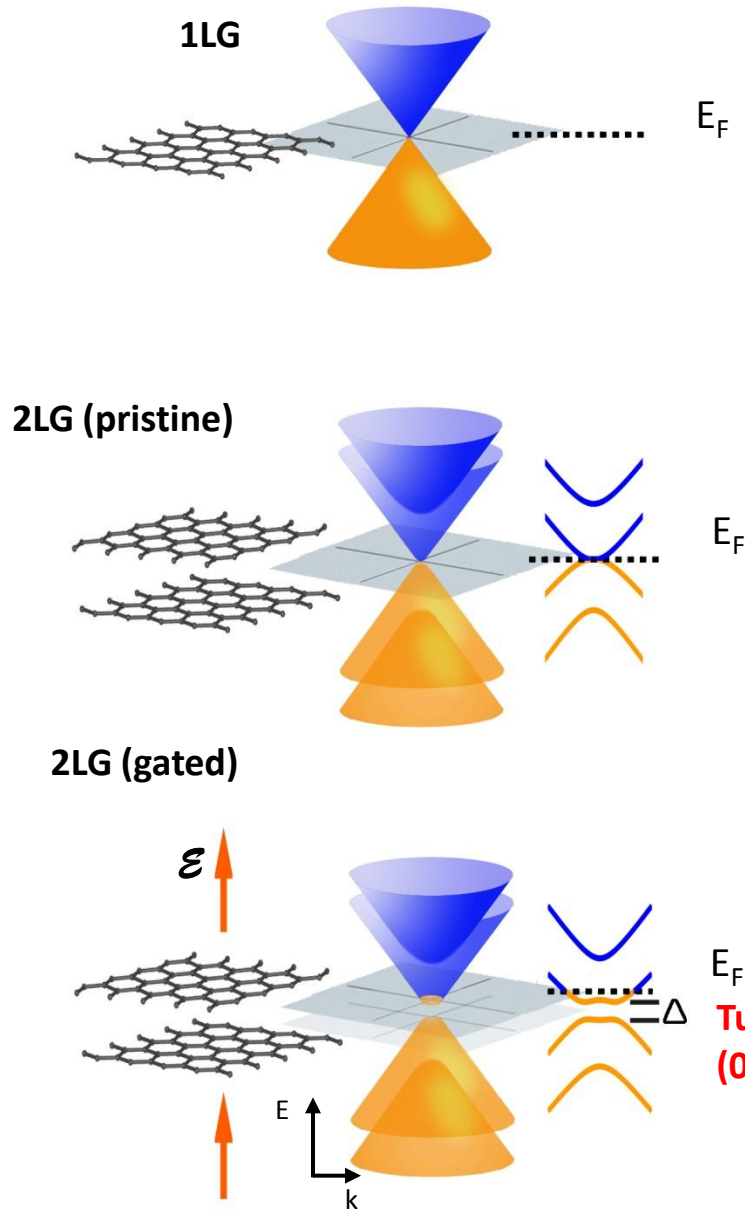


- ☑ Very recent theoretical predictions shows that the inversion symmetry breaking is directly related to an electronic gap opening in bilayer graphene.
- ☑ The removal of inversion symmetry in bilayer graphene due to unequal strain fields between the 2 layers may have important implications in the band gap engineering, providing an alternative route to induce the formation of a band gap.

[Nano Letters 12, 687 (2012)]

The results suggest that in the marked region the 2 graphene layers experience unequal strain field resulting in a local inversion symmetry breaking and the activation of the E_u mode.

Dual-gated bilayer graphene

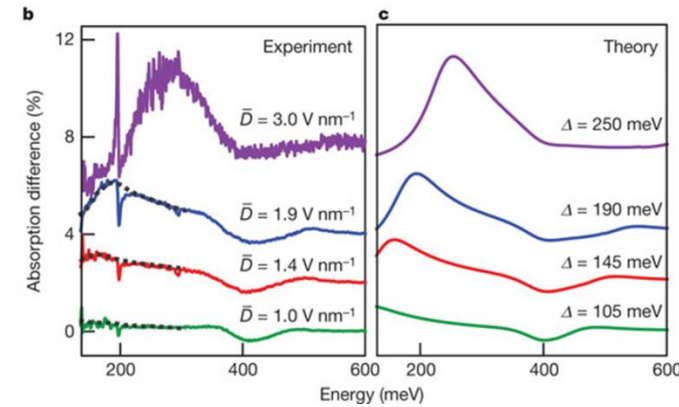
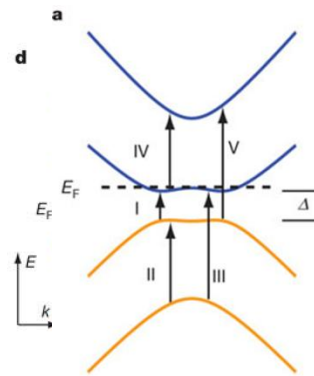
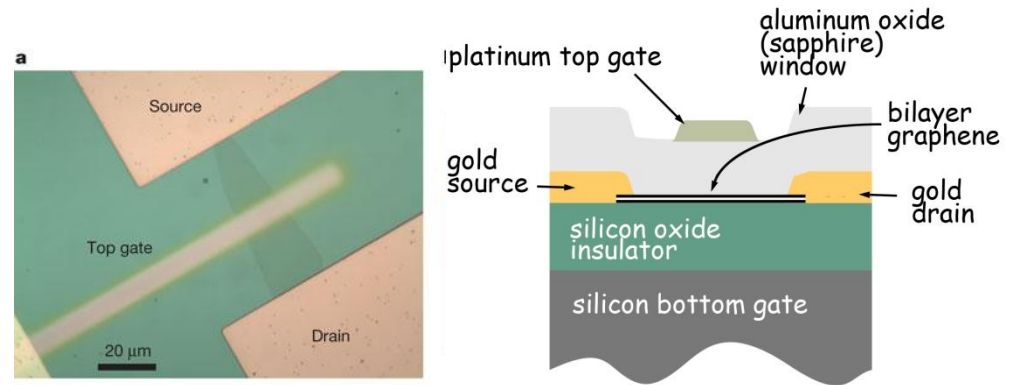


E_F

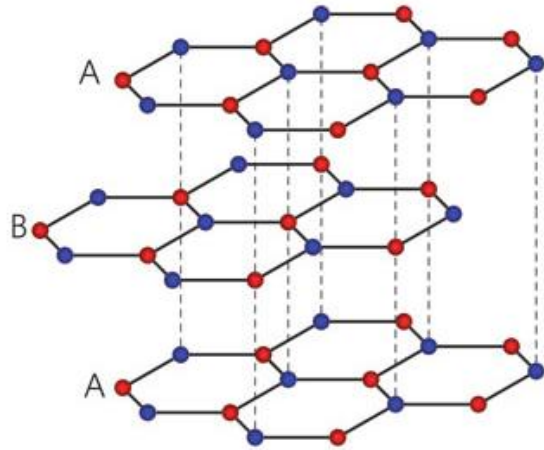
E_F

E_F

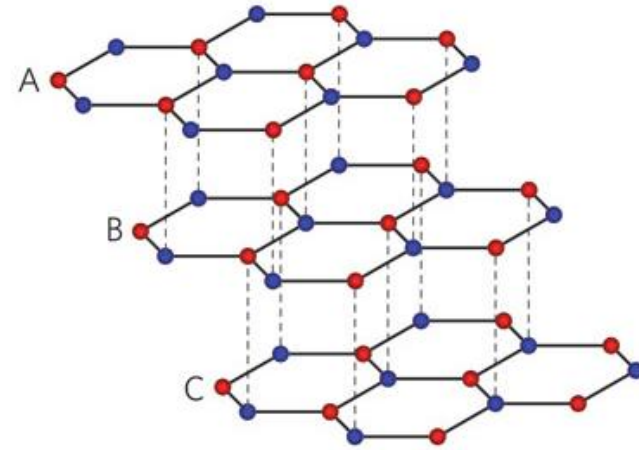
**Tunable bandgap
(0-.25eV)**



Trilayer graphene

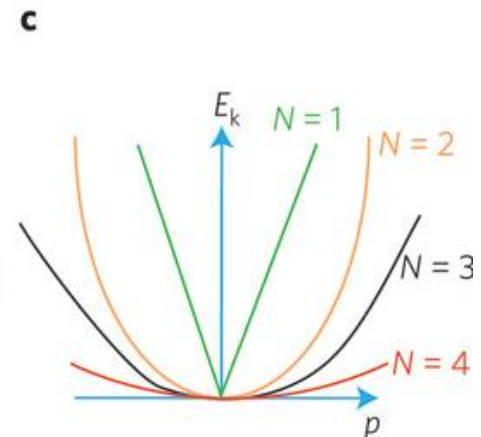
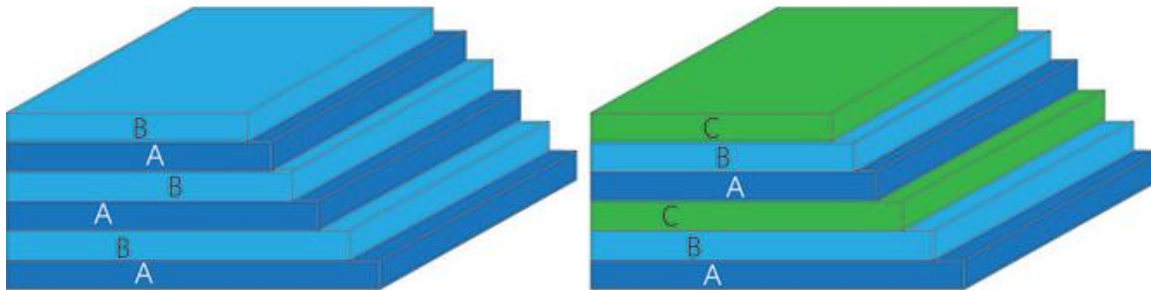


Bernal stacking
(ABA)



Rhombohedral stacking
(ABC)

b Multilayer graphene



Acknowledgements/ Collaborations

FORTH/ ICE-HT & University of Patras:

STAFF

C. Galiotis
J. Parthenios
D. Tasis
G. Kalosakas
P. Lianos

POSTDOCS

I. Polyzos
P. Pappas
E. Koukaras
D. Sfiris

POSTGRADS

G. Tsoukleri
P. Ravani
G. Trakakis
H. Androulidakis
L. Seremetis
N. Delikoukos
A. Paxinou
K. Ntoukakis

External:

K. Novoselov, A. Geim (Manchester, UK)
C. Thomsen & J. Maultzsch (TU Berlin)
A. Ferrari (Cambridge, UK)
O. Frank, L. Kavan (J. Heyrovský Institute, CR)
N. N. Lathiotakis (E.I.E)
G. Konstantinidis & G. Deligeorgis (FORTH/IESL)

Financial support:

- ❖ FORTH GRAPHENE CENTRE (<http://graphene.iceht.forth.gr/>)
- ❖ “THALIS”- Ministry of Education